UNIVERSITY OF OKLAHOMA

GRADUATE COLLEGE

BRANCHED POLYETHYLENIMINE RE-SENSITIZES METHICILLIN-RESISTANT *STAPHYLOCOCCUS AUREUS* TO BETA-LACTAM ANTIBIOTICS THROUGH A NOVEL MECHANISM OF ACTION

A DISSERTATION

SUBMITTED TO THE GRADUATE FACULTY

in partial fulfillment of the requirements for the

Degree of

DOCTOR OF PHILOSOPHY

By

MELISSA ANN FOXLEY
Norman, Oklahoma
2018

Downloaded from SHAREOK. Persistent Handle URL: https://hdl.handle.net/11244/301396

BRANCHED POLYETHYLENIMINE RE-SENSITIZES METHICILLIN-RESISTANT *STAPHYLOCOCCUS AUREUS* TO BETA-LACTAM ANTIBIOTICS THROUGH A NOVEL MECHANISM OF ACTION

A DISSERTATION APPROVED FOR THE
DEPARTMENT OF CHEMISTRY AND BIOCHEMISTRY

BY

_____
Dr. Charles Rice, Chair

_____
Dr. Daniel Glatzhofer

_____
Dr. Mark Nanny

_____
Dr. George Richter-Addo

_____
Dr. Si Wu

© Copyright by MELISSA ANN FOXLEY 2018
All Rights Reserved.

Acknowledgements

If I could write another dissertation worth of acknowledgements, it still would not be enough to express my gratitude to all that have been integral throughout my graduate school career. Thus, I will be brief in my thanks, but so many have been vital to the construction of this dissertation.

First and foremost, I would like to thank my advisor, Professor Charles Rice, for all of his support and help throughout this journey. He provided me with infinite amounts of knowledge and tools to allow me to succeed; for this, I am forever grateful. Professor Rice and his wife, Toni, welcomed me from the start and treated me as part of their family. As my time in the laboratory comes to an end, I am able to see how I have grown as an individual (academically, professionally, and personally) which in large part is due to both of their aid, encouragement, and, at times, nudging over the past four years.

I would also like to thank my graduate committee: Professor Mark Nanny, Professor Daniel Glatzhofer, Professor George Richter-Addo, and Professor Si Wu. Their time and guidance allowed me to stay on track to graduate in four years. I must also acknowledge the University of Oklahoma and the Department of Chemistry and Biochemistry for accepting me into their graduate program and allowing me to complete my studies. The professors here have also provided me with unlimited amounts of knowledge and information.

I have been very fortunate to have great colleagues in the Rice Research Group. Each of them helped me in ways that I could never fully thank. A large portion of my initial training in the laboratory was thanks to Dr. Anthony Friedline and Dr. Kieth

Thomas. My fellow graduate researchers: Anh Lam and Anita Ly have been wonderful sounding boards for ideas, and I wish them nothing but success in the future. I have had the most wonderful army of undergraduates: Stoffel Strange, Min Xiao, Summer Wright, Katie Grogan, Madeline Harney, Erika Moen, Beatrice Wilson, Jennifer Pusavat, and Casey Wouters. A special acknowledgement goes to Erika Moen for her amazing editing skills for this dissertation.

The work in this dissertation utilizes a large variety of techniques and instruments. The microscopy laboratory personnel have been immensely helpful: Professor Scott Russell, Dr. Preston Larson, Dr. Tingting Gu, Dr. Ben Smith, and Greg Strout. I would like to acknowledge Dr. Susan Nimmo for all of her assistance with the NMR experiments. When we initially started working with MRSA, Professor Robert Cichewicz and Jarrod King provided us with laboratory space, assistance, and information at the start of this project. Since we did not have the laboratory space to perform mammalian cell culture, Professor Anthony Burgett provided us with the laboratory space, and Professor Rama Kothapalli helped me optimize the cytotoxicity assays. I would like to thank Professor Glatzhofer for all of his help with understanding BPEI.

I would like to thank all of my professors at the University of Minnesota Duluth and my teachers from Proctor High School. My first chemistry class was taught by Professor Sangeeta Mereddy who made me fall in love with chemistry. I am especially thankful to my academic advisor Professor Paul Siders for all of his advice on life and careers. I would like to acknowledge all of the people that ran the Pathways to Advanced Degrees in Life Sciences, especially Professor Ben Clarke and Mary

Keneddy-Clarke, for getting me involved in undergraduate research. A special acknowledgement goes out to my research advisor Professor Venkatram Mereddy and all of the students in his research laboratory: Grady Nelson, Sravan Jonnalagadda, Shirisha Jonnalagadda, Luke Solano, Mike Williams, Conor Ronayne, Erica Lueth, and Melissa Just. Professor Mereddy provided me with my first research experience and helped me grow as a researcher.

At the University of Oklahoma, I have found the strongest support system and group of friends. These friends have taught me so much and provided me with a tremendous amount of help. My time at OU has been vastly more enjoyable because of these wonderful people.

Last, but not least, my appreciation for my family throughout the process of graduate school and the rest of my life. My mom and dad, Deborah and Daniel Hill, have always supported my dreams and have always pushed me to rise above the expectations I set for myself. My late Grandma Towner always taught me to be kind to everyone and always find the joys life has to offer. My Grandma and Grandpa Hill showed me the meaning of working hard and that life is what you make it to be. I married into the best family: Lori Foxley, Christina Foxley, Joseph Foxley, and Opa and Oma Krause have been the most wonderful second family. Finally, I would like to thank my husband, Curt Foxley. Thank you, Curt, for standing by me through all the craziness of graduate school and life.

Table of Contents

Acknowledgements iv

List of Tables xi

List of Figures xii

Abstract xx

Chapter 1: Methicillin-resistant *Staphylococcus aureus* 1

Antibiotic Resistance 1

Pathogenesis and Prevalence of *Staphylococcus aureus* 3

Bacteria Cell Walls 7

β-Lactam Antibiotics 9

Resistance Mechanisms 13

Drugs of Last Resort 15

Chapter 2: 600-Da BPEI is a Non-Toxic Cationic Polymer 18

Background 18

Structure of BPEI 19

Uses for BPEI 20

Drug Design 21

Purpose of Experiment 23

Experimental Procedures 24

Preparation of Cationic Polymers 24

pH Titration of BPEIs 24

Maintenance of Eukaryotic Cell Lines 24

CellTiter Viability Assay 25

Nephrotoxicity Assay 25
Results and Discussion 26
Characterization of BPEI 26
600-Da BPEI has low cytotoxicity in vitro 28
Conclusion 30
Chapter 3: Efficacy of β-lactam antibiotics against MRSA Restored Through Synergy with BPEI 32
Background 32
Purpose of Experiment 34
Experimental Procedures 35
Cell Lines Used 35
In Vitro Efficacy Checkerboard Assays 36
Minimum Bactericidal Concentrations 37
Clinical Isolates of MRSA 37
Growth and Time-Killing Curves 38
Results and Discussion 38
BPEI has synergy with β-lactam antibiotics against MRSA 40
BPEI creates synergy with β-lactam antibiotics to stop VISA growth 43
BPEI potentiates oxacillin against clinical isolates of MRSA 45
Intermediate molecular weight BPEI has higher efficacy 48
BPEI:oxacillin combination is bactericidal 50
BPEI does not have synergy with other antibiotics 54
BPEI:β-lactam efficacy is specific to MRSA 56

Conclusions 58

Chapter 4: Targeting Wall Teichoic Acid *In Situ* with Branched Polyethylenimine Potentiates β-Lactam Efficacy against MRSA 61

Background 61

Structure and Function of Teichoic Acids 62

Principles of NMR, Confocal Microscopy and Fluorescently Labelled Proteins. 64

Principles of Nuclear Magnetic Resonance 64

Principles of Laser Scanning Confocal Microscopy 66

Principles of Fluorescence Labels 68

Purpose of Experiment 70

Experimental Procedures 72

Synthesis of the BPEI:Dye Conjugate 72

Labeling Cells with the BPEI:Dye Conjugate 72

Confocal Microscopy and Image Processing 73

WTA Purification 73

NMR Spectroscopy 74

Checkerboard Assay of WTA-Deficient Cells 75

Imaging of Fluorescently Labeled Proteins 75

Results and Discussion 76

BPEI localizes on the cell wall of Gram-positive bacteria 76

BPEI electrostatically binds to WTA 80

WTA is important for BPEI potentiation of β-lactam antibiotics 85

BPEI prevents proper localization of cell wall machinery 88

Conclusions 92
Chapter 5: Morphological Examination of the Effect of BPEI on MRSA 95
Background 95
Principle of Electron Microscopy 96
Purpose of Experiment 100
Experimental Procedures 101
Phase Contrast Imaging 101
Scanning Electron Microscopy 101
Autolysis Assay 102
Transmission Electron Microscopy 102
Results and Discussion 103
BPEI alters the cell morphology of Bacillus subtilis cells 103
BPEI prevented autolysis of MRSA cells 106
WTA-deficient knockout mutants have altered cell wall structure and cell division 108
BPEI increased cell size of MRSA 109
Cell division was altered when cells were treated with BPEI 111
BPEI degraded the cell wall and caused stress response 114
Conclusions 117
References 119

List of Tables

Table 1. Structure and classification of commonly used β-lactam antibiotics. 11

Table 2. The pKa of BPEIs and Tris base. 28

Table 3. *In vitro* mammalian cytotoxic activity of BPEI 29

Table 4. Bacterial strains used in study. 36

Table 5. Minimum inhibitory concentrations and fractional inhibitory values of BPEI in combination with β-lactam antibiotics against MRSA. 42

Table 6. Synergy of 600-Da BPEI and β-lactams against MRSA 700787. 44

Table 7. Treatment of clinical isolates of MRSA. Data shows the concentration of BPEI required to reduce the MIC of oxacillin to the susceptibility cutoff of 2 μg/mL. 46

Table 8. Treatment of clinical isolates of MRSA. Data shows the concentration of oxacillin required to reduce the MIC of BPEI to 4 μg/mL. 47

Table 9. Minimum inhibitory concentrations and fractional inhibitory values of BPEI in combination with non-β-lactam antibiotics against MRSA. 55

Table 10. Lack of synergy of 600-Da BPEI and β-lactams against MSSA 25923. 57

Table 11. BPEI prevents MRSA USA300 cells from separating efficiently. 114

List of Figures

Figure 1. Colonization, infection, and pathogenesis of *S. aureus* bacteria in the human body. 5

Figure 2. Structure of Gram-positive and Gram-negative bacteria are distinct from one another. Gram-positive cell walls have a much thicker peptidoglycan layer and the presence of teichoic acids. Gram-negative cell walls have an outer membrane that acts as a barrier. 9

Figure 3. An example of one molecule of 600-Da BPEI is shown. 19

Figure 4. Titration curve (A) and the buffer capacity curve (B) of BPEI polymers and Tris-base. 27

Figure 5. 600-Da BPEI had minimal LDH release in a primary kidney proximal tubule cell line (PCS-400-010). The 1800-Da and 10-kDa BPEIs had higher LDH release than the nephrotoxic drug colistin. Error bars denote standard deviation (n=3). 30

Figure 6. *In vitro* assay of ampicillin against MRSA. When BPEI (2.7 µg/mL) is added, the MIC for ampicillin is between 12 and 25 µg/mL (checkered columns) while ampicillin without BPEI does not inhibit MRSA below 50 µg/mL concentration (solid red columns). The growth of MRSA was evaluated by measuring the change in OD_{600} after 20 hours. Cell growth in TSB without additives is denoted as Control. 39

Figure 7. Checkerboard assays show synergy between BPEI and β-lactams on MRSA USA300 and MRSA MW2. BPEI had synergy with oxacillin (A, B), ceftizoxime (C, D), and imipenem (E, F) against MRSA USA300 (A, C, E) and MRSA MW2 (B, D, F). Each assay was performed as three separate trials, and the presented data is shown as the average change in OD_{600} 41

Figure 8. Checkerboard assays show synergy between BPEI and β-lactams on MRSA 252 and MRSA 33592. BPEI had synergy with ampicillin against hospital-acquired MRSA 252 (A). BPEI had synergy with oxacillin against MRSA 33592 (B). Each assay was performed as three separate trials, and the presented data is shown as the average change in OD_{600}. 43

Figure 9. BPEI potentiates β-lactam activity against MRSA 700787. Checkerboard assays show that BPEI potentiates oxacillin (A), amoxicillin (B), and ampicillin (C) activity against MRSA 700787. Each assay was performed as three separate trials, and the presented data is shown as the average change in OD_{600}. 44

Figure 10. BPEI and oxacillin together are effective at preventing growth of a clinical isolate of MRSA. The concentration of BPEI required to inhibit MRSA OU14 was reduced when simultaneously grown in 2 μg/mL oxacillin (A). Similarly, the concentration of oxacillin required to inhibit growth was reduced while simultaneously treated with 4 μg/mL of BPEI (B). The black line indicates the cutoff for growth at a change in OD_{600} of 0.05. Each data point is reported as the average of four trials. 47

Figure 11. Low and intermediate MW BPEI potentiate MRSA to oxacillin. 600-Da BPEI (A), 1200-Da BPEI (B) and 1800-Da BPEI (C) potentiate oxacillin acitivity against MRSA 700787 but 10-kDa BPEI (D) does not. Each assay was performed as three separate trials, and the presented data is shown as the average change in OD_{600}. 49

Figure 12. *In vitro* linear PEI assay against MRSA. LPEI alone does not affect the growth of MRSA through 54 μg/mL (striped red columns); addition of 9.3 μg/mL ampicillin provides some effect, though not enough to inhibit MRSA growth (thatched red columns). Growth of MRSA was evaluated by measuring the change in OD_{600} after

20 hours. Cell growth in media (Control) or media with 1% DMSO show the increase in OD_{600} (solid red columns), while 50 µg/mL chloramphenicol serves as a negative control. 50

Figure 13. 600-Da BPEI and oxacillin comprise a bactericidal combination in MRSA 700787. Cells treated individually with BPEI or oxacillin were still able to grow but growth was inhibited when both BPEI and oxacillin were used (A). A time-kill curve shows that the combination has a bactericidal mechanism of action as seen with the drop in viable cell counts after 4 hours (B). Error bars denote standard deviation (n=3). 52

Figure 14. BPEI: oxacillin combination is bactericidal against MRSA. Dark shaded circles indicate wells where the bacteria grew as determined by an OD_{600} greater than 0.05. Lighter shaded circles show where cells were not killed but did not reach an OD_{600} of 0.05. Unshaded circles had less than 500 cells/µl. Bolded circles show an FIC less than 0.5. 54

Figure 15. BPEI does not potentiate synergy with vancomycin or linezolid. Checkerboard assays show that BPEI did not have synergy with vancomycin (A,B) or linezolid (C,D) against MRSA USA300 or MRSA MW2. Chloramphenicol and BPEI do not have synergy against MRSA 700787 (E). Each assay was performed as three separate trials, and the presented data is shown as the average change in OD_{600}. 56

Figure 16. BPEI does not potentiates β-lactam activity against MSSA 25923, *B. subtilis* 6051, or *E. coli* 11775. BPEI and ampicillin have synergy against MRSA MW2 (A). Checkerboard assays show that BPEI not potentiates ampicillin (B) activity against MSSA 25923. No synergy is seen between β-lactams and BPEI against *B. subtilis* 6051

(C) or *E. coli* 11775 (D). Each assay was performed as three separate trials, and the presented data is shown as the average change in OD_{600}. 58

Figure 17. Proposed clinical application. 60

Figure 18. Structure of *S. aureus* teichoic acid (modified from Sewell and Brown).(*126*) R=H, D-ala, N-acetylglucosamine; n= 40 to 60 repeats. 63

Figure 19. Diagram of a simplified LSCM. 67

Figure 20. A Jablonski diagram showing the different energy levels that are encountered in fluorescence. 68

Figure 21. Optical sections of BPEI binding to MRSA and *B. subtilis*. MRSA, stained with BPEI: Alexa Fluor 488 (A) and DAPI (B), is imaged by LSCM. The merged image (C) shows BPEI binding to the cell surface but not within the cytoplasm. Similarly, *B. subtilis* stained with BPEI: Alexa Fluor 488 (D) and DAPI (E), and the merged image (F), shows a high affinity between BPEI and *B. subtilis*. Scale bars equal 5 µm. 77

Figure 22. Alexa Fluor 488 signal was caused by conjugated BPEI. Images shown are *B. subtilis* cells treated with BPEI:Alexa Fluor 488 (top row), unconjugated Alexa Fluor 488 (middle row), or unconjugated BPEI (bottom row). The left column shows the detected Alexa Fluor 488 signal. The middle column shows the detected Dapi signal. The right column shows the merged images with both signals. Each image shows raw intensity. Scale bars equal 5 µm. 78

Figure 23. Optical sections of BPEI binding to *E. coli* 11775. *E. coli* stained with BPEI-Alexa Fluor 488 (A) and DAPI (B), is imaged by LSCM and the absolute fluorescence intensity is shown. The merged image (C) shows non-specific localization of BPEI.

BPEI is not seen when normalized to the fluorescence intensity of BPEI on *B. subtilis* (D-F). Scale bars equal 5 µm. 79

Figure 24. The cationic amine groups of BPEI electrostatically bind to the anionic phosphate groups of WTA. 80

Figure 25. ^{31}P NMR spectra of WTA before (A) and after the addition of low-M_W BPEI (B) show significant changes in phosphate chemical shift caused by changes in the chemical environment. 82

Figure 26. Spectral changes are also manifested in the heteronuclear multiple-bond correlation (HMBC) spectra when comparing pure WTA (A) and WTA with BPEI (B). The P-31 signals near 4 ppm are correlated with the proton signals of NAG sugar groups. However, clear identification of specific interactions is prevented by the heterogeneous nature of WTA functional groups, BPEI branching, and WTA:BPEI binding interactions. 83

Figure 27. Mechanism by which BPEI makes MRSA susceptible to oxacillin is through WTA. BPEI and oxacillin have synergy against MRSA MW2 (A). Synergy is lost against MRSA MW2 Δ*tarO* (B) and MRSA MW2 with sub-lethal tunicamycin (0.250 µg/mL; C). Tunicamycin potentiates oxacillin against MRSA MW2 (D). Each assay was performed as three separate trials, and the presented data is shown as the average change in OD_{600}. 87

Figure 28. WTA is required for synergy between ampicillin and 600-Da BPEI. BPEI and ampicillin are synergistic (FIC=0.188) on the wild-type MRSA MW2 (A). MRSA cells lacking WTA through deletion of *tarO* (B) do not have synergy (FIC=0.5). Each

assay was performed as three separate trials, and the presented data is shown as the average change in OD_{600}. 88
Figure 29. LSCM of MRSA Col PBP4:YFP shows that PBP4 primarily localizes at the division septum of dividing cells (A, B). BPEI delocalizes the PBP4 from the division septum (C, D). Quantitative analysis of the fluorescence intensity at the division septum (S) versus fluorescence intensity at non-septum regions (L) was performed for untreated and BPEI-treated samples. Analysis was done for 100 cells of each sample that shows a visible closed septum. The PBP4 for untreated cells (S/L= 0.62 ± 0.18) localized heavier at the division than the BPEI-treated samples (S/L= 0.47 ± 0.18). p-values < 0.0001. Scale bars equal 2 μm. 91
Figure 30. LSCM of MRSA PBP2:GFP shows that PBP2 primarily localizes at the division septum of dividing cells. BPEI does not appear to delocalize PBP2. Scale bars equal 2 μm. 92
Figure 31. Our proposed mechanism of action is that BPEI electrostatically binds to WTA, which creates steric hindrance and prevents proper localization of PBP2a. Therefore, BPEI disables PBP2a through delocalization, and β-lactam antibiotics disable the other PBPs, which results in cells that are unable to crosslink the cell wall.94
Figure 32. Simplified diagrams of an SEM (left) and TEM (right). 99
Figure 33. Changes in morphology of *B. subtilis* due to exposure to BPEI during growth, observed using phase contrast microscopy. Cells not grown in BPEI (A-C) have a short, rod-shaped morphology. Cells grown in 128 μg/mL BPEI (D-F) have an elongated, curling morphology. Images on the left (A, D) were grown to an OD_{600} of

~0.2. Middle images (B, E) were grown to an OD_{600} of ~0.5. Images on the right (C, F) were grown to an OD_{600} of ~1.0. Scale bars equal 3 μm. 104
Figure 34. SEM images show the curling morphology of *B. subtilis* 6051 cells grown in BPEI. Cells were grown in the absence of BPEI (left) and in the presence of 150 μg/mL BPEI (right). The images were taken in early exponential phase of cell growth. Growth in the presence of BPEI shows a curling and twisting morphology that lacks septa formation. Scale bars equal 5 μm. 105
Figure 35. BPEI prevents Triton X-100 induced autolysis in MRSA 700787 in a concentration dependent manner. As the concentration of BPEI increased, the rate of autolysis decreased. Data points are presented as the average of three trials and error bars denote the standard deviation. 107
Figure 36. A WTA-deficient mutant, MRSA MW2 Δ*tarO* has altered cell division compared to the wild-type cell. Normal, wild-type MRSA MW2 is cocci shaped with a single division septum across the center (A). MRSA MW2 Δ*tarO* has multiple division septa found on one cell, and the septa are thicker (B). Scale bars equal 200 nm..... 109
Figure 37. BPEI caused a significant increase in MRSA 700787 cell size. The average cell size (largest diameter) for untreated cells is 0.86 ± 0.11 μm (A) but increases to 0.98 ± 0.14 μm when grown in 64 μg/mL BPEI (B). Normal cleavage furrows are shown with black arrows. Enlarged cells that do not have cleavage furrows present are shown with white arrows. Cells were fixed and imaged at late-lag phase. Scale bars equal 1 μm. A size analysis graph (C) shows the average cell size (center line), the standard deviation (outside of box), and minimum and maximum values (error bars) of 100 measured cells. (p-value <0.001)..... 110

Figure 38. MRSA 700787 cells have abnormal cell division when grown in BPEI. Untreated cells (A) show normal cell division septa versus treated cells (B). Black arrows indicate complete septa formation. White arrows indicate incomplete septa formation. Scale bars equal 200 nm. 112

Figure 39. SEM of MRSA USA300 shows multiple septa formations when treated with BPEI. Untreated cells (A) have a single septal formation (black arrows). Some BPEI-treated cells (B) have multiple septa formations (white arrows). Scale bars equal 1 μm. 113

Figure 40. TEM images of MRSA USA300 cells do not show drastic changes in division septa. Cells treated with BPEI (B and D) have thicker division septa in comparison to the untreated cells (A and C). Black arrows indicate complete septa formation. White arrows indicate incomplete septa formation. Scale bars equal 500 nm. 114

Figure 41. BPEI causes MRSA MW2 to show signs indicative of cell stress. TEM images of untreated (A) and BPEI-treated (B) show the difference in cell wall composition and septum formation. Scale bars equal 200 nm. SEM images of untreated (C) versus treated (D) show drastic alterations to the cell morphology. Scale bars equal 1 μm. 116

Abstract

Methicillin-resistant *Staphylococcus aureus* (MRSA) is a growing concern in the medical industry due to high morbidity and difficulty of treatment in infected patients. Conventional β-lactam antibiotics kill *Staphylococcus aureus* bacteria by inhibiting the function of cell-wall penicillin binding proteins (PBPs). However, β-lactams are ineffective against MRSA due to an extra PBP (PBP2a) that has a low binding affinity for β-lactam antibiotics. Branched polyethylenimine (BPEI), a non-toxic, cationic polymer, restores MRSA's susceptibility to β-lactam antibiotics including oxacillin, ampicillin, imipenem, ceftizoxime, and piperacillin. Checkerboard assays with MRSA demonstrated synergy between BPEI and β-lactam antibiotics. BPEI and oxacillin were effective against MRSA USA300, MRSA MW2, MRSA 700787, and clinical isolates of MRSA. A time-killing curve showed BPEI in combination with oxacillin to be bactericidal. BPEI did not potentiate vancomycin, chloramphenicol, or linezolid against MRSA. Additionally, the BPEI:β-lactam efficacy was specific to MRSA and was not observed against methicillin-susceptible *Staphylococcus aureus* (MSSA), Gram-negative *Escherichia coli*, or *Bacillus subtilis*.

When exposed to BPEI, MRSA cells increased in size and had difficulty forming septa. Nuclear magnetic resonance (NMR) data show that BPEI alters the teichoic acid chemical environment, an anionic polymer found in the cell wall of Gram-positive bacteria. Laser scanning confocal microscopy (LSCM) images depict BPEI residing on the MRSA cell wall, where teichoic acids and PBPs are located. BPEI electrostatically binds to wall teichoic acid (WTA), a polymer that is important for localization of certain cell wall proteins. BPEI does not potentiate ampicillin or

oxacillin when WTA is removed from the cell by genetic mutation or chemical inhibition of WTA synthesis. Using LSCM, we found that BPEI also prevents proper localization of PBP4, another PBP that aids in β-lactam resistance. Since PBP4 and PBP2a require WTA to properly localize in MRSA, *in situ* disabling of WTA using BPEI inhibits proper orientation and functioning of the enzymes. PBP2a requires teichoic acid to properly locate and orient the enzyme, and thus MRSA is susceptible to antibiotics that prevent teichoic acid synthesis in the bacterial cytoplasm. These data suggest that BPEI may prevent proper localization of cell wall machinery by binding to WTA and leading to cell death when administered in combination with β-lactam antibiotics. By creating steric hindrance through WTA binding, BPEI in combination with β-lactam antibiotics could be used as a viable treatment option for MRSA infections.

Chapter 1: Methicillin-resistant *Staphylococcus aureus*

Methicillin-resistant *Staphylococcus aureus* (MRSA) is a dangerous pathogen that causes Staph infections in humans that are difficult to treat. Conventional antibiotics, such as ampicillin, are unable to effectively treat MRSA. Consequently, amputation of the infected areas and drugs of last resort, vancomycin for instance, are leading treatment options. However, MRSA can also spread in the bloodstream, infect the heart and other internal organs, and cause sepsis. One in seven patients infected with MRSA die from their infection.(*1*) The Centers for Disease Control designate MRSA as a "serious threat."(*2*) Thus, a strong need exists to design and create new drugs that can effectively kill MRSA in the early stages of infection. My research involves branched polyethylenimine (BPEI), a non-toxic polymer that we found restores MRSA's susceptibility to conventional antibiotics, such as oxacillin and ampicillin. BPEI in combination with ampicillin and other antibiotics effectively prevents growth of MRSA. Additional research I have conducted includes determining BPEI's mechanism of action and understanding how BPEI removes MRSA's resistance factor. This research has been published in the Journal of Antibiotics and ACS Medicinal Chemistry Letters.(*3*, *4*) It is our hope, that in the future, BPEI will be used as a first-line treatment for MRSA infections.

Antibiotic Resistance

Antibiotic resistance is a growing concern in health communities. For many decades, the development of antibiotics to kill microbe infections saved millions of lives. Since the discovery of antibiotics, bacteria and other microbes have developed

resistance to those life-saving drugs. Antibiotic resistance refers to the ability of microbes, such as bacteria, to mutate in such a way that allows them to survive in the presence of different antibiotics. The Review on Antimicrobial Resistance predicts that by the year 2050, antibiotic-resistant superbugs will cause 10 million deaths annually, surpassing the number of annual deaths caused by cancer.(*5*) Overall, 2,049,442 drug-resistant infections occur each year in the United States alone.(*2*) Of those, 23,488 result in death; about 11,000 of which are caused by MRSA infections.(*2*) Globally, the burden is even worse: 700,000 deaths each year are attributed to antimicrobial-resistant pathogens.(*5*) Of the antibiotic-resistant pathogens, MRSA has the highest death to infection ratio (approximately 1:7).(*2*) Also, antibiotic resistance causes a $55 billion economic burden in the United States each year.(*6*) Since the initial discovery of antibiotics, overuse and improper use of antibiotics, as well as poor patient medication adherence, have sped up the evolution of resistant species.(*7*) Estimates state that 30% to 50% of prescribed antibiotics are ineffective.(*8*) Although certain steps can be taken to slow the development and prevalence of antibiotic-resistant pathogens, the evolution of resistance factors will inevitably outpace the current rate of development of new antibiotics. In order to reduce the current and future burden of antibiotic resistance, more treatment options must be discovered.

Although there is a call to create new antibiotics, only five new classes of antibiotics were approved for human use between 2000 and 2015.(*9*) Of which, the last completely new class of antibiotics was daptomycin, discovered in the 1980s.(*10-12*) Most antibiotics that are used today were discovered in the 1940s to 1960s, also known as the golden era of antibiotic discovery.(*12, 13*) Additionally, only one to three new

antibiotics were FDA-approved most years between 2000 and 2015.(*9*) Between 2000 and 2015, 30 new antibiotics and two new drug combinations were launched.(*9*) Today, pharmaceutical companies tend not to invest in new antibiotic discovery. This is largely because diseases cured in a short few days lead to smaller profit margins in comparison to other diseases that are longer-lasting or chronic.(*14*) Also, doctors tend to prescribe generic antibiotics to patients, which leads companies to focus on intravenously-administered antibiotics because these can be given at a higher cost.(*14*) Other obstacles to antibiotic development stem from difficulty in discovering novel compounds or new drug targets that can escape the already existing resistance mechanisms.(*14*) Additionally, more focus is placed on discovering antibiotics that have broad-spectrum activity since most infections have more than one infecting species.(*14*) Although antibiotics do not require long-term, chronic safety studies, the high dose requirements for efficacy causes a hurdle for getting FDA-approval.(*14*) Therefore, some research has focused on repurposing FDA-approved non-antimicrobial drugs for use against bacterial infections.(*15, 16*) Thus, despite the need for new antimicrobial treatments, little emphasis has been placed on discovery and development.

Pathogenesis and Prevalence of *Staphylococcus aureus*

The British surgeon Alexander Ogston was the first to report infections caused by Staphylococcus bacteria found in abscesses.(*17*) *Staphylococcus aureus,* a Gram-positive pathogen, causes minor to major skin infections as well as life-threatening diseases when it infects the blood stream or internal organs (Figure 1). Minor, localized skin infections include pimples, abscesses (pus build-up), and folliculitis (infection of

hair follicles). Staph skin infections can also be less localized causing impetigo (a contagious infection that typically forms red sores in children) or cellulitis (an infection of the inner skin layers). The majority of clinical isolates of *S. aureus* emanate from pus-filled chambers in the skin or soft tissues that are isolated from the blood system.(*18*) However, minor infections can become severe in immuno-compromised individuals or when spread internally. When *S. aureus* invades a patient's bloodstream, toxic shock syndrome, bacteremia, and sepsis are possible. Toxic shock syndrome occurs when *S. aureus* releases a superantigen toxin that attacks the immune system of healthy patients and often results in death within hours if not treated quickly. Bacteremia, the presence of bacteria in the bloodstream, leads to sepsis, which occurs when the patient's immune system injures the host's tissues while attacking the infection. *S. aureus* is capable of infecting the brain, heart, lungs, and bones, which can lead to meningitis, endocarditis, pneumonia, and osteomyelitis, respectively. *S. aureus* can also cause food poisoning. Despite its potential for serious infections, *S. aureus* normally resides in the anterior nares of 20% of healthy individuals.(*19*) Usually, these persistently colonizing bacteria do not negatively impact their host. However, about 82% of individuals infected with *S. aureus* are infected by their colonizing strain.(*20*) Colonizing strains provide the host with "protective immunity" and antibodies that help prevent toxic shock syndrome; therefore, non-carriers have higher mortality rates than carriers.(*21, 22*)

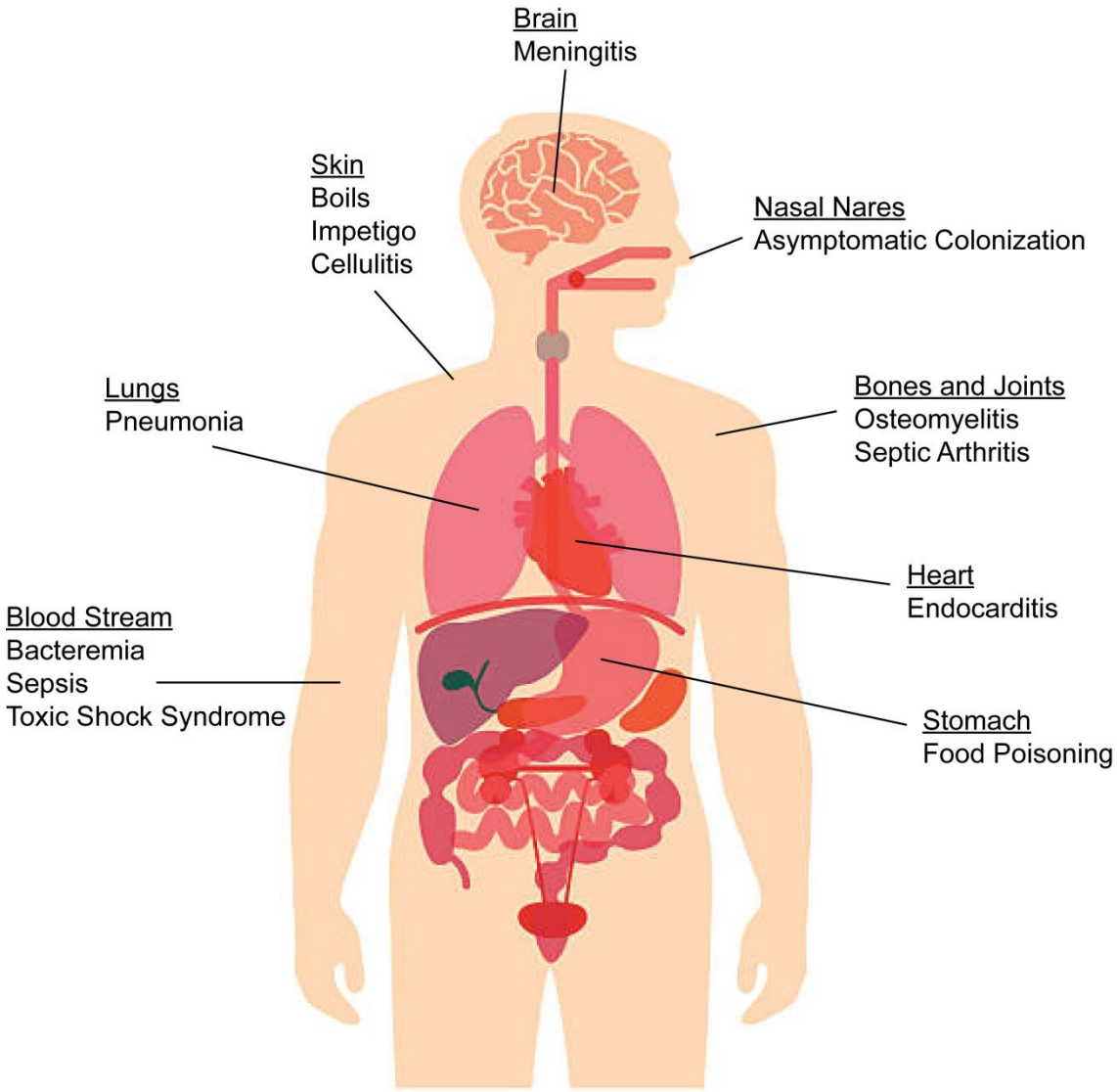


Figure 1. Colonization, infection, and pathogenesis of *S. aureus* bacteria in the human body.

S. aureus have multiple mechanisms to evade antimicrobials and host defenses such as making biofilms, hiding in epithelial cells, forming small-colony variants, and creating microcapsules. Each of these mechanisms allows for the bacteria to remain undetected by hosts, which makes the bacteria remain viable even after the initial infection is cleared.(*23-26*) Biofilms, groups of bacteria that are embedded in

extracellular polymeric substances (EPS), often form on the surfaces of medical devices, such as catheters or implants, and are difficult to treat due to the impenetrable properties of the EPS layer. Small-colony variants are very slow-growing bacteria that can persist in hosts without detection and cause recurrent infections.(*25*) Sometimes, microcapsules form around *S. aureus* cells, preventing the cells from being killed and allowing for adherence to surfaces.(*26*) By some bacteria being capable of evading cell death, *S. aureus* re-infects the patient and causes recurrent infections after the initial treatment.

S. aureus is capable of making a variety of toxins and proteins that can attack and injure host cells and tissues. One common toxin, Staphylococcal α-toxin, causes membrane damage in many different types of host cells, is found in most strains of *S. aureus*, and is considered to be the major cytotoxic agent aiding in virulence.(*27*) β-toxin, γ-toxin, and δ-toxin, are similar to α-toxin but attack more specific targets.(*28*) Also, β-toxin does not seem to be active at normal body temperatures; thus, it is not the primarily used toxin by *S. aureus*.(*28, 29*) The α-, β-, γ-, and δ-toxins all work by causing membrane damage and creating pores in host cells. Many of *S. aureus*'s toxins focus on harming host defense cells in order to evade elimination by the immune system.(*28*) Specifically, *S. aureus* attacks host immune systems through leukocidins, which create pores in leukocytes and neutrophils (important immune cells that work to kill pathogens) and can induce apoptosis and necrosis.(*30*) Additionally, *S. aureus* has numerous virulence factors that get released in the infected individual and allow for protection, spreading, and quorum-sensing.(*19*) Also, *S. aureus* secretes coagulase enzymes that clot plasma,(*31*) deoxyribonucleases that destroy host DNA,(*32*) and

staphylokinases that aid in digesting fibrin to allow spreading of the bacteria.(*33*) MRSA has the same virulence factors as methicillin-susceptible *S. aureus* (MSSA) with the addition of a few others. For example, Panton-Valentine leucocidin (PVL), a pore-forming toxin, is found in only 5% of *S. aureus* strains but is frequently found in MRSA.(*34, 35*) MRSA has pathogenicity similar to that of MSSA but cannot be treated with conventional β-lactam antibiotics that target the bacterial cell wall.

Bacteria Cell Walls

Bacteria are single-cellular organisms that are distinct from mammalian cells due to the presence of a complex cell wall that creates structural stability. These essential cell walls protect the bacteria and maintain the cell's morphology. The two main types of bacteria, Gram-positive and Gram-negative bacteria, differ in the structure of their cell walls (Figure 2). Gram-negative bacteria (such as *Escherichia coli*, *Pseudomonas aeruginosa*, and *Klebsiella pneumonia*) have a cytoplasmic membrane similar to Gram-positive bacteria covered by a thin peptidoglycan layer. Gram-negative bacteria also have an outer membrane that further protects the bacteria. The cytoplasmic membrane in bacteria is a phospholipid bilayer that acts as a barrier surrounding the entire cell. Eukaryotic cells also have a phospholipid bilayer. Peptidoglycan, which is unique to bacteria, strengthens the bacteria by creating a mesh of repeating N-acetylglucosamine (NAG) and N-acetylmuramic acid (NAM) sugars that are crosslinked with amine chains. The periplasmic space, found between the lipid membrane and the peptidoglycan, contains a gel-like storage matrix consisting of a high concentration of proteins that makes up 20% to 40% of the cell's volume.(*36*) The outer

membrane of Gram-negative bacteria is composed of phospholipids and lipopolysaccharides that prevent many larger molecules from entering the cell and periplasm. The outer membrane also imparts a negative charge on the outside of the cells. Gram-positive bacteria, such as *S. aureus* and *B. subtilis*, have a cytoplasmic membrane that is covered by a thick layer of peptidoglycan. Unlike Gram-negative bacteria, Gram-positive bacteria do not have an outer membrane. Teichoic acids, anionic polymers that attach to either the lipid membrane or the cell wall and extend to the extracellular space, are present in Gram-positive bacteria cell walls. The teichoic acids impart a negative charge to the bacterial cell wall. The bacteria cell wall is an extremely important target for antibiotics because of its uniqueness compared to mammalian cells which reduces the amount of side effects and complications to the patient.

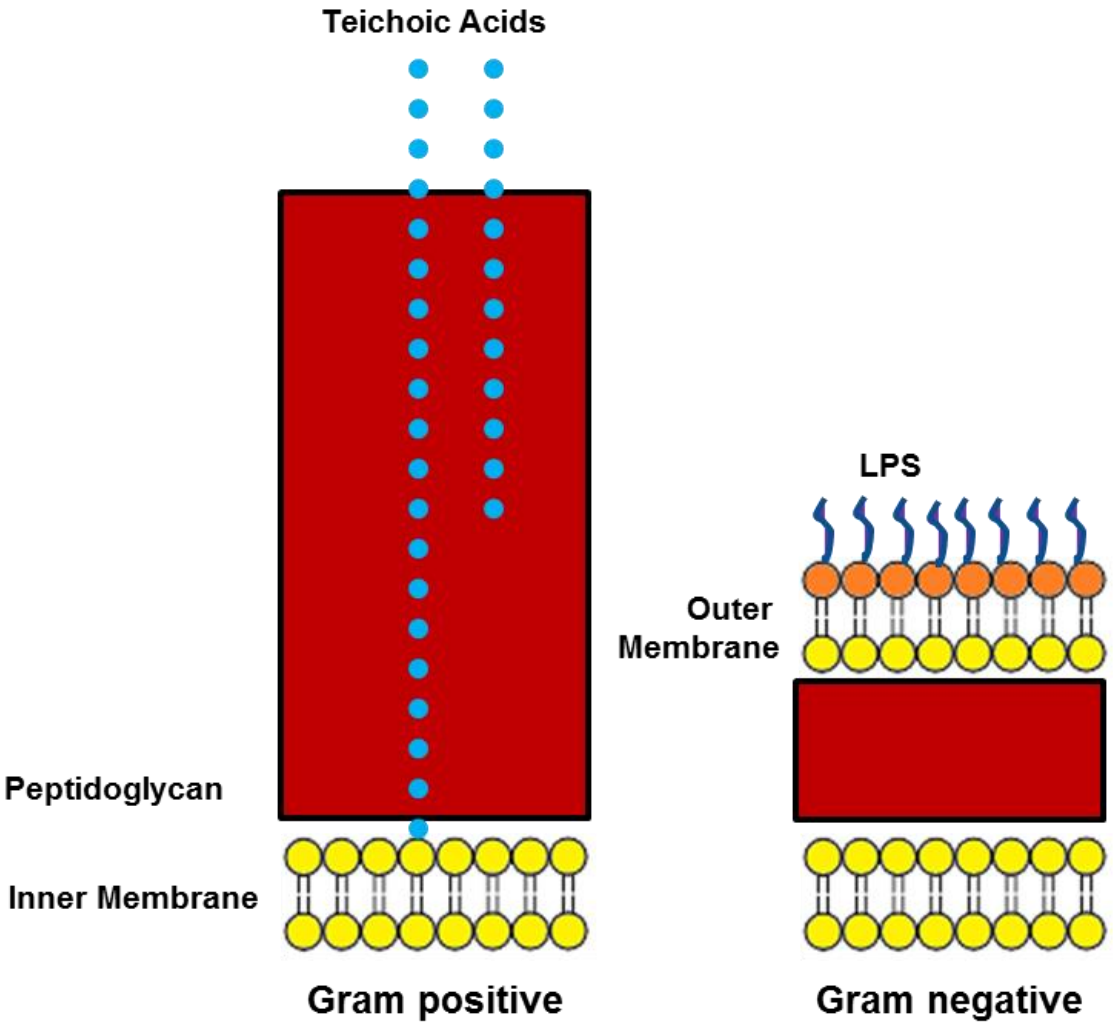


Figure 2. Structure of Gram-positive and Gram-negative bacteria are distinct from one another. Gram-positive cell walls have a much thicker peptidoglycan layer and the presence of teichoic acids. Gram-negative cell walls have an outer membrane that acts as a barrier.

β-Lactam Antibiotics

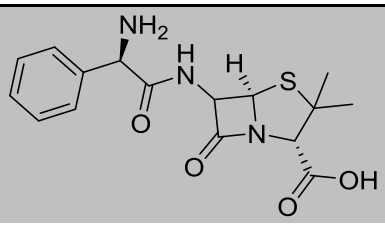
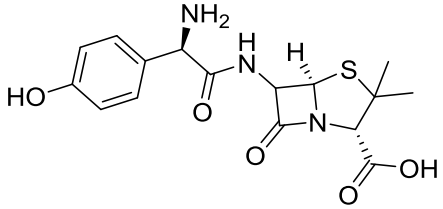
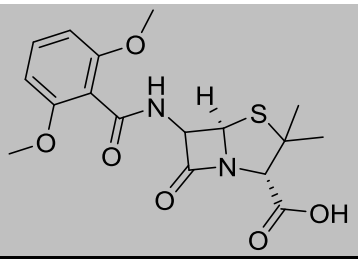
Penicillin, discovered in 1928 accidently by Alexander Fleming, was the first antibiotic used to treat Staph infections. Fleming noticed blue-green mold growing on his culture of *S. aureus*, causing a halo of inhibited bacteria growth around it.(*37*) The mold, later isolated and characterized as *Penicillium chrysogenum*, released penicillin into the agar, killing the bacteria. However, issues with the mass production of

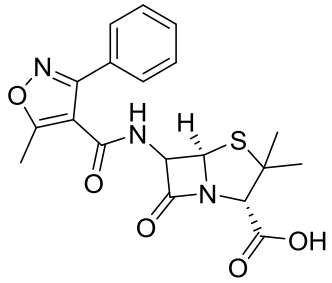
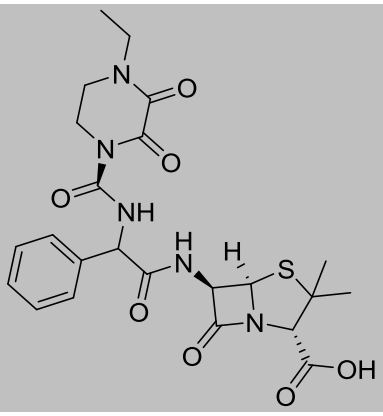
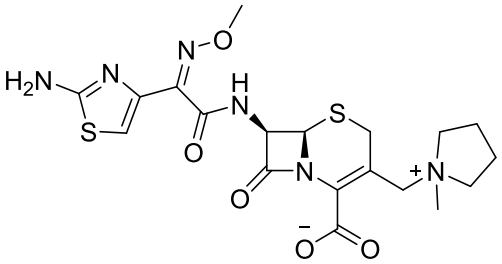
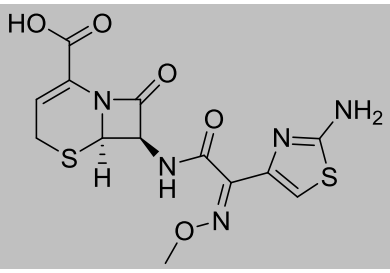
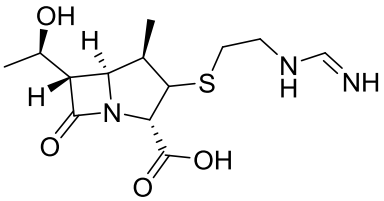
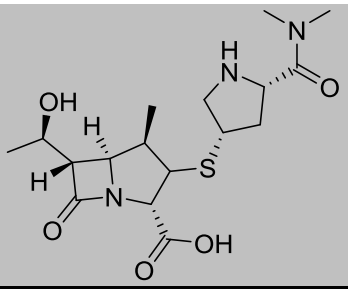
penicillin prevented it from becoming available to the general public until 1945. Prior to the discovery of penicillin, the rate of *S. aureus*-induced bacteremia was greater than 80% in infected individuals.(*38*) Today, β-lactams are still one of the most commonly-prescribed classes of antibiotics. In fact, approximately 118 million courses of β-lactam antibiotics were prescribed to treat bacterial infections in 2011.(*39*) β-lactam antibiotics are favored because of their broad-spectrum activity, specificity for bacteria, and low toxicity to humans.

Penicillin contains a β-lactam ring, the core component of the β-lactam antibiotic group. β-lactam antibiotics function by inhibiting bacteria cell wall crosslinking, which is necessary to make the bacterial cell wall strong and robust. Penicillin-binding proteins (PBPs) are the proteins responsible for cross-linking the cell wall. The β-lactam antibiotics mimic D-alanyl-D-alanine from the precursors of NAG and NAM subunits of peptidoglycan. The antibiotic then irreversibly binds to the active site of a PBP to inactivate the enzyme. Most species of bacteria have multiple PBPs that carry out transpeptidase activity (the crosslinking of peptides), transglycosylate activity (the synthesis of glycan strands), and carboxypeptidase activity (the cleaving of the peptide bonds that allows construction of the cell wall). All strains of *S. aureus* carry PBP1, PBP2, and PBP3. PBP1 and PBP3 are responsible for transpeptidation. PBP2 is responsible for the transglycosylase and transpeptidase activity. PBP4, important for resistance in some MRSA strains, has carboxypeptidase and transpepsidase activity. β-lactam antibiotics cause cell death via cell wall degradation, lysis, and cytoplasm leakage.(*40*)

Since the discovery of penicillin, numerous synthetic and natural derivatives of penicillin have been discovered. β-lactam antibiotics are classified into subclasses based on their core β-lactam ring structure (Table 1). Penams are rings similar to that found in penicillin. Carbapenems are used to treat multidrug-resistant bacteria. Some commonly prescribed β-lactam antibiotics are ampicillin, amoxicillin, oxacillin, piperacillin, cefepime, ceftaroline, imipenem, and meropenem. Certain β-lactams bind to some PBPs stronger than others. For example, antibiotics with high affinity binding to PBP2 are ampicillin, cefaclor, cefotaxime, ceftizoxime, cefuroxime, cephalothin, cloxacillin, nafcillin, oxacillin, penicillin G, and piperacillin.(*41-43*)

Table 1. Structure and classification of commonly used β-lactam antibiotics.

Antibiotic	**Subclass**	**Structure**
Ampicillin	Penam	
Amoxicillin	Penam	
Methicillin	Penam	

Oxacillin	Penam	
Piperacillin	Penam	
Cefepime	Cephem	
Ceftaroline	Cephem	
Imipenem	Carbapenem	
Meropenem	Carbapenem	

Resistance Mechanisms

Resistance to penicillin developed a few years after commercialization.(*44*) The first source of penicillin resistance was *blaZ*, which codes for a β-lactamase, a protein transcribed by the bacteria to degrade β-lactams.(*44*) β-lactamase enzymes are secreted by the bacteria to hydrolyze the β-lactam ring and thereby deactivate the antibiotic. β-lactamase inhibitors, such as clavulanic acid, sulbactam, and tazobactam, were designed to inhibit the β-lactamase and prevent deactivation of the β-lactam antibiotic. Typically, β-lactam antibiotics are prescribed in combination with β-lactamase inhibitors. Additionally, some newer β-lactam antibiotics have been designed to be less susceptible to cleavage by β-lactamases. Today, about 90% of *S. aureus* strains are resistant to the original penicillin.(*40*)

Methicillin was introduced in 1959 to treat penicillin-resistant infections, but resistance to methicillin developed two years later.(*45*) Resistance to methicillin was not due to *blaZ* but caused by intrinsic resistance and alteration in PBPs.(*46*) All *S. aureus* strains have at least three PBPs that cross-link the cell wall. However, MRSA has an extra PBP, known as PBP2a, which has a low binding affinity for β-lactam antibiotics and thus allows for crosslinking in the presence of methicillin and other β-lactam antibiotics. PBP2a is coded for by the *mecA* gene located on the Staphylococcal Chromosome Cassette mec (SCCmec). Specifically, PBP2a performs the transpeptidase activity of PBP2 in the presence of β-lactam antibiotics.(*42*) PBP4, which is not present in all *S. aureus* strains and not coded for by *mecA*, may also aid in β-lactam resistance due to its low affinity for β-lactam antibiotics.(*47*) Clinicians typically test for the presence of *mecA* to determine if the infecting microbe has methicillin-resistance. It is

unknown how *S. aureus* strains first obtained SCCmec, but the two active theories are that it was by bacteriophage-mediated transduction or through conjugation.(*48*) There are five different types of SCCmec, which vary in size and genetic composition. Genetic differences between the different SCCmec types do not play a role in resistance but are important for understanding the evolution of MRSA strains.(*49*) Methicillin is no longer used clinically because methicillin resistance is so widespread.

Hospital-acquired MRSA (HA-MRSA) was first found in hospital settings; however, community–acquired MRSA (CA-MRSA) became prevalent later. The classification of CA-MRSA versus HA-MRSA depends on the patient history; however, each type has distinct genotypic differences. CA-MRSA causes infections in healthy individuals who had not received hospital care prior to the onset of infection. HA-MRSA generally infects individuals during hospitalization, typically within a 48-hour window.(*18*) HA-MRSA caused the majority of infections before the 1990s, whereas CA-MRSA became widespread in the late 1990s.(*50*) Community-acquired strains are considered to be more virulent than hospital-acquired strains.(*51*) The two most prevalent strains of MRSA, MRSA USA300 and MRSA MW2, are both community-acquired. PVL, a pore-forming toxin, is not usually found in MSSA or HA-MRSA, but most CA-MRSA strains have the protein.(*52*) HA-MRSA tends to be more resistant to non-β-lactam antibiotics than CA-MRSA.(*18*) Thus, hospital- versus community-acquisition provides a means of differentiating MRSA strains.

Drugs of Last Resort

Typically, β-lactam antibiotics are prescribed to initially treat Staph infections. However, if an infection does not clear up with β-lactams, a drug of last resort must be given. Although estimates in different countries vary, the World Health Organization estimates that approximately 44% of *S. aureus* infections are caused by MRSA.(*12*) First sold in 1954, vancomycin is the most commonly prescribed antibiotic to treat MRSA.(*53, 54*) Vancomycin, a glycopeptide, prevents cell wall crosslinking by binding to the D-ala D-ala moieties instead of binding to PBPs like β-lactams. Hearing loss, allergic reactions, and kidney damage has occurred with vancomycin usage.(*55*) In a hospital setting, vancomycin is considered to be the first-line therapeutic to treat MRSA. However, vancomycin cannot pass through the stomach lining, so it must be given intravenously to treat systemic infections. Additionally, vancomycin-resistant MRSA (VRSA) strains have been found due to the presence of the *vanA* gene, but VRSA is still rare.(*56, 57*)

Linezolid and daptomycin are other drugs of last resort used to treat MRSA infections. Linezolid, approved for commercial use in 2000, inhibits protein synthesis to prevent bacterial reproduction. Linezolid has oral bioavailability, is safe for short-term use, and can be inexpensive to manufacture. Although linezolid can be prescribed as an oral antibiotic, it is typically given intravenously to better control dosage and reduce medication administration errors. Daptomycin, approved by the FDA in 2003, inserts into bacterial cell membranes causing leakage of intracellular contents and cell death. Daptomycin is considered to be the second-line therapy for MRSA, while linezolid is the third-line therapy. Linezolid and daptomycin are referred to as “reserve antibiotics,”

meaning that they are only used in incidents where vancomycin or β-lactams cannot be used, allowing them to remain effective and prevent onset of resistance.(*58*) MRSA resistance to linezolid and daptomycin is rare but has been discovered.(*59, 60*)

Ceftaroline (FDA-approved in 2010) and telavancin (FDA-approved in 2009) have recently been approved for patient use in severe cases but must be administered intravenously.(*54*) Ceftaroline, also called Teflaro, is a β-lactam that has efficacy against MRSA. Ceftaroline is a prodrug, meaning it is prescribed in its inactive form and gets metabolized to the active form in the body. Although ceftaroline is a β-lactam antibiotic, the anti-MRSA property of the drug comes from its thiazole group rather than the β-lactam ring.(*61*) Telavancin, a synthetic derivative of vancomycin, works similarly to vancomycin in that it also disrupts bacterial membranes.(*62*) Since both of these antibiotics have been approved for human use within the last ten years, they are only used in rare instances where other antibiotics cannot be used or are not effective.

Other last-resort therapies to treat MRSA are tigecycline and quinupristin/dalfopristin. Tigecycline can be used to treat certain Gram-positive and Gram-negative bacteria by inhibiting protein synthesis.(*63*) Quinupristin/dalfopristin can be used to treat staph infections and vancomycin-resistant Enterococci infections. Quinupristin and dalfopristin work synergistically to inhibit protein synthesis.(*64*) Oral antibiotics are not often given to treat MRSA but some have been shown to be effective. Trimethoprim/sulfamethoxazole, a broad-spectrum antibiotic, synergistically inhibits folate synthesis, an important process for a variety of cellular components in the bacteria.(*65*) Trimethoprim/sulfamethoxazole is effective against approximately 80% of

MRSA infections.(*66*) These therapies are used rarely to treat MRSA infections and must be given intravenously.

Despite the number of FDA-approved drugs to treat MRSA infections, bacteria are very successful at mutating to create new resistance mechanisms. Resistance to vancomycin, coded for by the *vanA* gene, was discovered in 2002.(*56, 57*) MRSA infections that are resistant to daptomycin and linezolid have also been discovered but are currently rare.(*59, 60*) Today, there is no record of infections that are resistant to more than one drug of last resort. Although prudence when prescribing antibiotics has slowed down the evolution of antibiotic resistance, it is impossible to fully prevent antibiotic resistance from eventually occurring.

Chapter 2: 600-Da BPEI is a Non-Toxic Cationic Polymer

Background

Our lab started working with branched polyethylenimine (BPEI), an inexpensive, cationic polymer, as a tool to prevent metal-binding in bacteria. Metals, such as calcium and magnesium, are necessary for a variety of functions in bacteria. Magnesium, for example, coordinates to negative charges on nucleotide phosphate groups, regulates DNA replication and transcription, and neutralizes cell membranes.(*67*) Calcium has been suggested to be important for bacteria motility, virulence, cell adhesion, pH homeostasis, quorum sensing, and spore formation.(*68, 69*) Although metal cations are important for a variety of functions, their transportation into the cytoplasm of the bacteria was not well understood. Porins transport the metals through the cell membrane, but our lab wanted to understand how these metals go through the cell wall of bacteria and what phenotypically happens to the bacteria when metal binding is blocked.(*70*) *Bacillus subtilis* 1A578 was used because it is a non-pathogenic bacterium that is resistant to the antibiotic chloramphenicol, which allows for leniency in sterile techniques. Thomas found that BPEI caused the bacteria to form long, curling, filamentous bacteria instead of the normal, short, rod-shaped bacteria. Additionally, he found that the bacteria was unable to grow in chloramphenicol when simultaneously treated with BPEI.(*70*) This discovery laid the groundwork for subsequent research.

Structure of BPEI

Polyethylenimines (PEI) are polymers with repeating amine groups separated by ethyl groups. Linear PEI (LPEI) contains only secondary amines that make the polymer a long chain. Branched PEI (BPEI) contains primary, secondary, and tertiary amine groups that make it is a very flexible polymer (Figure 3). The primary amines of BPEI are protonated at neutral pH, which contributes to the highly cationic nature of the polymer. Due to the presence of primary amines, BPEI has a higher charge density than LPEI. Because of the presence of a large number of primary amines and a high charge density, we investigated BPEI more thoroughly than LPEI.

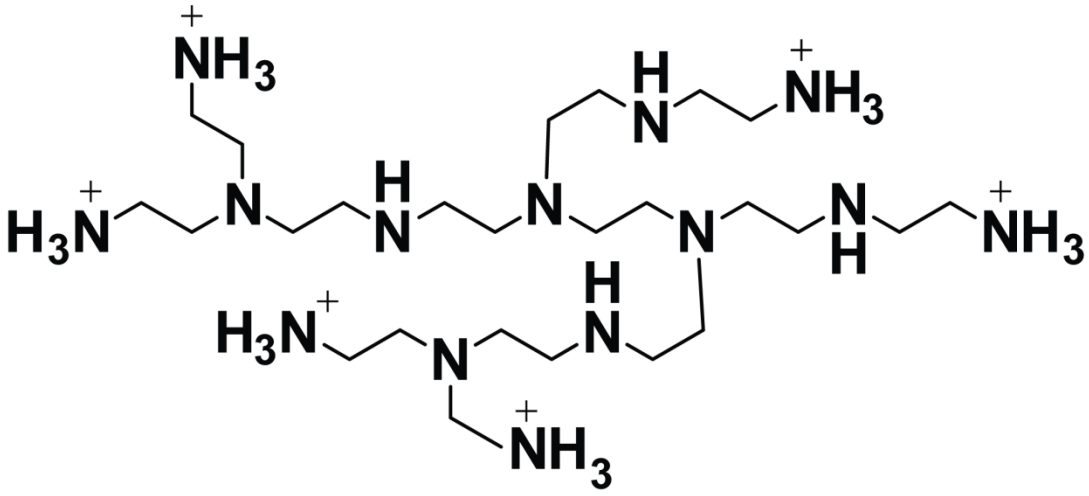


Figure 3. An example of one molecule of 600-Da BPEI is shown.

PEIs come in a range of sizes as small as 500-Da up to 1,000,000-Da and higher. BPEIs with molecular weights lower than 10-kDa have ratios of primary: secondary: primary amines of approximately one: two: one. BPEIs with molecular weights higher than 25,000-Da have ratios of amines that are closer to one another.(*71*) The repeating units of the polymers cause a distribution of sizes around an average MW.

Commercially-available low-MW BPEIs have larger size dispersity than the higher MW BPEIs.(*72*)

Uses for BPEI

PEIs are used for a variety of industrial, environmental, and research purposes. PEI was used in the 1950s to improve paper's wet strength to increase the paper's ability to retain strength when saturated with water.(*73*) Additionally, PEIs have been used as a water treatment option because they are able to coagulate and flocculate a variety of contaminants.(*74*) PEIs have also been used in research laboratories for a variety of reasons. For instance, PEIs are used to flocculate contaminants to aid in purification of proteins.(*75-77*) Cell tissue culture can utilize PEI because the cationic charge attracts the overall negative charge of eukaryotic cells, causing them to attach to the plating surface.(*78*) BPEI, a commonly-used and heavily-researched polymer, can also be synthesized easily and inexpensively.

PEIs have been heavily researched as transfection agents for gene therapy. The positive charges of the PEI electrostatically interact with the negatively-charged phosphate groups of DNA, which condenses the DNA and allows for insertion into cells.(*79, 80*) PEIs are one of the most effective systems for gene transfer in mammalian cells. Higher-MW PEIs are more cytotoxic but also more efficient at transfecting.(*81*) For gene therapy, LPEI is typically a better transfecting agent than BPEI.(*82, 83*) Also, higher-MW LPEIs are more effective than lower-MW LPEIs.(*79, 81*) BPEI less than 2,000-Da was unable to transfect eukaryotic cells.(*84*) Higher-MW PEIs are able to compact the DNA tighter and have a higher PEI:DNA complex surface charge, which

allows for easier insertion into eukaryotic cells.(*79*) The success with PEIs for gene therapy proves promising for other biological purposes.

Cationic polymers have antimicrobial properties, because they are able to interact with the negatively-charged cell wall of bacteria. The proposed mechanism by which they work is thought to be that they destabilize the cell wall and permeabilize the cytoplasmic and outer membranes.(*72, 85*) Many of these cationic polymers are used as biocides. However, to date, no cationic polymers have been approved for solution-based clinical treatment of microbial infections. Cationic polymers derived from polystyrene and poly(vinylpyridine) are the most commonly-researched polymers for antimicrobial activity.(*85*) Although BPEI has the highest charge density of the cationic polymers with antimicrobial activities, it has insufficient antimicrobial activity for clinical practices.(*85*) Modifications of BPEI have been made to increase the antimicrobial efficacy, typically by increasing the hydrophobic group to cationic moiety ratio.(*86, 87*) Thus, utilizing BPEI for antimicrobial development may be possible with structural or formulation changes.

Drug Design

Historically, many drug candidates have failed due to similar structural and chemical properties. Consequently, chemicals were determined to be "drug-like" if they fit a set of parameters denoted as the rule of five (RO5) concept.(*88*) The RO5 determines the likelihood of a compound to be orally bioavailable and to have favorable pharmacokinetic characteristics. Approximately 90% of drug compounds in Phase II clinical trials or further fit with the RO5.(*89*) The RO5 states that drugs should have a

molecular weight lower than 500 g/mol, no more than 5 H-bond donors or 10 H-bond acceptors, and the computationally calculated Log P should be less than 5.(*88*) Of the RO5 parameters, molecular weight and lipophilicity have proven to be the most important.(*90*) The molecular weights of drugs in Phase I clinical trials are proportionally larger than the molecular weights of established drugs. The average molecular weight of drugs in clinical trials decreases as the trials progress. This is partially due to larger molecules having a higher probability of containing toxic moieties.(*90*) Lipophilic drugs are unlikely to advance far in clinical trials because they get metabolized faster, have low solubility, and have poor absorption.(*90*) Discovery and development of new antibiotics takes a minimum of 10 years to reach clinical trials. Thus, understanding a compound's ability and probability of becoming a lead drug is important.

However, the RO5 does not pertain well to antibiotic discovery, but for largely unknown reasons.(*91*) Specifically, sulfa drugs are the only antibiotics that fall into the RO5.(*91*) Of the FDA-approved drugs, up to 95% of drugs are ionizable, and 67.5% are ionizable between pHs of 2 and 12 (75% weak bases, and 20% weak acids).(*92, 93*) The majority of basic drugs have pKas between 6.5 and 10.5.(*93*) Antibacterials (Gram-positive and Gram-negative) are more hydrophilic and more polar compared to non-antibiotic medicine.(*91*) The average molecular weight for Gram-positive targeting antibiotics is 813 g/mol, which is higher than the 600 g/mol cutoff of Gram-negative targeting antibiotics (average of 414 g/mol).(*91*) Natural product derivatives make up the majority of current antibiotics. However, natural product discovery has not been a focus of pharmaceutical companies recently because of the labor and funding required

to characterize and purify compounds , as well as the tendency to identify known compounds.(*94*)

Combination treatments are commonly used by clinicians to treat bacterial infections and are necessary to treat difficult infections. Combination therapies reduce the onset of resistance because bacteria have a harder time evolving when multiple targets are being inhibited.(*13*) Augmentin is one of the most prescribed drug combinations, consisting of the β-lactam amoxicillin and the β-lactamase inhibitor clavulanic acid. Previously, combination treatments were composed of existing antibiotics, but recent work has focused on designing new combinations with non-established drugs.

Purpose of Experiment

The purpose of the experiment was to determine the drug-like capabilities of BPEIs of varying molecular weights. Cytotoxicity assays were performed on immortal human cells (Hela, HCT-166, and Hek-293) and on a primary kidney cell line (PCS-400-010). Cytotoxicity assays showed that 600-Da BPEI was the least cytotoxic of the tested molecular weights. As molecular weight increased, toxicity increased. For this reason, 600-Da BPEI was determined to be the lead potentiator for future studies.

Experimental Procedures

Preparation of Cationic Polymers

BPEI (600, 1200, 1800, and 10,000-Da) was purchased from Sigma-Aldrich. BPEI was easily dissolved in water. Due to BPEI's stability, it can be stored in water for over one month without degradation.

pH Titration of BPEIs

BPEIs were diluted with distilled water to 6 g/L concentration (0.01 M for 600-Da BPEI). 50 mL of BPEI was titrated with 1.0 M HCl dropwise. The pH (measured on an Orion 3 Star pH meter) was recorded throughout. The titration curve was graphed. Data analysis was followed using the procedure outlined by Gibney et al.(*72*) In order to determine the pKas, the maximum buffer capacity for each pH range was determined. Buffer capacity is defined as the change in the amount of HCl added divided by the change in pH. Each titration was done twice and the data is presented as the average.

Maintenance of Eukaryotic Cell Lines

Cell lines were purchased from ATCC and maintained by following company protocols. Hela (cervical cancer), HCT-116 (colon cancer), and HEK-293 (kidney cancer) cells were incubated at 37 °C, 5% CO_2. Growth media was changed every three days. Cells were sub-cultivated when cell density reached 80% coverage to prevent the cell density from becoming too high. Sterile technique was used throughout.

CellTiter Viability Assay

A CellTiter-Blue (Promega) assay was performed as described by Burgett et al.(*95*) Briefly, cells were plated in 96-well culture plates and grown at 37 °C for 20-24 hours. Compounds (dissolved in water) were delivered to the cells and grown for another 48 hours. Cell morphology and viability was qualitatively observed with a cell culture light microscope. CellTiter-Blue was added and allowed to react for one hour. Viable cells convert the resazurin dye in the assay to a fluorescent resorufin end product. Thus, the fluorescence signal detected is proportional to the number of viable cells. The fluorescence (544 nm excitation; 590 nm emission) was measured on a Tecan Infinite M20 plate reader. Growth relative to untreated cells was calculated. The required concentration to inhibit growth of 50% of the cells (IC_{50}) was determined by graphing all concentrations versus relative growth and establishing the concentration where relative growth is 50%. All concentrations were done in triplicate.

Nephrotoxicity Assay

A Pierce Lactate Dehydrogenase (LDH) Cytotoxicity (Thermo) assay was performed with PCS-400-010 cells. Cells were plated (2,500 cells/well) and grown for 24 hours at 37 °C. The cells were treated and grown for another 24 hours. Supernatant (50 µL) was transferred to the reaction mixture (50 µL) for each well and the plates were incubated further at room temperature for 30 minutes. Stop solution (50 µL) was added to each well after 30 minutes. Absorbance was measured at 490 nm and 680 nm. To determine LDH activity, the 680 nm absorbance value was subtracted from the 490 nm value. The percent cytotoxicity was calculated by subtracting the spontaneous LDH

activity from the treatment LDH activity and comparing to the maximum LDH activity. The study was done in triplicate.

Results and Discussion

Characterization of BPEI

Because BPEIs have primary, secondary, and tertiary amines, there should be three different pKas for BPEI. The majority of drugs are weak acids and bases, so understanding pKas is critical to understanding ionic forms throughout the body. The pKa of a drug affects pharmacokinetic characteristics, and establishing pKas are important for FDA regulation compliance.(*93*) The literature reports conflicting pKa values for BPEI. Therefore, the pKas for 600-Da, 1800-Da, and 10-kDa BPEIs were determined using potentiometric titrations with HCl. A titration curve of each BPEI shows a substantial buffering region around 7-9 pH for each polymer (Figure 4A). Another small shelf between 5-6 pH indicates another buffer region. In order to determine the pKa, the buffering capacity at each pH was determined by dividing the change in HCl added by the change in pH and plotting against the pH (Figure 4B). Then the pH of each buffer capacity peak was determined. The pKa1 for each BPEI was around 8.7 and pKa2 was around 5.1 (Table 2). The pKa of Tris base was determined to be 8.3 ± 0.1 which is less than 3% that of the accepted value of 8.1.(*96*) Each pKa determined was about 10% less than those determined by Gibney et al. using a similar method.(*72*) Increasing the molecular weight of BPEI does not drastically change the pKa.

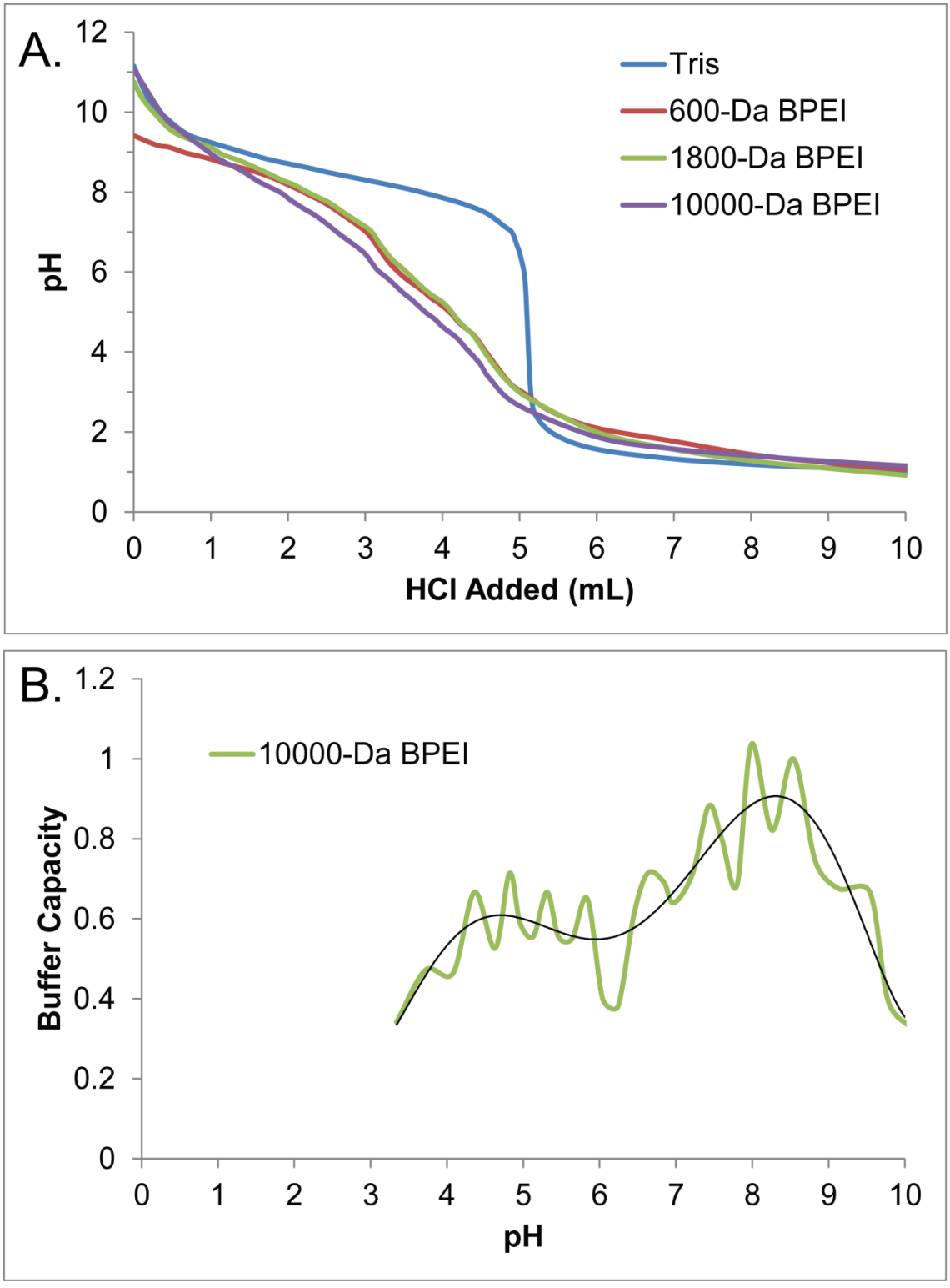


Figure 4. Titration curve (A) and the buffer capacity curve (B) of BPEI polymers and Tris-base.

Table 2. The pKa of BPEIs and Tris base.

	pKas	
	Experimental	Literature
600-Da BPEI	5.1±0.1	6.2[A]
	8.7±0.3	9.4
1800-Da BPEI	5.5±0.1	6.2[A]
	8.7±0.2	9.6
10-kDa BPEI	4.7±0.3	5.8[A]
	8.0±0.1	9.0
Tris Base	8.3±0.1	8.1[B]

The reported value is the average of two separate trials ± standard deviation. Gibney et al.[A](*72*) Haynes et al.[B](*96*)

600-Da BPEI has low cytotoxicity in vitro

A possible critique of utilizing BPEI in drug discovery is misunderstanding that cationic BPEIs are cytotoxic and thus unlikely to be useful as clinical antibacterial treatments. Reports show that cationic compounds, such as aminoglycosides and polymyxins, lead to nephrotoxicity.(*97, 98*) However, presumptions that all BPEIs are toxic overlook the stipulation that toxicity depends on molecular weight and concentration. High molecular weight BPEIs (over 25,000 Da) are cytotoxic, whereas the lower molecular weight BPEIs are non-toxic unless their concentrations are orders-of-magnitude higher than the amount required for potentiation.(*72, 99, 100*) Low cytotoxicity was confirmed in our lab with *in vitro* cytotoxicity data using mouse fibroblasts,(*3*) human HeLa, human colon, and human kidney cell lines (Table 3). The IC_{50} values for 600-Da BPEI (100-1,000 μg/mL) are orders of magnitude higher than the amount required for potentiation (~1 μg/mL). An *in vitro* hemolysis assay, published by Gibney et al., showed that 600-Da BPEI had no hemolytic activity and 10-kDa BPEI had minimal hemolysis (>5%) up to 2,000 μg/mL.(*72*) Drug-induced nephrotoxicity refers to irreversible kidney damage caused by a pharmaceutical.

Because of BPEI's cationic nature, some may believe that the polymer could cause nephrotoxicity. An *in vitro* nephrotoxicity assay was performed using primary human renal proximal tubule epithelial cells (hRPTECs). The assay detects the release of the metabolic enzyme, lactate dehydrogenase (LDH). A lack of LDH release suggests that the membrane is not damaged and the test agent does not cause *in vitro* nephrotoxicity. Exposure to 600-Da BPEI caused minimal release of LDH (~1% at 8 μg/mL, 16 μg/mL, and 31 μg/mL; 3.5% at 62 μg/mL; and 8% at 125 μg/mL, Figure 5). As per the literature, these values are indicative of low toxicity.(*101*) These values are much lower than the LDH release values for cationic and nephrotoxic, colistin (1% at 8 μg/mL; 2.3% at 16 μg/mL; 18% at 31 μg/mL; 26% at 62 μg/mL; and 28% at 125 μg/mL, Figure 5). The 1200-Da, 1800-Da, and 10-kDa BPEIs were more toxic than the 600-Da BPEI as seen with the CellTiter Blue cell viability (Table 3) and LDH assays (Figure 5). These data suggest 600-Da BPEI is preferred as a lead potentiator in drug discovery due to its low toxicity and low nephrotoxicity.

Table 3. *In vitro* mammalian cytotoxic activity of BPEI

Human Cell line	**Mean IC_{50} ± S.D. (μg/mL)**			
	600-Da	1200-Da	1800-Da	10 kDa
Cervical cancer (Hela)	1,090 ± 150	813 ± 16	935 ± 62	6.56 ± 0.89
Colon cancer (HCT116)	292 ± 45	548 ± 58	180 ± 75	11.1 ± 2.2
Kidney cancer (HEK293)	691 ± 79	186 ± 28	59 ± 24	1.9 ± 0. 5

Notes: Values are reported as the average of three trials ± standard deviation. Cells were treated for 48 hours and assayed with the CellTiter Blue method.

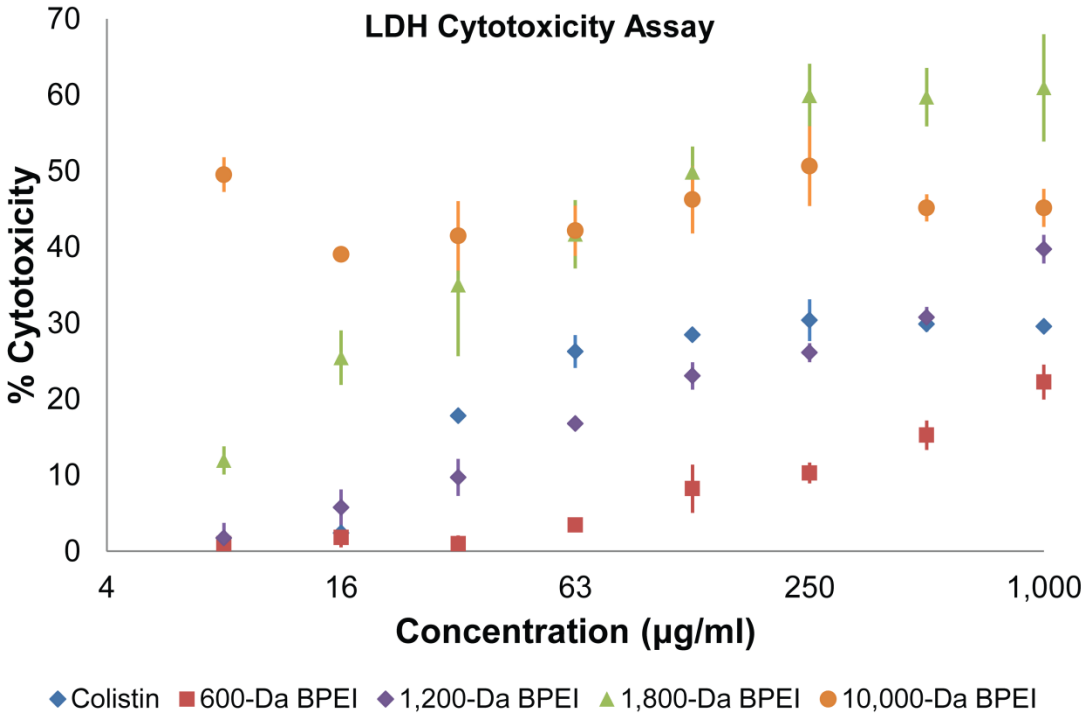


Figure 5. 600-Da BPEI had minimal LDH release in a primary kidney proximal tubule cell line (PCS-400-010). The 1800-Da and 10-kDa BPEIs had higher LDH release than the nephrotoxic drug colistin. Error bars denote standard deviation (n=3).

Conclusion

We found that lower molecular weight BPEI is less cytotoxic than higher molecular weight BPEI. While the IC_{50}s of 600-Da BPEI was between 100-1,000 µg/mL for each tested cell line, 10-kDa BPEI was more toxic with IC_{50}s between 1-10 µg/mL. The LDH cytotoxicity assay showed 600-Da BPEI had minimal LDH release. However, 1800-Da and 10-kDa released more LDH than the nephrotoxic drug colistin. Thus, we designated 600-Da to be the lead potentiator for future studies. The low toxicity of our lead potentiator is the result of its hydrophilic nature. 600-Da BPEI is very hydrophilic and completely miscible with water. Also, 600-Da BPEI molecules are very small and do not contain regions of hydrophobic character, as seen with cationic

peptides, aminoglycosides, and polymyxins. Thus, 600-Da BPEI lacks the energetic force that drives hydrophobic compounds into lipid membranes. Higher molecular weight BPEIs had higher toxicity and caused nephrotoxicity. BPEI ranging from 10,000 – 1,000,000-Da possess less hydrophilic interiors that increase their lipophilicity and lead to membrane penetration and damage.

Chapter 3: Efficacy of β-lactam antibiotics against MRSA Restored Through Synergy with BPEI

Background

Methicillin-resistant *Staphylococcus aureus* (MRSA) is a current and growing risk to human health. It causes serious infections that show remarkable resistance to antibiotic treatments. Originally acquired exclusively in healthcare settings, MRSA is now regularly found outside the healthcare environment.(*102*) Diagnosed or suspected MRSA infections require treatment with vancomycin, linezolid, or daptomycin.(*54*) Although resistance has developed to all three drugs of last resort, to date, no MRSA strain is resistant to more than one of them.(*59, 103*) Other drugs, such as ceftaroline and telavancin, have been approved for patient use in severe cases but must be given intravenously.(*54*) Yet, people suffer from MRSA infections because, MRSA is either misdiagnosed or not suspected, and ineffective first-line antibiotics, usually β-lactams,(*39*) are given. After MRSA diagnosis, clinicians turn to drugs of last resort, but treatment delays can result in mortality or increased morbidity due to release of MRSA toxins into tissue.(*103, 104*) In 2011, MRSA infected 80,500 people; nearly 1 in 7 cases resulted in death (11,300; 14%).(*1*) Drug resistance hinders efforts to develop safe clinical treatments for MRSA infections. Fortunately, progress has been made towards developing new antibiotics such as oxadiazoles,(*105*) tedizolid,(*106*) and teixobactin.(*107*) The timing coincides with a critical period in antibiotic research and development, as MRSA is developing resistance to drugs of last resort, such as vancomycin.(*57, 108, 109*) Therapeutic approaches to overcome resistance factors include efflux-pump inhibitors that increase the intracellular concentration of

antibiotics.(*110*) Bacteria can also use β-lactamase enzymes to degrade the antibiotics; thus, treatment requires β-lactamase inhibitors. However, development of new antibiotics has slowed within the last 20 years, with the last new antibiotic class having been discovered over 30 years ago.

Little research has examined BPEI as an antibacterial agent. Of that which has been done, the majority has focused on BPEI used alone to combat Gram-negative infections. Wiegand et al. tested LPEI and BPEI against *E. coli* and found low efficacy, regardless of molecular weight.(*100*) In studies that looked at *S. aureus*, LPEIs had better activity than BPEIs but still had MICs of 30-40 μg/mL, with no effect caused by molecular weight.(*100*) Gibney et al. mirrored this observation and found that both LPEI and BPEI are selective against *S. aureus* over *E. coli*, because they gave lower MICs.(*72*) The MIC of BPEI was not dependent on the molecular weight and consistently had an MIC of around 100 μg/mL, which is too high to be considered effective for clinical purposes.(*100*) Previous research in the laboratory found that low-MW BPEI prevented growth of chloramphenicol-resistant *B. subtilis* 1A578 in chloramphenicol.(*70*) This led to the idea that BPEI could potentially remove antibiotic resistance from pathogenic bacteria such as MRSA.

Determination of Synergy

When developing new drug combinations, the drug interaction refers to the effect that the drugs have on one another. Synergy occurs when the drugs work together in order to increase the effectiveness. The opposite of synergy, antagonism, occurs when the effectiveness is reduced when the drugs are given together. Additivity occurs

when both drugs have an effect but are not increasing the efficacy of each other. Combination therapies of antibiotics are advantageous because they increase efficacy and reduce the onset of resistance.(*13*) Determination of synergy of antibiotic combinations is important for reducing dosage size, understanding drug mechanism, and obtaining novel patents.

A common technique for determining the *in vitro* level of synergy between drugs is a checkerboard assay. On a checkerboard assay, different combinations of antibiotics are added to 96-well plates. A consistent amount of bacteria is added to each well and allowed to grow for a certain amount of time. After, the fractional inhibitory concentration index (FICI) can be determined. For each antibiotic, the minimum inhibitory concentration (MIC) is the minimum concentration of one antibiotic required for the bacteria to not grow. For each well of bacteria that did not grow, an FICI is calculated using Equation 1 with the concentrations of each antibiotic in the specific well. An FICI less than 0.5 indicates synergy. An FICI greater than 1.0 indicates antagony. Between 0.5 and 1.0 indicates additivity. By determining the drug interactions of antibiotics using checkerboard assays, we can better understand the efficacy of the combination therapy and the mechanism of action.

$$\frac{\mathrm{Conc_A}}{\mathrm{MIC_A}} + \frac{\mathrm{Conc_B}}{\mathrm{MIC_B}} = \mathrm{FIC_A} + \mathrm{FIC_B} = \mathrm{FICI} \qquad \text{(Equation 1)}$$

Purpose of Experiment

Although BPEI alone had impractically high MICs, it was hypothesized that BPEI would potentiate the activity of antibiotics against drug-resistant pathogens. Thus, the purpose of this experiment was to determine whether synergy was present between

BPEI and antibiotics against MRSA. We found that BPEI synergistically re-sensitized MRSA to β-lactam antibiotics. However, BPEI did not potentiate non-β-lactam antibiotics against MRSA. Additionally, the BPEI:β-lactam combination was effective for only MRSA and did not display synergy against MSSA, *Escherichia coli*, or *Bacillus subtilis*.

Experimental Procedures

Cell Lines Used

Bacterial cell lines were obtained from American Tissue Culture Collection: MRSA USA300 (ATCC BAA-1717™), MRSA 33592 (ATCC 33592™), MRSA 252 (ATCC BAA-1720™), and *Bacillus subtilis* 6051 (ATCC 6051™). MRSA MW2 (ATCC BAA-1707™) was a generous gift from Professor Suzanne Walker. MRSA 700787 (ATCC 700787™), MSSA 25923 (ATCC 25923™), and *Escherichia coli* 11775 (ATCC 11775™) were generous gifts from Professor Robert Cichewicz and Jarrod King. Clinical isolates were obtained from patient swabs at the University of Oklahoma Health Sciences Center and provided by Cindy McCloskey M.D. following institutional review board (IRB) approval. Table 4 lists bacteria strains used in the study and their characteristics. Since MRSA and MSSA are classified as biosafety level 2 organisms (BSL-2), extra precautions were taken for all procedures. All studies were performed in a biological safety cabinet with appropriate personal protective equipment.

Table 4. Bacterial strains used in study.

Bacteria Species	Strain	Gram reaction	Characteristics
MRSA	USA300	+	Most commonly diagnosed strain of MRSA. Resistant to triple action antibiotic ointments.(*111*)
MRSA	MW2	+	High rate of diagnosis. Particularly virulent strain.
MRSA	700787	+	Vancomycin-intermediate resistance.
MRSA	33592	+	Gentamicin-resistant.
MRSA	252	+	Hospital-acquired strain.
MSSA	25923	+	Methicillin-susceptible *S. aureus* strain.
B. subtilis	6051	+	Non-virulent reference bacillus strain.
E. coli	11775	-	Non-virulent Gram-negative strain.

In Vitro Efficacy Checkerboard Assays

Checkerboard assays were used to determine synergy of BPEI with β-lactam antibiotics against bacteria. Stock solutions of oxacillin were made in DMSO and added to pre-sterilized 96-well plates with cation-adjusted Mueller-Hinton Broth so that the final DMSO concentration was <1%. Bacteria were added to each well on the plate so that the final cell density was ~5 x 10^5 cells/mL. Optical density readings were made immediately after inoculation using a Tecan Infinite M20 plate reader with a wavelength of 600 nm. The plates were incubated for 20 hours in a humidified incubator at 35 °C and a final OD_{600} reading was recorded. The change in OD_{600} was calculated by subtracting the initial OD_{600} from the final OD_{600} reading. A change in OD_{600} greater than 0.050 was considered to be positive for growth. The minimum inhibitory concentration (MIC) was assigned as the lowest concentration of antibiotic or

BPEI that did not allow growth. The fractional inhibitory concentration index (FICI) was calculated using the previously-established equation.(*112*) An FICI lower than 0.5 indicates synergy, between 0.5 and 1 represents additivity, and greater than 1 shows antagonism. Each assay was done as three separate trials and reported as the modal FICI value.

Minimum Bactericidal Concentrations

Minimum bactericidal concentrations (MBC) were determined by counting colonies on agar plates inoculated with the contents of the 96-well plates after the final OD_{600} readings were taken. Specifically, 5 μL of cell suspension was transferred to a TSB agar plate for each well. The agar plates were grown for 24 hours at 35 °C. After growth, colony forming units were counted.

Clinical Isolates of MRSA

The MIC of oxacillin and BPEI against 16 strains of MRSA and 5 strains of MSSA were determined using the Clinic Practice Guidelines.(*54*) The MIC of BPEI and oxacillin were determined by serially diluting each in 96-well plates with MHB. In separate wells, decreasing concentrations of BPEI were added to MHB with a constant amount of oxacillin (2 μg/mL). The same was done for decreasing concentrations of oxacillin with a constant amount of BPEI (4 μg/mL). Bacteria was added (5×10^5 cells/ mL) to each well and grown until confluency at 35 °C. The OD_{600} was measured before and after growth. A change in OD_{600} greater than 0.05 was considered positive for

growth. Each MIC was determined in quadruplicate, and the values are presented as the average of four trials.

Growth and Time-Killing Curves

TSB growth media augmented with various amount of BPEI and/or oxacillin was inoculated at 0.5% from an overnight culture of MRSA 700787. During cell growth at 35 °C, with shaking (200 rpm), the OD_{600} was monitored with a Jenway Genova UV/Visible Spectrophotometer hourly for each sample. Aliquots were taken at 0 hour, 4 hours, 8 hours, and 24 hours. Each aliquot was serially diluted in fresh TSB and transferred to TSB agar plates. The agar plates were grown at 35 °C for 24 hours. After growth, colony forming units were counted. Each study was done in triplicate.

Results and Discussion

Methicillin was initially introduced in 1959 to treat penicillin-resistant infections, but reports of methicillin-resistance began appearing just two years later.(*45*) Today, improved β-lactam antibiotics have clinically replaced methicillin. Some β-lactams, such as oxacillin, ampicillin, and ceftizoxime are still used to treat Staph infections, but the increased prevalence of MRSA infections has made vancomycin a first-line antibiotic against septic *S. aureus* infections. Vancomycin is unable to cross the stomach lining and therefore must be given intravenously, which often requires hospitalization, can be symptomatic, and can cause complications such as hearing loss, allergic reaction, and kidney damage.(*55*) Furthermore, cases of vancomycin-resistant *S. aureus* (VRSA) have been found.(*57, 108*) Last-resort drugs such as daptomycin and

linezolid are effective against MRSA but are rarely prescribed in order to slow the onset of resistance. Thus, development of an orally-administered combination therapy that employs β-lactams could replace vancomycin as a first-line MRSA treatment. Because BPEI removed chloramphenicol resistance from *B. subtilis* 1A578 (chloramphenicol-resistant strain), we hypothesized that BPEI could also remove MRSA's resistance to ampicillin and other β-lactams. A quick screen (Figure 6) showed that BPEI is capable of reducing MRSA's growth in ampicillin.

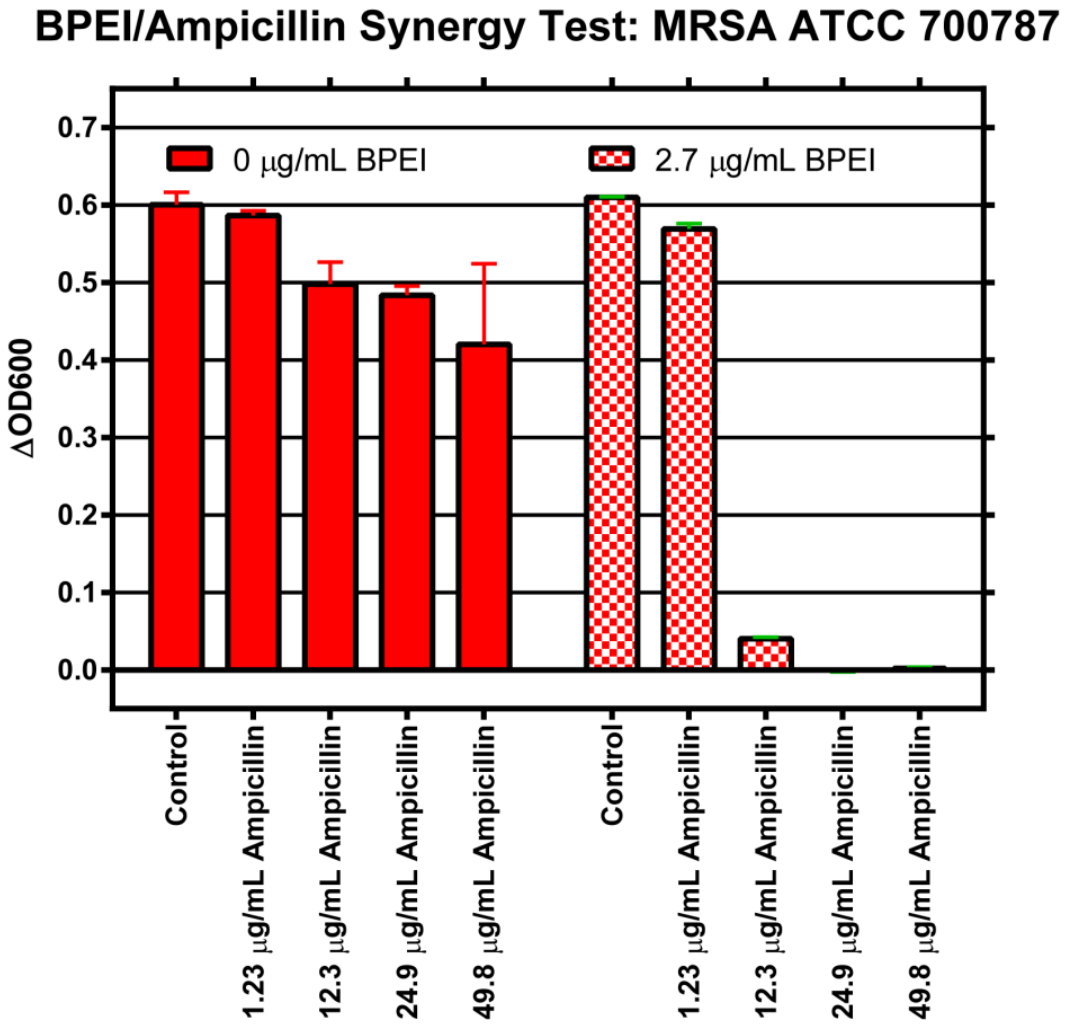


Figure 6. *In vitro* assay of ampicillin against MRSA. When BPEI (2.7 μg/mL) is added, the MIC for ampicillin is between 12 and 25 μg/mL (checkered columns) while ampicillin without BPEI does not inhibit MRSA below 50 μg/mL concentration (solid

red columns). The growth of MRSA was evaluated by measuring the change in OD_{600} after 20 hours. Cell growth in TSB without additives is denoted as Control.

BPEI has synergy with β-lactam antibiotics against MRSA

Checkerboard assays were used to determine synergy between BPEI and β-lactam antibiotics. Here we look at the two most common strains of CA-MRSA: USA300 and MW2. MRSA USA300 is the most common community-associated strain, which could be partially due to its low susceptibility to over-the-counter triple antibiotic ointments.(*111, 113, 114*) MRSA MW2 (also referred to as MRSA USA400) has additional toxins that make it particularly virulent. BPEI in combination with oxacillin showed synergy against multiple cell lines (Table 5). The BPEI:oxacillin combination against MRSA USA300 had a fractional inhibitory concentration index (FICI) of 0.266 (Figure 7A). An FICI less than 0.5 indicates synergy, greater than 1.0 indicates antagony, and between 0.5 and 1.0 indicates additivity. MRSA MW2, had an FICI of 0.250 for the BPEI:oxacillin combination (Figure 7B). BPEI (4 μg/mL) reduced the MIC of ceftizoxime from 256 μg/mL to 8 μg/mL against MRSA USA300 (FICI= 0.313; Figure 7C). Similarly, BPEI (8 μg/mL) reduced the MIC of ceftizoxime from 256 μg/mL to 16 μg/mL against MRSA MW2 (FICI= 0.156; Figure 7D). Imipenem and BPEI exhibited synergy against both MRSA USA300 (FICI= 0.375; Figure 7E) and MRSA MW2 (FICI= 0.25; Figure 7F).

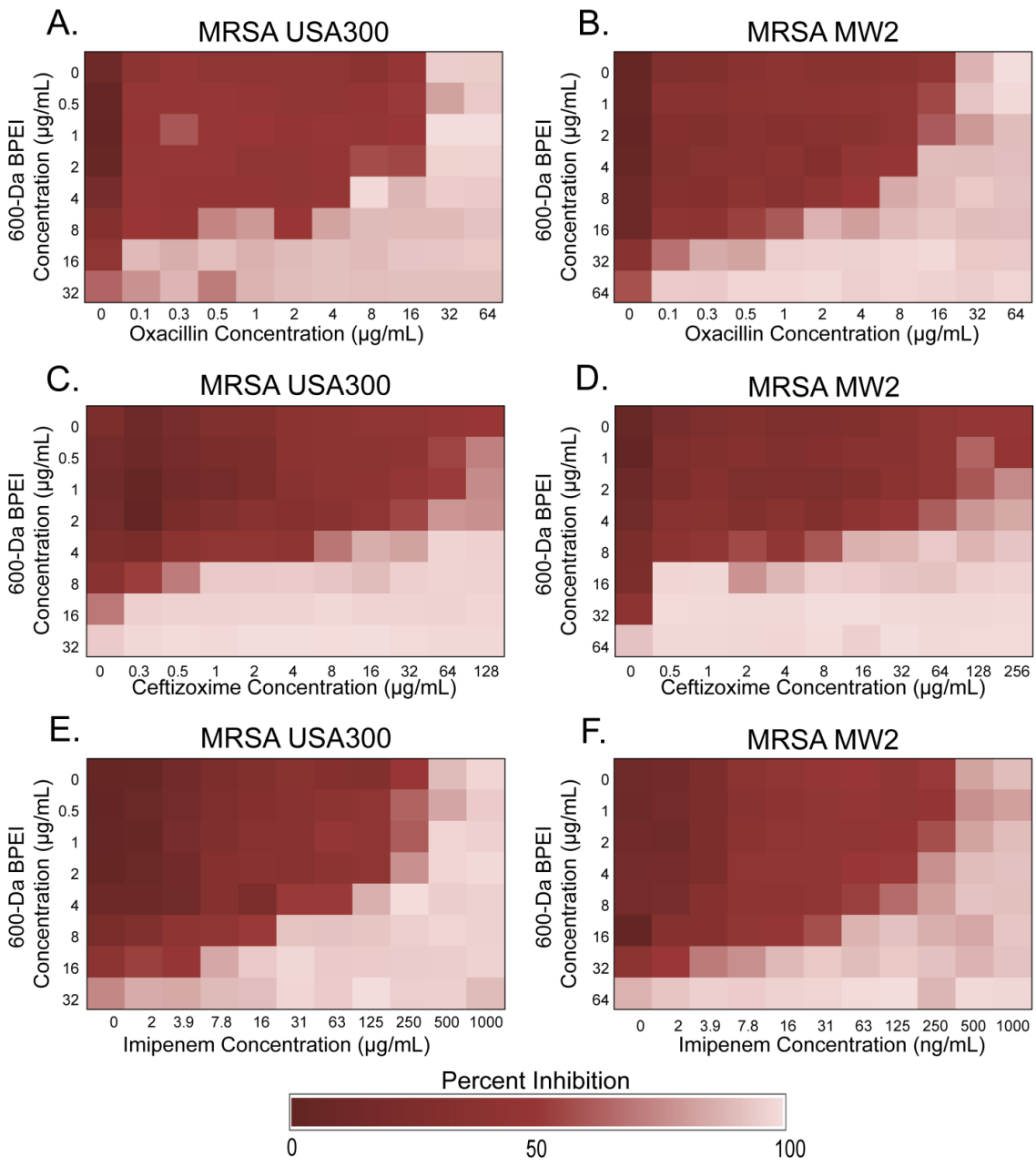


Figure 7. Checkerboard assays show synergy between BPEI and β-lactams on MRSA USA300 and MRSA MW2. BPEI had synergy with oxacillin (A, B), ceftizoxime (C, D), and imipenem (E, F) against MRSA USA300 (A, C, E) and MRSA MW2 (B, D, F). Each assay was performed as three separate trials, and the presented data is shown as the average change in OD_{600}.

Table 5. Minimum inhibitory concentrations and fractional inhibitory values of BPEI in combination with β-lactam antibiotics against MRSA.

Strain / Antibiotic	MRSA MW2		MRSA USA300		MRSA 252		MRSA 33592	
	MIC	FICI	MIC	FICI	MIC	FICI	MIC	FICI
BPEI	64	-	32	-	32	-	32	-
Oxacillin	32	0.250	32	0.266	>256	0.501	256	0.281
Ampicillin	128	0.188	2	0.516	256	0.375	256	0.516
Amoxicillin	128	0.250	4	0.5	256	0.500	256	0.375
Meropenem	2	0.313	4	0.250	32	0.504	8	0.563
Ceftizoxime	>256	0.156	256	0.313	>256	0.254	>256	0.5
Piperacillin	>256	0.266	16	0.313	>256	0.501	>256	0.501
Cephalothin	4	0.5	2	0.5	32	0.281	32	0.375
Imipenem	0.5	0.375	0.25	0.25	64	0.508	32	0.281

Notes: MIC=minimum inhibitory concentration. FICI=fractional inhibitory concentration index. Each value is the average of three separate trials.

Two other commercially-available MRSA strains were also tested: MRSA 252 and MRSA 33592. MRSA 252, a HA-MRSA strain, is one of the major strains found in the United Kingdom. Additionally, MRSA 252 is genetically diverse compared to other strains of MRSA.(*115*) MRSA 33592 (also denoted as MRSA 1063) is a CA-MRSA strain that also has resistance to gentamicin. Other β-lactam antibiotics such as amoxicillin, meropenem, and piperacillin had synergy with BPEI against MRSA MW2 and USA300, but the synergistic effect was less prominent against MRSA 252 and MRSA 33592 (Table 5). MRSA 252, a HA-MRSA strain, only had synergy between BPEI and ampicillin (FICI=0.370; Figure 8A). BPEI had synergy with oxacillin (FICI=0.281; Figure 8B), amoxicillin (FICI=0.375), and cephalothin (FICI=0.375) against MRSA 33592. All other tested BPEI and β-lactam combinations had only additivity or no effect against MRSA 252 or MRSA 33592.

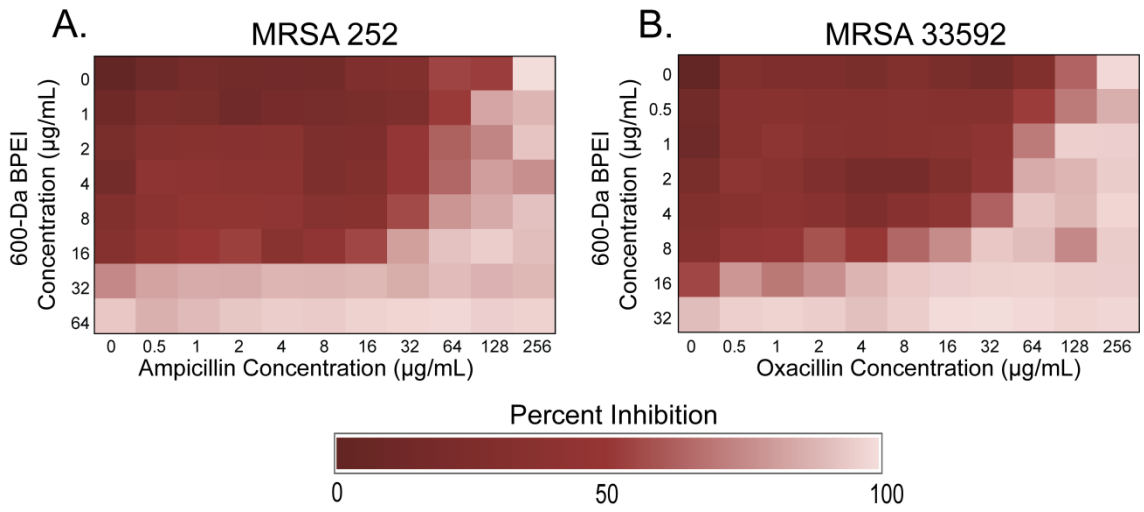


Figure 8. Checkerboard assays show synergy between BPEI and β-lactams on MRSA 252 and MRSA 33592. BPEI had synergy with ampicillin against hospital-acquired MRSA 252 (A). BPEI had synergy with oxacillin against MRSA 33592 (B). Each assay was performed as three separate trials, and the presented data is shown as the average change in OD_{600}.

BPEI creates synergy with β-lactam antibiotics to stop VISA growth

Checkerboard assays demonstrate anti-MRSA properties of 600-Da BPEI mixed with β-lactam antibiotics (Table 6) against a MRSA strain containing PBP2a (ATCC 700787™) that is also moderately resistant to vancomycin (vancomycin-intermediate *S. aureus*, VISA). BPEI has synergy (FICI<0.5) with oxacillin, ampicillin, amoxicillin, and meropenem (Figure 9A-C). Adding 600-Da BPEI (0.5 µg/mL) reduced the MIC of oxacillin from 64 µg/mL to 4 µg/mL against MRSA 700787. Increasing the concentration of 600-Da BPEI to 1 µg/mL resulted in a 128-fold decrease of the MIC of oxacillin to 0.5 µg/mL. Likewise, increasing the 600-Da BPEI concentration increases potentiation and decreases MIC values of amoxicillin, ampicillin, and meropenem. However, BPEI did not have synergy with methicillin; the FICI equals 0.563 which indicates additivity (Table 6).

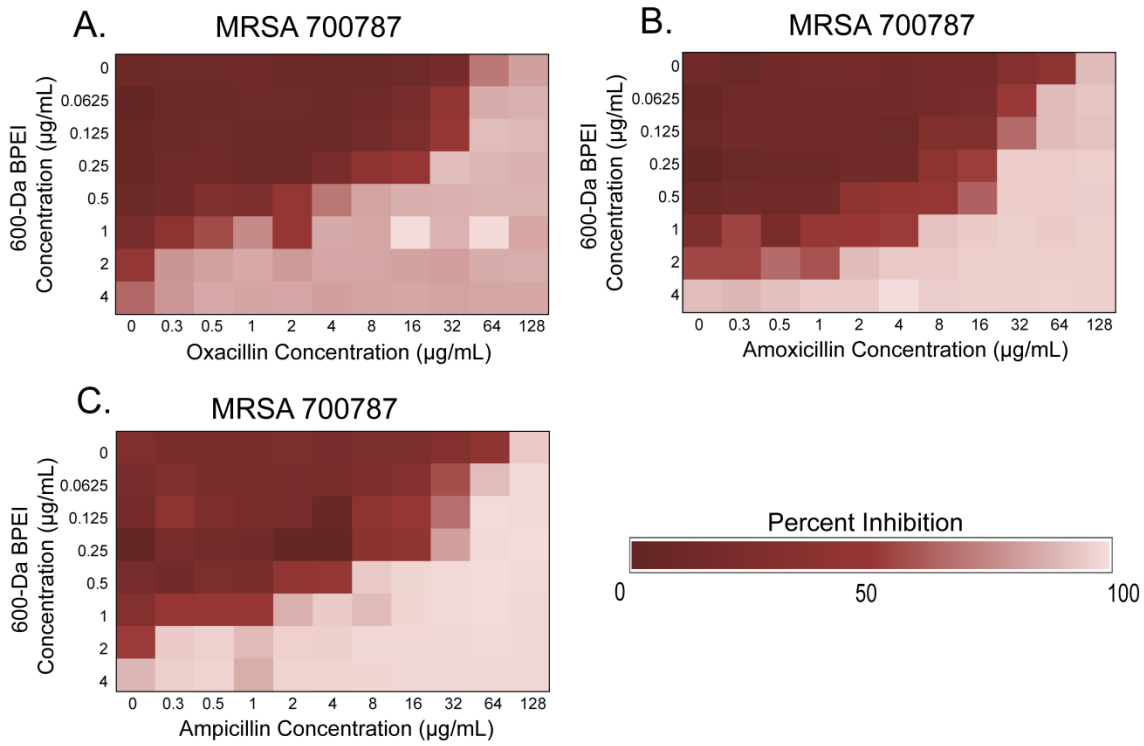


Figure 9. BPEI potentiates β-lactam activity against MRSA 700787. Checkerboard assays show that BPEI potentiates oxacillin (A), amoxicillin (B), and ampicillin (C) activity against MRSA 700787. Each assay was performed as three separate trials, and the presented data is shown as the average change in OD_{600}.

Table 6. Synergy of 600-Da BPEI and β-lactams against MRSA 700787.

Strain	Antibiotic	MIC_A (μg/mL)		MIC_B (μg/mL)		FICI	Outcome
		Alone	Comb.	Alone	Comb.		
MRSA 700787	Oxacillin	64	4 0.5	4	0.5 1	0.188 0.258	Synergy
	Ampicillin	128	8 2	4	0.5 1	0.188 0.266	Synergy
	Amoxicillin	128	8	4	1	0.313	Synergy
	Methicillin	64	4	4	2	0.563	Additivity
	Meropenem	2	0.5	4	0.5	0.375	Synergy

Notes: MIC_A is minimum inhibitory concentration of the antibiotic; MIC_B is minimum inhibitory concentration of BPEI; FICI is fractional inhibitory concentration index.

BPEI potentiates oxacillin against clinical isolates of MRSA

We have been able to demonstrate synergy between BPEI and β-lactams against five commercially-available reference strains of MRSA. Since the long-term goal is for BPEI to be combined with β-lactams to treat clinical MRSA infections, clinical isolates of MRSA obtained from patients at the University of Oklahoma College of Medicine were tested. The laboratory of Cindy McCloskey M.D. confirmed that each isolate contained the *mecA* gene and therefore was resistant to oxacillin. The BPEI:oxacillin showed the best efficacy against the tested commercially-available MRSA panel, so this combination was used for further studies. We were motivated to see if the BPEI:oxacillin combination would be efficient against clinical isolates of MRSA. The MICs for oxacillin and BPEI separately were determined for each isolate. The minimum concentration of BPEI required to inhibit growth of the bacteria in the presence of 2 μg/mL oxacillin (the breakpoint of susceptibility) was compared to the MIC of BPEI alone (Figure 10A, Table 7). In this test, eleven of the sixteen tested strains had an FICI less than 0.5. Additionally, the minimum concentration of oxacillin required to inhibit growth in the presence of 4 μg/mL BPEI was compared to the MIC of oxacillin alone (Figure 10B, Table 8). In this test, ten of the sixteen tested strains had an FICI less than 0.5. Between the two tests, twelve strains showed synergy and the other four strains saw a reduction in MIC representative of additivity. This data demonstrates that BPEI:oxacillin shows broad efficacy against clinical strains of MRSA.

Table 7. Treatment of clinical isolates of MRSA. Data shows the concentration of BPEI required to reduce the MIC of oxacillin to the susceptibility cutoff of 2 μg/mL.

Strain #	Oxacillin MIC (μg/mL)	Removing Resistance		BPEI MIC (μg/mL)	FICI
		Concentration Oxacillin (μg/mL)	Concentration BPEI (μg/mL)		
1	256	2	16	32	0.508
2	8	2	1	32	0.281
3	64	2	16	16	1.03
4	64	2	8	32	0.281
5	128	2	16	64	0.266
6	32	2	8	64	0.188
7	128	2	16	64	0.266
8	256	2	8	8	1.01
9	32	2	16	64	0.313
10	16	2	32	256	0.25
11	256	2	32	64	0.508
12	64	2	32	128	0.281
13	16	2	4	8	0.625
14	32	2	8	64	0.188
15	16	2	2	256	0.133
16	32	2	2	256	0.125

Notes: FICI is the fractional inhibitory concentration. MIC is the minimum inhibitory concentration. Each value is the average of four trials.

Table 8. Treatment of clinical isolates of MRSA. Data shows the concentration of oxacillin required to reduce the MIC of BPEI to 4 µg/mL.

Strain #	BPEI MIC (µg/mL)	Removing Resistance		Oxacillin MIC (µg/mL)	FICI
		Concentration BPEI (µg/mL)	Concentration Oxacillin (µg/mL)		
1	32	4	128	256	0.625
2	32	4	2	8	0.375
3	16	4	16	64	0.5
4	32	4	8	64	0.25
5	64	4	16	128	0.188
6	64	4	0.5	64	0.078
7	64	4	64	128	0.563
8	8	4	64	256	0.75
9	64	4	16	32	0.563
10	256	4	4	16	0.266
11	64	4	32	256	0.188
12	128	4	8	64	0.156
13	8	4	0.125	16	0.508
14	64	4	4	32	0.188
15	256	4	2	16	0.141
16	256	4	8	32	0.266

Notes: FICI is the fractional inhibitory concentration. MIC is the minimum inhibitory concentration. Each value is the average of four trials.

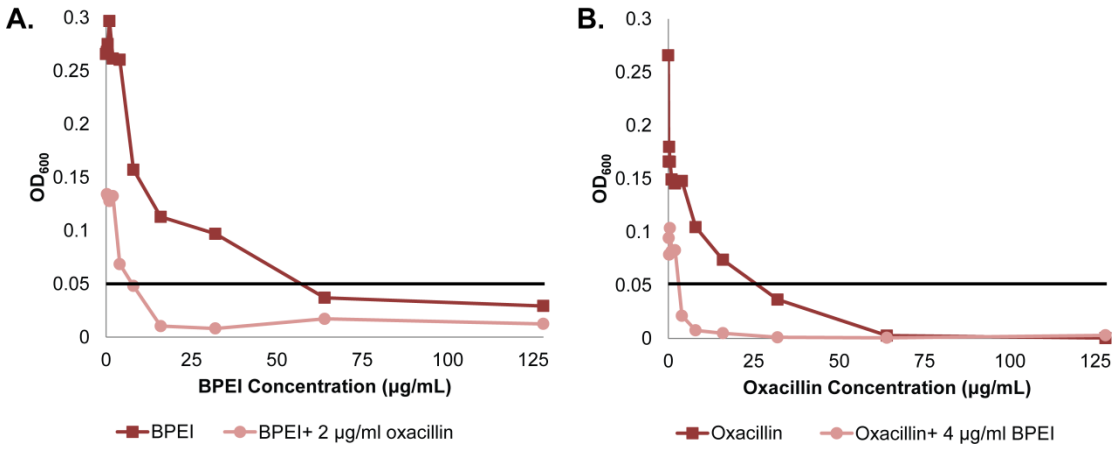


Figure 10. BPEI and oxacillin together are effective at preventing growth of a clinical isolate of MRSA. The concentration of BPEI required to inhibit MRSA OU14 was reduced when simultaneously grown in 2 µg/mL oxacillin (A). Similarly, the concentration of oxacillin required to inhibit growth was reduced while simultaneously treated with 4 µg/mL of BPEI (B). The black line indicates the cutoff for growth at a change in OD_{600} of 0.05. Each data point is reported as the average of four trials.

Intermediate molecular weight BPEI has higher efficacy

BPEI is commercially available in a wide range of sizes (600 to 1,000,000-Da). We were motivated to determine whether increasing the molecular weight of BPEI increases its efficacy against MRSA 700787. The MICs of 1200-Da and 1800-Da BPEI alone (0.5 μg/mL) were lower compared to that of 600-Da BPEI alone (4 μg/mL; Figure 11 A). The 1200 and 1800-Da BPEI had synergy with oxacillin (Figure 11B, C). Only 0.125 μg/mL 1200-Da BPEI was required to reduce the MIC of oxacillin from 128 μg/mL to 8 μg/mL against MRSA 700787. 10-kDa BPEI had an MIC of 4 μg/mL but did not demonstrate synergy with oxacillin (FICI= Figure 11D). Compared to the 600-Da BPEI + β-lactam combination, the 1200-Da and 1800 Da + β-lactam combinations have superior *in vitro* efficacy. However, as shown previously, 600-Da BPEI shows negligible *in vitro* cytotoxicity against mammalian cells whereas toxicity increases for 1200-Da, 1800-Da, and 10-kDa BPEI. Also, we did not anticipate LPEI would have activity; a short study confirmed this hypothesis. The 600-Da form of LPEI did not inhibit MRSA growth and did not potentiate ampicillin unless the concentration was high (54 μg/mL; Figure12). Because 600-Da BPEI was determined to be the lead potentiator, no more studies were done on other PEIs.

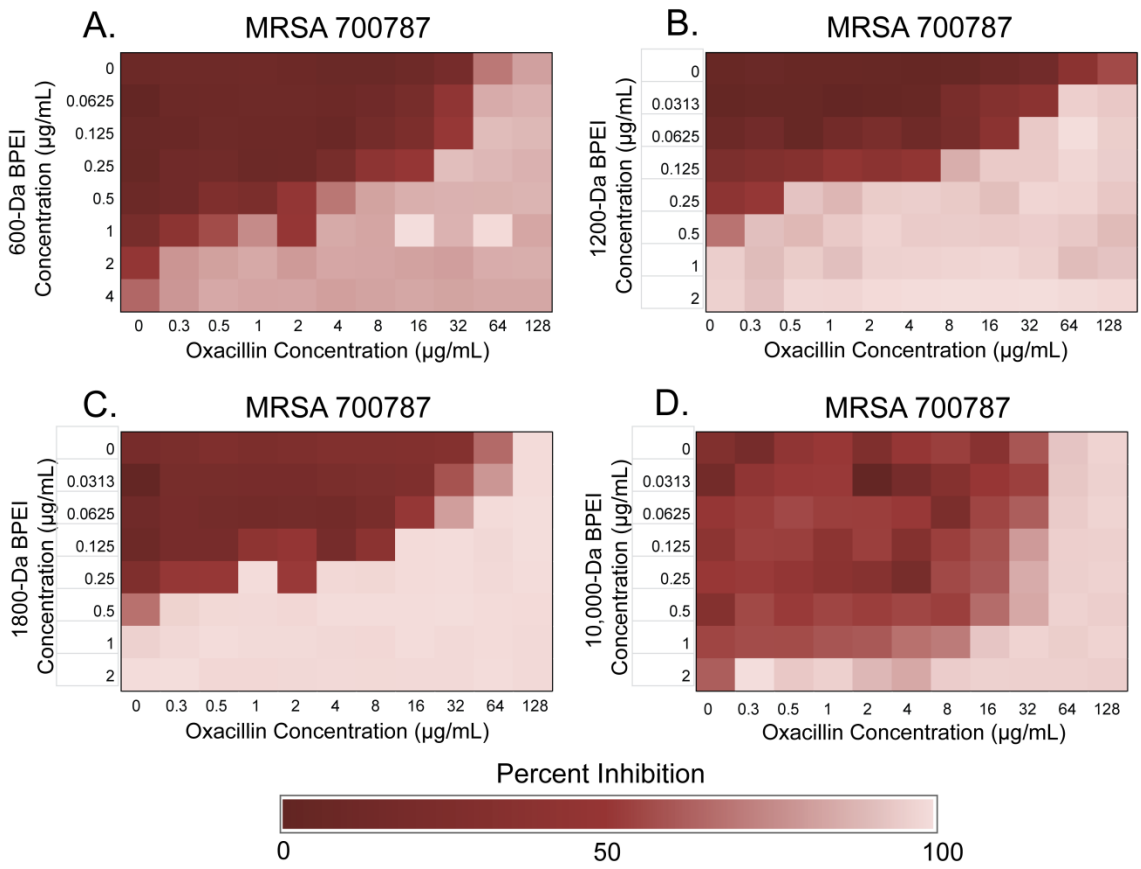


Figure 11. Low and intermediate MW BPEI potentiate MRSA to oxacillin. 600-Da BPEI (A), 1200-Da BPEI (B) and 1800-Da BPEI (C) potentiate oxacillin acitivity against MRSA 700787 but 10-kDa BPEI (D) does not. Each assay was performed as three separate trials, and the presented data is shown as the average change in OD_{600}.

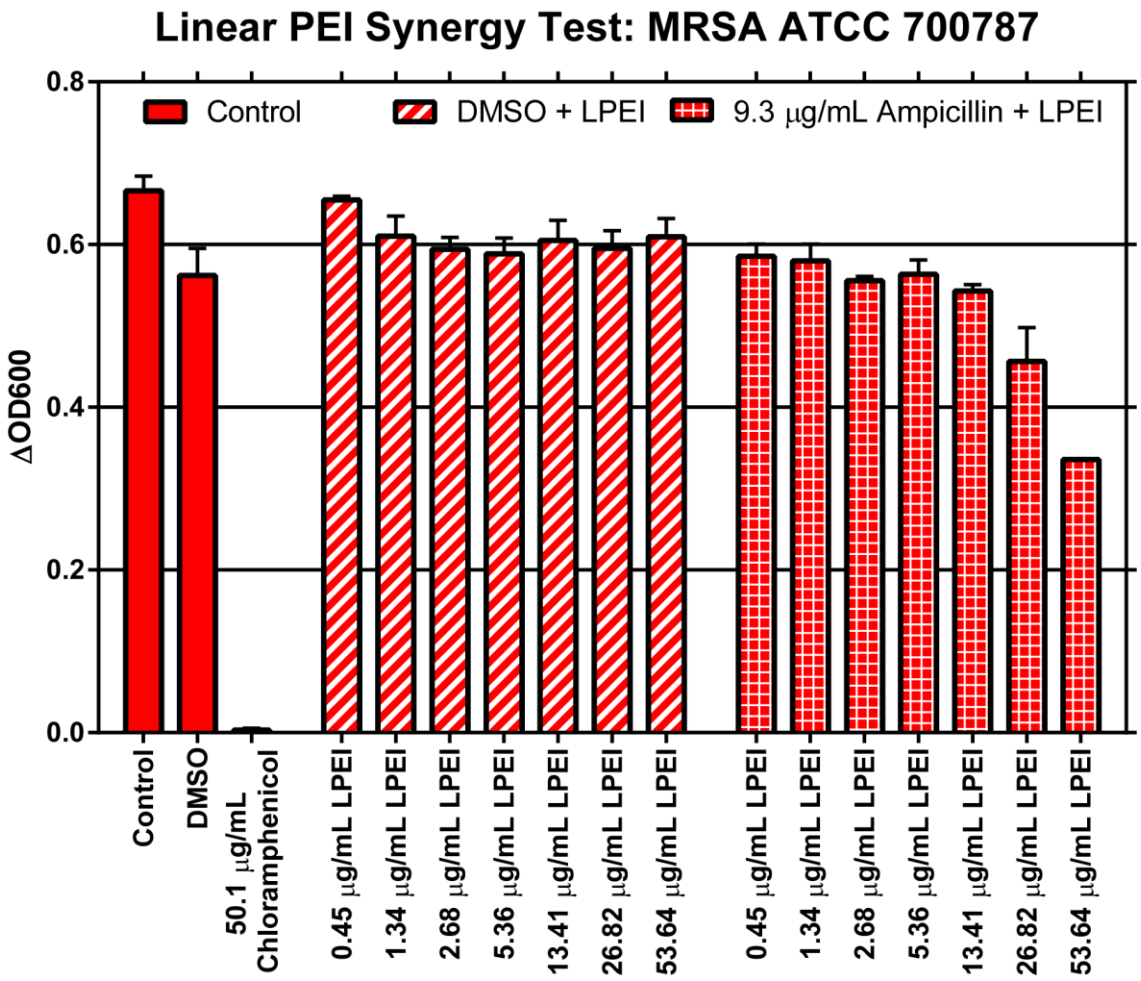


Figure 12. *In vitro* linear PEI assay against MRSA. LPEI alone does not affect the growth of MRSA through 54 µg/mL (striped red columns); addition of 9.3 µg/mL ampicillin provides some effect, though not enough to inhibit MRSA growth (thatched red columns). Growth of MRSA was evaluated by measuring the change in OD_{600} after 20 hours. Cell growth in media (Control) or media with 1% DMSO show the increase in OD_{600} (solid red columns), while 50 µg/mL chloramphenicol serves as a negative control.

BPEI:oxacillin combination is bactericidal

Monitoring the growth of MRSA 700787 reveals that bacteria exposed to sub-inhibitory concentrations of BPEI and oxacillin fail to reach exponential phase when the two compounds are combined (Figure 13A). Aliquots were transferred to agar plates, and CFUs were counted from the 0 hour, 4 hour, 8 hour, and 24 hour time points to

determine if the lack of growth observed for the BPEI and oxacillin combination was bacteriostatic or bactericidal. After 8 hours, the control sample had the highest cell density (1×10^9 cells/μL). The samples that contained BPEI or oxacillin had lower viable cell numbers in comparison to the control sample, but these values were still higher than the initial cell density ($>1 \times 10^5$ cells/μL). The viable cell count decreased for growth in both BPEI and oxacillin (47 CFUs/μL at 8 hours growth) and did not increase after 24 hours (Figure 13B). This data demonstrates that the mechanism by which BPEI and oxacillin prevents growth of MRSA is bactericidal.

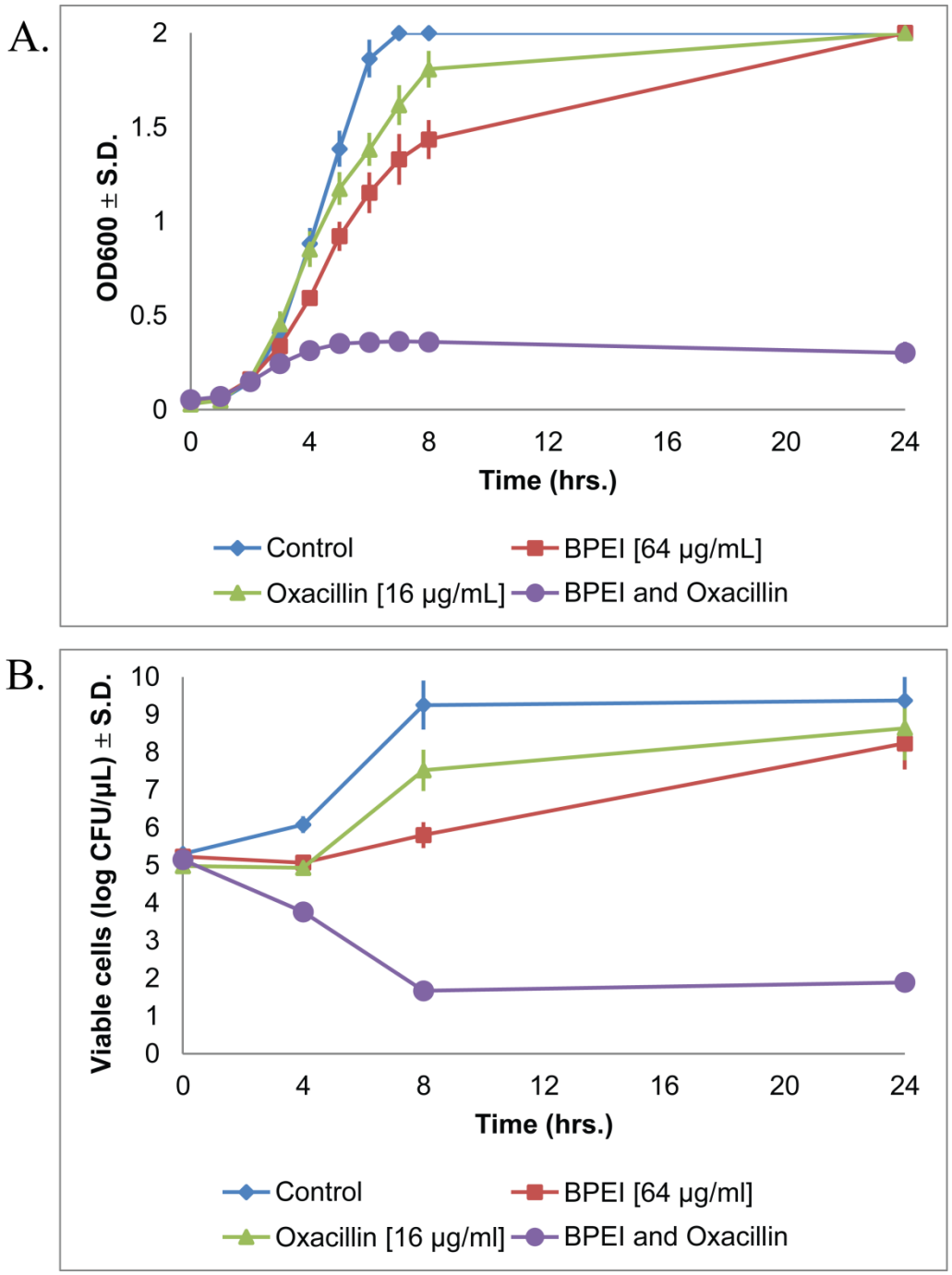


Figure 13. 600-Da BPEI and oxacillin comprise a bactericidal combination in MRSA 700787. Cells treated individually with BPEI or oxacillin were still able to grow but growth was inhibited when both BPEI and oxacillin were used (A). A time-kill curve shows that the combination has a bactericidal mechanism of action as seen with the drop in viable cell counts after 4 hours (B). Error bars denote standard deviation (n=3).

To support this conclusion, minimum biocidal concentrations (MBCs) were determined from a checkerboard assay of MRSA containing BPEI and oxacillin. The MBC of BPEI was the same as the MIC (4 μg/mL) while the MBC for oxacillin was at least twice as large as the MIC (MIC= 64 μg/mL; MBC>128 μg/mL). The MBCs for the combination (1 μg/mL BPEI, 2 μg/mL oxacillin; Figure 14) were 2-fold greater than the combination's MICs (1 μg/mL BPEI, 1 μg/mL oxacillin). If the MBC is less than 4-fold the MIC, the drug is considered bactericidal and does not require the assistance of host defenses.(*116*) Since the MBC for BPEI and its oxacillin combination is not greater than four times the MIC, both BPEI alone and the BPEI: oxacillin combination is bactericidal.

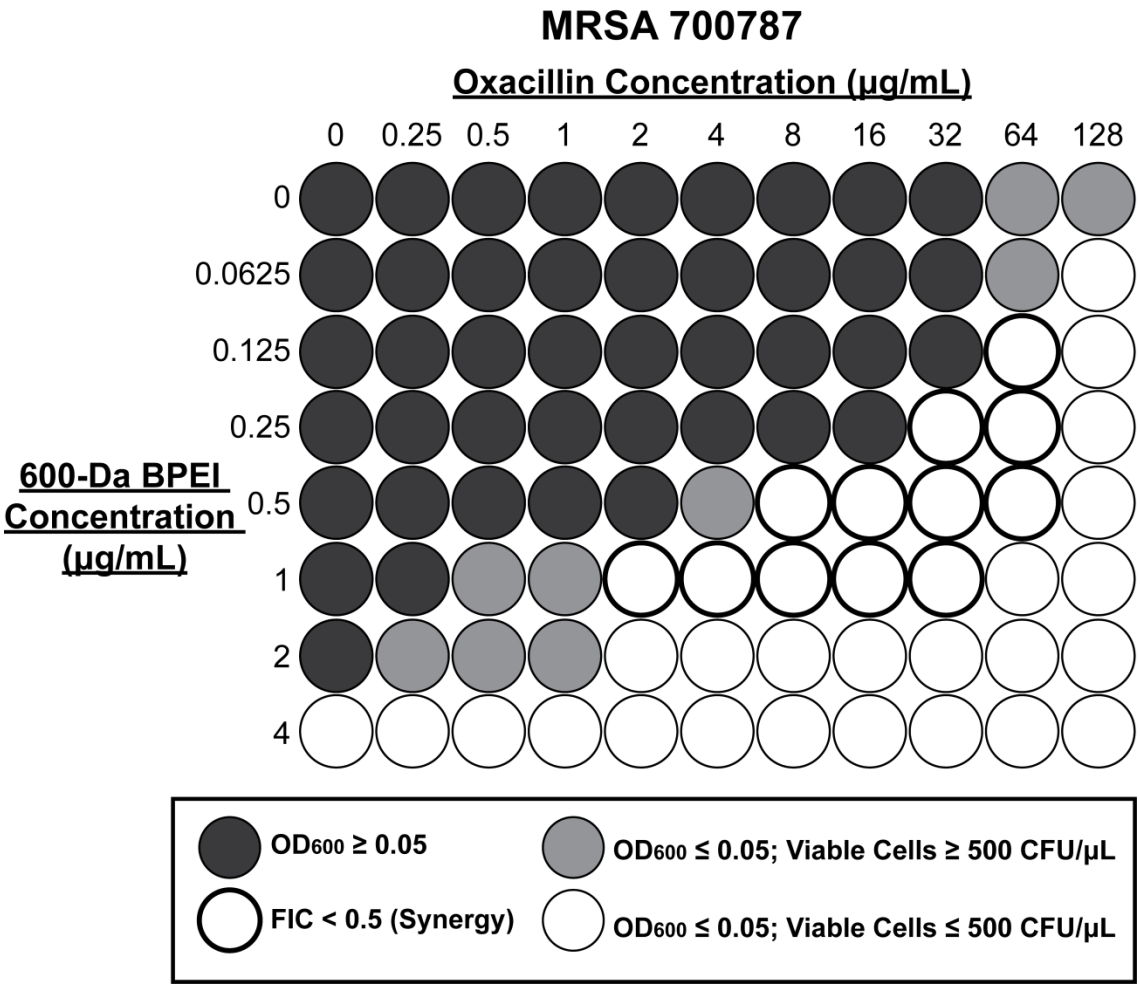


Figure 14. BPEI: oxacillin combination is bactericidal against MRSA. Dark shaded circles indicate wells where the bacteria grew as determined by an OD_{600} greater than 0.05. Lighter shaded circles show where cells were not killed but did not reach an OD_{600} of 0.05. Unshaded circles had less than 500 cells/µl. Bolded circles show an FIC less than 0.5.

BPEI does not have synergy with other antibiotics

Since BPEI has synergy with most of the tested β-lactams antibiotics, non-β-lactam antibiotics were also tested. Vancomycin, linezolid, and chloramphenicol each have different mechanism of actions. Vancomycin is a large a glycopeptide that targets cell wall synthesis. Linezolid, an oxazolidinone, inhibits protein synthesis and localizes intracellularly. Vancomycin and linezolid are prescribed to treat systemic MRSA

infections. Chloramphenicol inhibits protein synthesis but is not used to treat MRSA infections. Vancomycin, linezolid, and chloramphenicol did not yield significant MIC reductions in the presence of BPEI against any of the tested strains (Table 9). For both MRSA USA300 and MRSA MW2, the FICI for vancomycin and BPEI was 1.00 (Figure 15A, B). Linezolid showed additivity with BPEI against MRSA USA300 (FICI= 0.5; Figure 15C) and MRSA MW2 (FICI= 0.5; Figure 15D). Chloramphenicol was only tested against MRSA 700787 and only showed additivity with BPEI (FICI=0.5; Figure 15E). BPEI's efficacy at potentiating antibiotics is specific to β-lactam antibiotics which indicates that the mechanism of action involves PBPs.

Table 9. Minimum inhibitory concentrations and fractional inhibitory values of BPEI in combination with non-β-lactam antibiotics against MRSA.

Strain / **Antibiotic**	**MRSA MW2**		**MRSA USA300**		**MRSA 252**		**MRSA 33592**		**MRSA 700787**	
	MIC	FICI	MIC	FICI	MIC	FICI	MIC	FICI	MIC	FICI
BPEI	64	-	32	-	32	-	32	-	4	-
Vancomycin	1	1	1	1	1	1	2	0.5	2	1
Linezolid	2	0.5	1	0.5	1	0.5	1	0.5	2	0.5
Chloramph-enicol	-	-	-	-	-	-	-	-	8	0.5

Notes: MIC= minimum inhibitory concentration. FICI=fractional inhibitory concentration. Each value is the average of three separate trials.

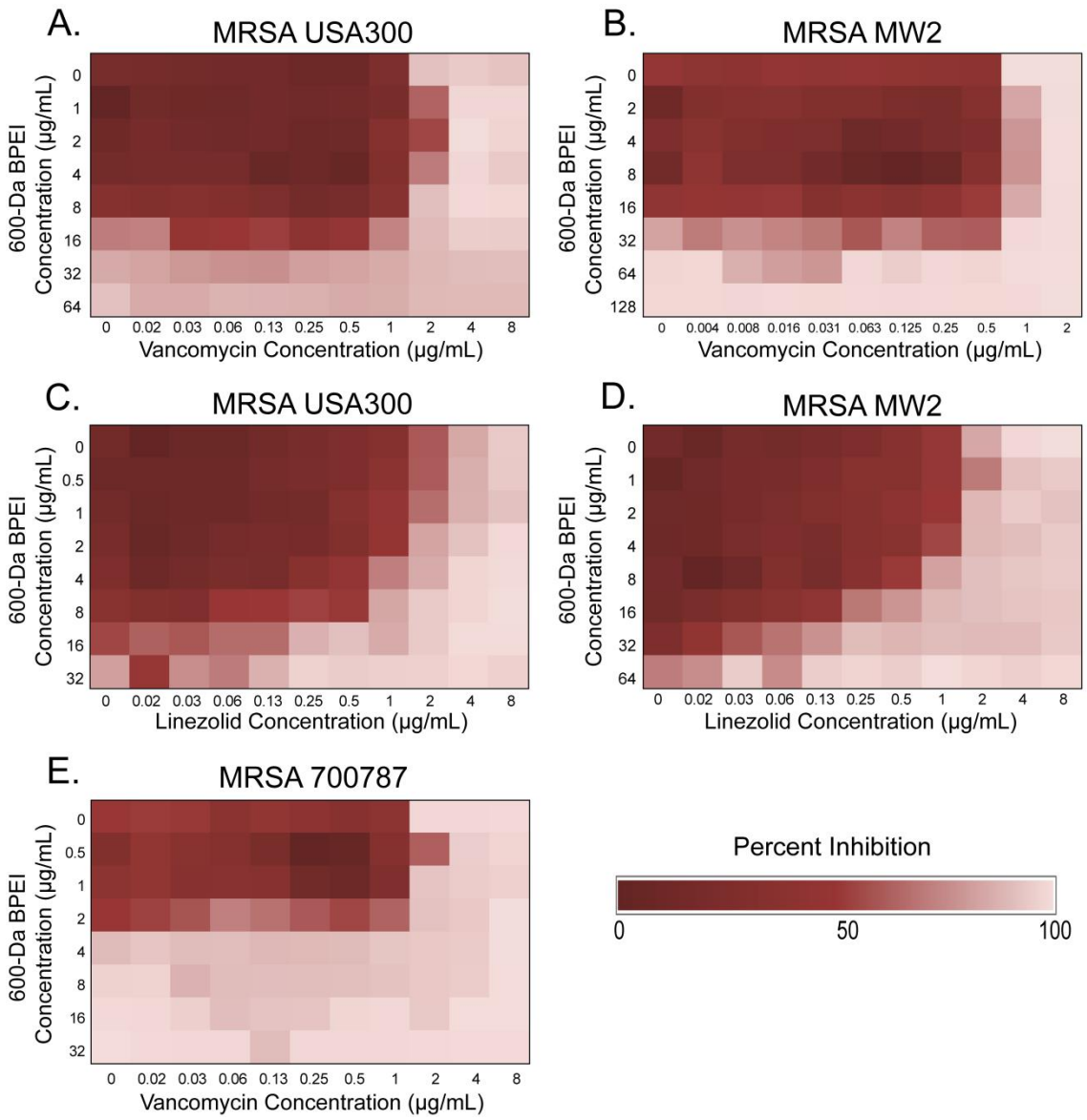


Figure 15. BPEI does not potentiate synergy with vancomycin or linezolid. Checkerboard assays show that BPEI did not have synergy with vancomycin (A,B) or linezolid (C,D) against MRSA USA300 or MRSA MW2. Chloramphenicol and BPEI do not have synergy against MRSA 700787 (E). Each assay was performed as three separate trials, and the presented data is shown as the average change in OD_{600}.

BPEI:β-lactam efficacy is specific to MRSA

BPEI potentiation of β-lactam antibiotics is specific to MRSA. A methicillin-susceptible *S. aureus* strain (MSSA 25923) was tested. BPEI only had modest additivity with oxacillin (FICI=0.750), ampicillin (FICI=0.750; Figure 16B), and amoxicillin

(FICI=0.750) against MSSA 25923 (Table 10). The different BPEI potentiation effects against MRSA versus MSSA support a mechanism involving PBP2a, which is present in MRSA but not in MSSA. We also report that the combination of BPEI and ampicillin does not have synergy against Gram-positive *B. subtilis* 6051 (FICI=1.0; Figure 16C) or Gram-negative *E. coli* 11775 (FICI=1.0; Figure 16D). These data lead us to believe that the mechanism by which BPEI potentiates β-lactams is specific for MRSA.

Table 10. Lack of synergy of 600-Da BPEI and β-lactams against MSSA 25923.

Strain	Antibiotic	MIC_A (μg/mL)		MIC_B (μg/mL)		FICI	Outcome
		Alone	Comb.	Alone	Comb.		
MSSA 25923	Oxacillin	0.064	0.032	32	8	0.75	Additivity
	Ampicillin	0.064	0.032	32	8	0.75	Additivity
	Amoxicillin	0.064	0.016	32	16	0.75	Additivity

Notes: MIC_A is minimum inhibitory concentration of the antibiotic; MIC_B is minimum inhibitory concentration of BPEI; FICI is fractional inhibitory concentration index.

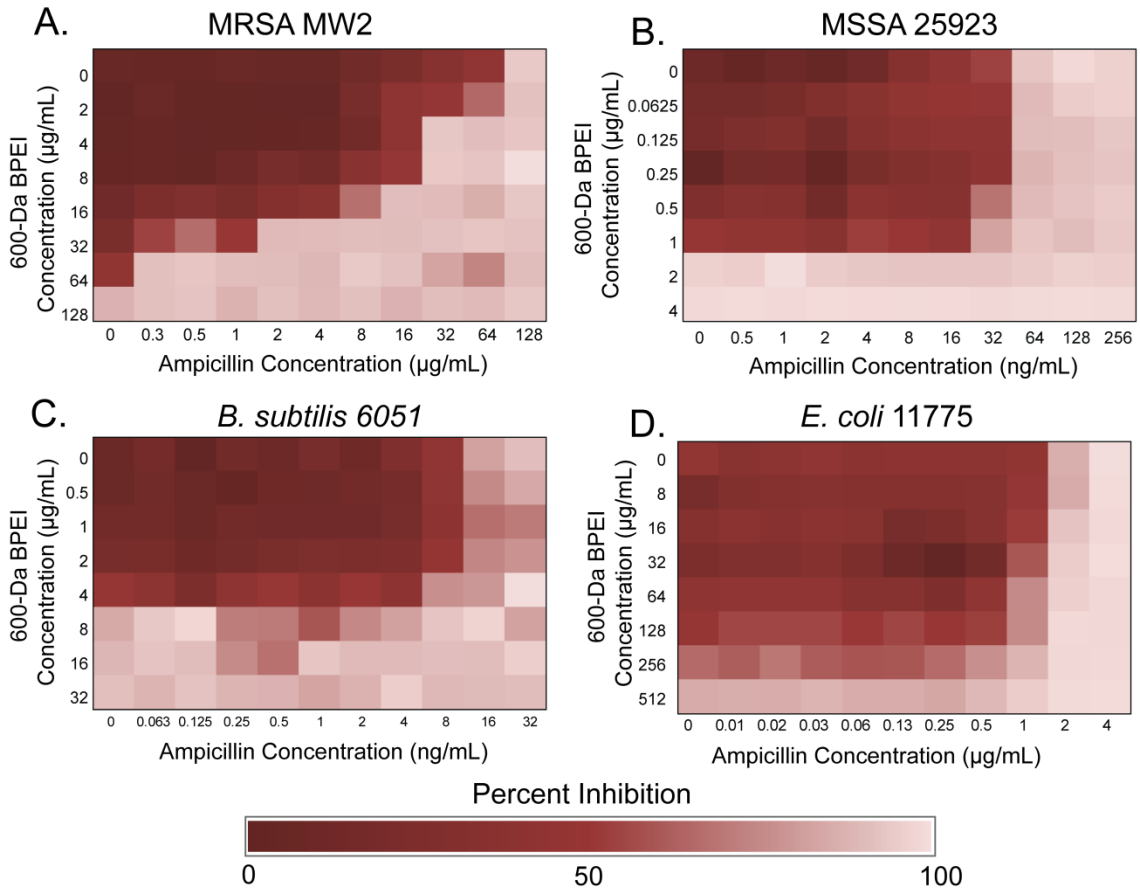


Figure 16. BPEI does not potentiates β-lactam activity against MSSA 25923, *B. subtilis* 6051, or *E. coli* 11775. BPEI and ampicillin have synergy against MRSA MW2 (A). Checkerboard assays show that BPEI not potentiates ampicillin (B) activity against MSSA 25923. No synergy is seen between β-lactams and BPEI against *B. subtilis* 6051 (C) or *E. coli* 11775 (D). Each assay was performed as three separate trials, and the presented data is shown as the average change in OD_{600}.

Conclusions

Rather than developing new inhibitors which require exhaustive clinical testing, we have discovered that some FDA-approved β-lactam antibiotics, such as oxacillin, can regain their efficacy against MRSA. The cost to the patient for treating Staph infections caused by MRSA is $695 to $29,000 more than treating MSSA infections.(*6*) The benefits to human health could be dramatic if the β-lactam + BPEI combination, used as a routine antibiotic therapy, can eliminate MSSA infections while

simultaneously preventing the growth of MRSA. Importantly, the data for *S. aureus* ATCC 25923 provide a potential route to treat, and prevent, antibiotic-resistant infections. By using a combination of BPEI and oxacillin to treat a non-resistant *S. aureus* infection, the emergence of β-lactam-resistant strains *in vivo* could be slowed. This benefit would not be possible with oxacillin alone. Currently, if a patient goes to the doctor with a Staph infection, the doctor will often prescribe antibiotics that are only effective if the infection is methicillin-susceptible. However, if the infectious agent is MRSA, the patient will have to undergo more vigorous treatments, such as intravenously antibiotics or amputation/ excision. Even still, one in seven patients infected with MRSA will end up dying from their infection.(*1*) Our proposal is that all patients with Staph infections will be prescribed BPEI in combination with a β-lactam (Figure 17). This would prevent the infection from getting worse in case the infectious agent is in fact MRSA; and therefore, increase the likelihood of success.

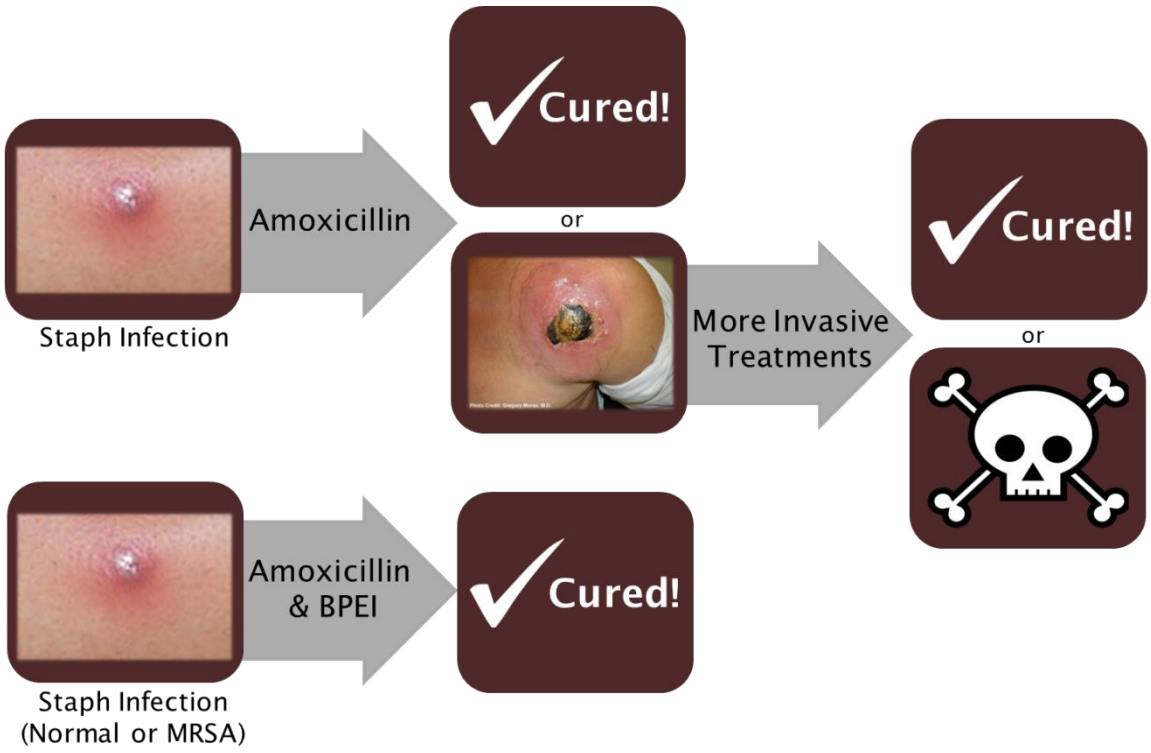


Figure 17. Proposed clinical application.

Chapter 4: Targeting Wall Teichoic Acid *In Situ* with Branched Polyethylenimine Potentiates β-Lactam Efficacy against MRSA

Background

The ability of BPEI to potentiate β-lactams against MRSA shows an interesting way of disabling resistance. BPEI was only able to potentiate β-lactams and did not have synergy with any of the other antibiotic classes tested. Additionally, the BPEI: β-lactam combination was only effective against MRSA which indicates a narrow-spectrum mechanism of action. A new focus to antibiotic development has been for narrow-spectrum agents because more available targets exist compared to broad-spectrum.(*94*) Thus, understanding the mechanism by which BPEI re-sensitizes MRSA to β-lactams would potentially open a new target and area for antibiotic development.

The cell envelope of Gram-positive bacteria is composed of a membrane, peptidoglycan, and teichoic acids. Methicillin, a β-lactam antibiotic, occupies the active site of penicillin binding proteins (PBP) 1, 2, and 3 to prevent the enzymatic cell-wall synthesis function in *S. aureus*. In the presence of β-lactam antibiotics, MRSA performs cell-wall synthesis using PBP2a, a transpeptidase enzyme with very low affinity for β-lactams. Hartman and Tomasz recognized and identified PBP2a in MRSA.(*117*) The β-lactam/transpeptidase complex is stable; however, resistance arises because the rate of complex formation is much slower than the *S. aureus* cell division time. Thus, it is nearly impossible for the complex to form *in vivo.(118)* Fuda et al. also presented a structure of PBP2a with no realistic access to the active site, suggesting there had to be a conformational change that took place as a result of binding non-crosslinked peptidoglycan at a location other than the active site, setting the groundwork for future

allosteric regulation papers.(*118*) Nevertheless, the cell wall remains an especially rich antimicrobial target, containing many opportunities for disruption, such as peptidoglycan, teichoic acids,(*41, 119*) and novel proteins.(*120*) While these targets have shown promise, side-effects and slow progress towards clinical usage have hindered efforts to reduce the rate of MRSA infection and mortality.(*121*) While it is possible to stop teichoic acid expression in the cytoplasm, thereby disabling the function of PBP2a,(*41*) the quantity of drug required for activity prevented development into a clinical MRSA treatment.(*121*)

Structure and Function of Teichoic Acids

Teichoic acids are anionic polymers that span the length of peptidoglycan in the cell walls of Gram-positive bacteria. Two types of teichoic acids exist: wall teichoic acid (WTA) and lipoteichoic acid (LTA). The teichoic acid portions of WTA and LTA have similar chemical structures, but they are linked to different cell regions. WTA covalently attaches to the NAM groups of peptidoglycan and extends to the extracellular space. LTA anchors to the lipid bilayer of the inner membrane with a linker and also extends to the extracellular space. Each teichoic acid consists of ribitol or glycerol phosphate groups and carbohydrates linked together with phosphodiester bonds (Figure 18). Diversity exists for the chemical structure of teichoic acids among bacterial species. Typically, *S. aureus* contains 1,5-D-ribitol-phosphates, but diversity can be seen even in the same strain.(*122*) *B. subtilis* WTA has a similar structure to that of *S. aureus* but has glycerol phosphates instead of ribitol phosphates and glycerol instead of N-acetylglucosamine. Gram-negative bacteria do not have teichoic acids.

Because of the large number of phosphate groups, teichoic acids provide an overall negative charge to the cell wall of bacteria. WTA constitutes up to 60% of the cell wall mass.(*123, 124*) Approximately one in nine peptidoglycan NAM units have WTA attached.(*123, 125*) Thus, WTA is an abundant and important component of the cell envelope.

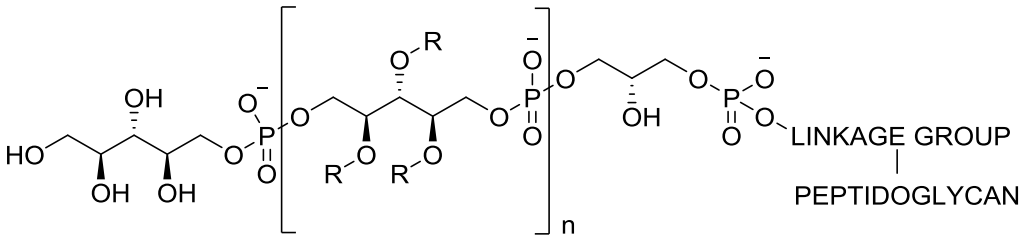


Figure 18. Structure of *S. aureus* teichoic acid (modified from Sewell and Brown).(*126*) R=H, D-ala, N-acetylglucosamine; n= 40 to 60 repeats.

Teichoic acids are known to be important for a variety of functions, including cell adhesion (*127, 128*) and biofilm production (*128, 129*) as well as host infection.(*127, 130*) However, their mechanisms are not well understood. Knockout strains of teichoic acid lost virulence and were unable to colonize *in vivo*.(*127, 131*) Gene knockout studies have shown that WTA mutants have clumping morphologies and reduced septa formations.(*132*) Lipoteichoic acid (LTA)-deficient mutants, conversely, have a drastically elongated morphology.(*133*) Additionally, WTA and LTA impart an overall negative charge to the cell wall, attracting metal cations.(*134-136*) Teichoic acids have proven essential for cell wall protein localization. Specifically, WTA is necessary for localization and activation of cell wall machinery, such as penicillin binding proteins (PBPs) and autolysins.(*123, 137, 138*) Inhibition of WTA synthesis led to improper localization of PBP2a/4, making MRSA susceptible to β-lactams.(*41, 139*) Although previously thought to be necessary, WTA is not essential to

viability but may be involved in β-lactam resistance.(*132, 140*) Atilano et al. found that WTA helps guide PBP4 to the division septum, which agrees with the knowledge that WTA mutants have decreased levels of crosslinking.(*137*) However, Gautam et al. contend that crosslinking in *S. aureus* occurs at both the division septum and the peripheral cell wall after division.(*141*) WTA was reported to be involved in bringing the autolysin Atl to the division septum.(*142*) FmtA, a protein upregulated in *S. aureus* in the presence of cell wall inhibitors, also lost septal localization in WTA knockout strains.(*138*) Preventing WTA synthesis or effectively preventing proper WTA function is a potentially viable area of antibiotic discovery. Thus, we were motivated by the connection between WTA deletion and cell wall morphology to disable WTA with a chemical agent that binds WTA in an electrostatic manner.

Principles of NMR, Confocal Microscopy and Fluorescently Labelled Proteins.

Principles of Nuclear Magnetic Resonance

Nuclear magnetic resonance (NMR) spectroscopy is a commonly used technique that can determine the structure and physical properties of organic and inorganic compounds. Magnetic fields around nuclei of atoms produce radio waves that can be detected with the instrument. Only nuclei with a spin can be detected in NMR spectroscopy; thus, not all nuclei are considered NMR active. Some commonly-used NMR active nuclei are ^{1}H, ^{13}C, ^{19}F, and ^{31}P. For NMR spectroscopy, the sample is placed inside a large magnet, which applies a constant magnetic field throughout the sample. After the sample is excited with a radio pulse, the weak signal is measured with radio receivers. A Fourier transform converts information from the time-domain to the

frequency domain. The magnetic moment of a nuclei is proportional to the spin of the nuclei and depends on the energy difference between the two spin states of the nuclei. However, differences in the electric environment lead to shifts in the frequency of the signals because the electrons around the nucleus oppose the applied magnetic field. Shielding occurs when the nucleus feels a weaker magnetic field due to an increased electron density around the nucleus. De-shielding occurs when the nucleus feels a stronger magnetic field because the electron density around the nucleus has been reduced. Differences in shielding versus de-shielding are often caused by neighboring atoms. Thus, the chemical shifts provide information about the chemical structure of the compound.

1D-NMR spectroscopy only provides information about one type of nuclei as frequency versus intensity. 2D-NMR spectroscopy plots two frequency axes which can relate adjacent atoms. 2D-NMR is helpful in understanding more complicated structures. Many types of 2D-NMR experiments exist. One of the most common types of 2D-NMR, also discussed in this dissertation, is heteronuclear multiple-bond correlation spectroscopy (HMBC). HMBC examines correlations between different nuclei (heteronuclear) over longer ranges (2-4 bonds). Other common methods are correlation spectroscopy (COSY) which looks at the same nuclei (homonuclear) correlations from adjacent atoms, total correlation spectroscopy (TOCSY) which looks at homonuclear correlations from longer ranges, or heteronuclear single-quantum correlation spectroscopy (HSQC) which looks at heteronuclear correlations of adjacent atoms. The intensity of these spectra are typically shown using a third-dimension and

displayed as contours. Ultimately, 1D- and 2D-NMR are valuable tools to better understand chemical structures, physical parameters, and molecular interactions.

Principles of Laser Scanning Confocal Microscopy

Light microscopy suffers from limitations in resolution at high magnifications because of diffraction rings. This phenomenon, called diffraction-limited resolution, equals the wavelength of light divided by two times the numerical aperture of the microscope. Resolution refers to the minimum distance between two objects that can be distinguished as separate points. The best resolution that can be obtained on a light microscope is approximately 200 nm. However, normal light microscopes rarely reach that limit because of a large depth of focus and lens aberrations.

Laser scanning confocal microscopy (LSCM), a high resolution fluorescence microscopy technique (Figure 19), can reach diffraction-limited resolution. For LSCM, a laser is scanned onto a specimen by the scanning unit. The laser excites a fluorophore on the sample which then emits a lower energy photon. A dichromatic mirror removes excitation rays and allows emitted rays through to the detector. The emitted ray then focuses through a pinhole aperture that removes any out of focus rays and prevents them from reaching the detector. The pinhole aperture allows for the microscope to view optical sections and overcomes limitation issues caused by a large depth of focus. The detector measures the number of photons from each spot of the imaging plane which creates a pixel. Then, each pixel is reconstructed to create the final image. LSCM makes it possible to reach diffraction-limited resolution limits and allows for imaging of interior cell components.

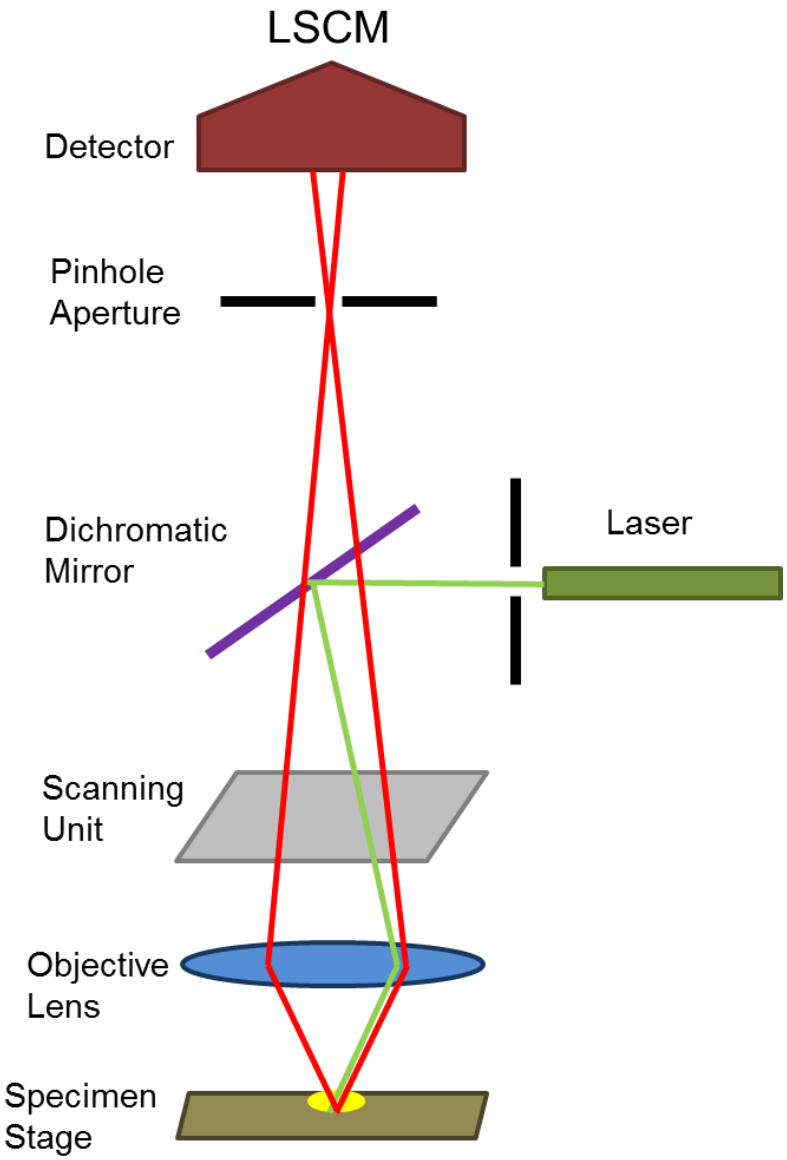


Figure 19. Diagram of a simplified LSCM.

Fluorescence occurs when a substance absorbs light radiation and emits that light as a form of luminescence. Typically, the emitted fluorescence has a longer wavelength and lower energy than the excitation radiation. A Jablonski diagram can be used to visualize this phenomenon (Figure 20). An electron in the ground state (S_0) absorbs a photon which excites that electron to an excited state (S_1). The excited

electron undergoes vibrational relaxation to the lowest vibrational level causing the electron to lose a small amount of energy. After, fluorescence occurs when the electron goes from the excited state to the ground state; in which, a photon of lower energy is released. The difference in wavelength between the excitation wavelength and the emission wavelength is known as the Stokes shift. For confocal microscopy, a fluorescent compound is excited with a laser beam.

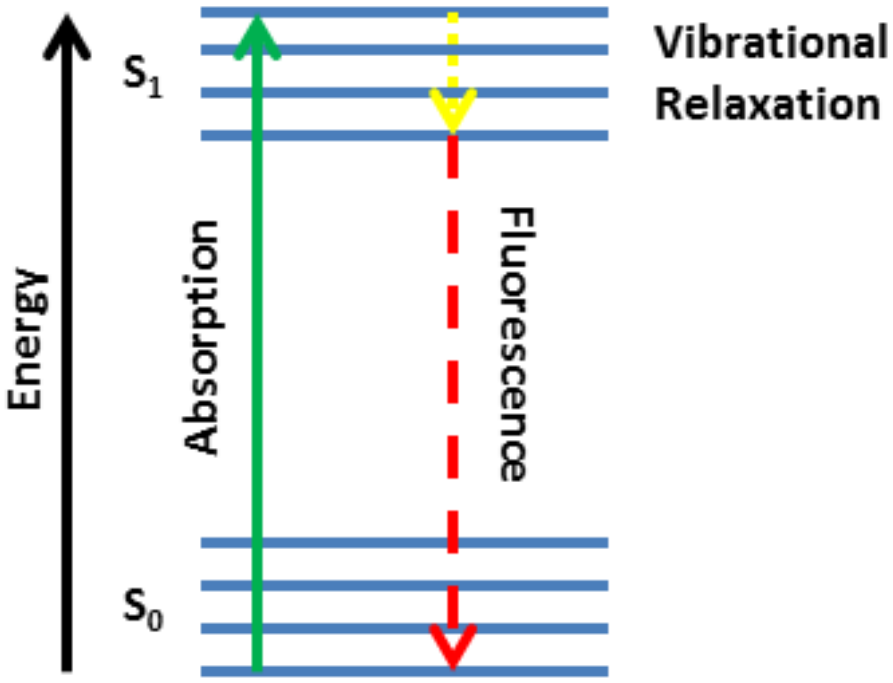


Figure 20. A Jablonski diagram showing the different energy levels that are encountered in fluorescence.

Principles of Fluorescence Labels

Fluorescent probes or dyes are commonly used for biological imaging. For fluorescent labelling, a specific protein, biomolecule, or functional group is tagged with a fluorophore. The fluorophore selectively binds to an area of concern and emits a fluorescence signal when excited by light of a certain wavelength. Each probe has a

different excitation wavelength spectrum and emission wavelength spectrum which allows for imaging of multiple probes in the same cell. Fluorescent labels can be either small fluorescent probes such as DAPI or fluorescent proteins such as green fluorescent protein (GFP). With the use of fluorescent dyes, we are able to accurately track the location of different biological components.

Small molecule fluorescent probes (typically 20-100 atoms), also called fluorophores, contain several π-bonds which allow for emission of light when excited with a light source. The π-system of the fluorophore is capable of absorbing photons of a certain wavelength range which excites an electron to an excited state. These probes usually have conjugated doubled bonds or aromatic groups which create an electronic environment favorable for fluorescence. Environmental factors such as pH, solvent, and chemical environment can affect the properties of the probe. Quantum yield refers to the efficiency of the number of emitted photons per absorbed photon. Each probe has a unique molar absorption coefficient which references how strongly the probe holds the light. Another important characteristic is the lifetime, the time required for an excited electron to return to the ground state. Photobleaching is another characteristic to consider which refers to loss of fluorescence upon continuous excitation.

The first fluorescent protein discovered, GFP, was discovered in the sea pansy in the early 1960s by Osamu Shimomura.(*143*) Since then, many GFP-derivatives have been made that excite and emit at different wavelengths, have increased stability, and can serve different functions. Most of the fluorescently labelled proteins have a beta barrel structure that creates a cylinder shape that protects the inner sidechains. The inward-facing sidechains of the barrel induces fluorescence in the protein and affect the

color of the chromophore because they create a hydrogen-bonding network and electron-stacking interaction. Fluorescent proteins tag other proteins or areas of interest without compromising the function of either protein. A large advantage of fluorescent proteins is that they can be introduced into the genome of bacteria which then allows for consistent expression after multiple growth cycles.

For this study, many different fluorescent probes were used. DAPI was used as a DNA stain to distinguish the cell wall from the cytoplasmic space. DAPI binds to A-T regions of DNA found in the cytoplasmic region. It has an excitation maximum wavelength of 358 nm and an emission wavelength of 461 nm. Another stain used was Alexa Fluor 488, a dye from the Alexa Fluor family of dyes. Alexa Fluor 488 was tagged to BPEI in order to track BPEI's localization in the cell. It has a maximum excitation of 495 nm and an emission wavelength of 519 nm. Fluorescent proteins were tagged to specific proteins in the cells. Green fluorescent protein (GFP), tagged to PBP2, has an excitation of 395 nm and an emission of 509 nm. Yellow fluorescent protein (YFP), tagged to PBP4, has an excitation peak of 514 nm and an emission peak of 527 nm. Each of these probes served specific purposes in order to determine the mechanism of action of the BPEI: β-lactam combination.

Purpose of Experiment

The continued emergence of resistance could be stemmed by re-sensitizing resistant strains of *S. aureus* to currently ineffective antibiotics, such as the β-lactam oxacillin. This approach will be viable only if the expression and/or functionality of proteins that contribute to resistance, such as PBP2a, are inhibited. PBPs are

indispensable for cell growth as they create essential crosslinks between adjacent peptidoglycan segments. Targeting PBP2a with inhibitors has been shown to re-sensitize resistant strains to methicillin.(*144*) In contrast, BPEI may indirectly disable PBP2a as evidenced by our discovery that BPEI administered in concert with β-lactams, makes MRSA susceptible to the antibiotics. The purpose of these experiments was to determine the mechanism by which BPEI potentiates β-lactam antibiotic activity against MRSA. Laser scanning confocal microscopy (LSCM) images show that BPEI binds to the cell wall where it can interrupt the function of teichoic acids, inactivate PBP2a, and restore β-lactam activity. NMR spectroscopy data demonstrate that BPEI binds to WTA, an anionic polymer found in MRSA cell walls, likely via electrostatic attraction between the cationic polymer and the anionic teichoic acid. Checkerboard assays using BPEI and β-lactams indicate that synergy is not present on a WTA-deficient mutant. Thus, WTA is necessary for BPEI's synergistic effect with β-lactams against MRSA. WTA is important for localization of MRSA's resistance factors, PBP2a and PBP4.(*137, 145*) LSCM of fluorescently-labelled proteins show that BPEI delocalized PBP4 from the division septa. Thus, the proposed mechanism behind BPEI's synergistic properties with β-lactam antibiotics is that the polymer indirectly disables PBP2a and PBP4 making MRSA susceptible to β-lactam antibiotics that then disables PBP1, 2, and 3.

Experimental Procedures

Synthesis of the BPEI:Dye Conjugate

Low-molecular weight BPEI (Sigma-Aldrich) was added to Alexa Fluor 488 dye provided in the Alexa Fluor 488 Protein Labeling Kit (Life Technologies) at a ratio of 200 µL BPEI (3 mg/mL stock in Milli-Q H_2O) per tube of powdered dye. After allowing the dye and BPEI to form the conjugate over 1.5 h at 25 °C, the product was stored at 4 °C and used without further purification. Images of unconjugated Alexa Fluor 488 and unconjugated BPEI were imaged to confirm that localization patterns were created by the BPEI:Alexa Fluor 488.

Labeling Cells with the BPEI:Dye Conjugate

Cultures of *E. coli* 11775, *B. subtilis* 6051 and MRSA 700787 at mid-log growth phase were pelleted by centrifugation at 2,000x g for 5 minutes, and the growth media supernatant was removed. 6 µM DAPI in phosphate-buffered saline (1X PBS, pH 7.2) was added to re-suspend the cell pellet, which was allowed to incubate for 5 minutes at room temperature. The BPEI-dye conjugate was then added to a final concentration of 100 µg/mL. Two control samples were prepared with either unconjugated BPEI or Alexa Fluor 488 alone and added to MRSA cells as described above. The stained bacterial cells were immediately fixed by resuspension with 4% paraformaldehyde (PFA) followed by a 10-fold dilution in 1X PBS. Cells were added to a microscope slide immediately prior to imaging.

Confocal Microscopy and Image Processing

PFA-fixed cells were mounted in 1X PBS and imaged using a Leica SP8 LSCM with a 63x/1.4NA oil objective. A 405 nm GaN diode laser line was used to image DAPI, and a 488 nm argon laser line was used to observe Alexa Fluor 488 fluorescence. Single optical sections were acquired of cells that had adhered to the coverslip, for highest axial resolution, with a pixel resolution of 80 nm × 80 nm. Instrument settings were kept fixed for all imaging to allow for direct comparison of fluorescence intensity.

To visualize the relative localization of fluorescence, independent of intensity, images were processed (ImageJ v1.49m) such that the total fluorescence intensity within each image was visible. To determine the relative fluorescence intensity between images, the fluorescence intensity of both the DAPI and the Alexa Fluor 488 were normalized to the respective intensities in the MRSA sample treated with BPEI conjugated with Alexa Fluor 488.

WTA Purification

The NMR experiments require 10–20 mg WTA isolated from 2-4 liters of bacterial cell culture. The poly(ribitol phosphate) WTA used in this work was isolated from *B. subtilis* W23(*146, 147*) (*B. subtilis* (Ehrenberg) Cohn ATCC 23059) rather than from MRSA, allowing high volumes of culture to be processed with minimal risk to personnel. This also allows us to take the sample into the NMR facility room, which is not rated for BSL-2 work. In the rare instance of sample breakage, using WTA from *B. subtilis* W23 does not present a clean-up hazard nor require decontamination of the expensive NMR analysis probes, magnets or spectrometers.

B. subtilis W23 cells were grown in LB media to an OD_{600} reading of approximately 0.8. After growth, the cells were harvested by centrifugation and physically disrupted using an Avestin® EmulsiFlex-C3 homogenizer. The insoluble cell wall was collected, placed in boiling 6% (w/v) SDS for 1 hour, washed with sterile water and EDTA then placed in 10% trichloroacetic acid (TCA) and treated for 48 hours at 4 °C. After allowing the TCA to remove the bound WTA from the cell wall, the WTA was collected in the supernatant and placed into a 500-Da molecular weight cutoff dialysis membrane. Membrane dialysis was performed at 4 °C in 1.5 L of sterile water with continual water changes over a 48-hour period. The final 4 hours of dialysis took place in a 1-kDa molecular weight cutoff membrane to assure sample purity. The sample was lyophilized and kept at -20 °C until use.

NMR Spectroscopy

NMR samples were prepared in Eppendorf tubes by mixing purified WTA with low-M_W BPEI in D_2O. The pH was measured with a microscopic pH probe and adjusted to 7.2 if necessary. A 3-mm NMR tube was filled with 160 μL of a 2 mM sample of WTA, BPEI, or a combination of 2 mM BPEI with 2 mM WTA in D_2O. All NMR experiments were performed in 3-mm tubes using 28 shims Agilent VNMRS-500 MHz equipped with a triple-resonance PFG probe. Pulse sequences for each experiment were supplied by Agilent. Data acquisition and processing were completed using VNMRJ 2.2C software on the Red Hat Linux 4.03 operating system. After processing, all experiments were analyzed using Sparky software. The NMR spectra were collected at 277K and referenced internally to the water signal at its correlating temperature.

Checkerboard Assay of WTA-Deficient Cells

MRSA MW2 and MRSA MW2 Δ*tarO* (referenced in Campbell et al., 2001)(*145*) were a generous gift from Professor Suzanne Walker. Checkerboard assays were used to determine synergy of BPEI with β-lactam antibiotics against bacteria. Stock solutions of antibiotics were made in DMSO and added to pre-sterilized 96-well plates with cation-adjusted Mueller-Hinton Broth so that the final DMSO concentration was <1%. Bacteria were added to each well on the plate so that the final cell density was ~5 x 10^5 cells/mL. Optical density readings were made immediately after inoculation using a Tecan Infinite M20 plate reader with a wavelength of 600 nm. The plates were incubated for 20 hours in a humidified incubator at 35 °C and a final OD_{600} reading was recorded. The change in OD_{600} was calculated by subtracting the initial OD_{600} from the final OD_{600} reading. A change in OD_{600} greater than 0.050 was considered to be positive for growth. The minimum inhibitory concentration (MIC) was assigned as the lowest concentration of antibiotic or BPEI that did not allow growth. The fractional inhibitory concentration index (FICI) was calculated using the previously-established equation.(*112*) An FICI lower than 0.5 indicates synergy, between 0.5 and 1 represents additivity, and greater than 1 shows antagonism. Each assay was done in triplicate and reported as the modal FICI value.

Imaging of Fluorescently Labeled Proteins

MRSA COL strains with green fluorescent protein (GFP)-labelled PBP2 or yellow fluorescent proteins (YFP)-labelled PBP4 were a generous gift from Professor

Mariana Gomes de Pinho. Bacteria were inoculated 0.5% into TSB media from an overnight culture. Some samples were grown in 64 μg/mL BPEI. The cells were grown to mid-log phase at 37 °C (OD_{600}=0.5). After growth, the cells were centrifuged, and the supernatant was removed. The cells were stained with DAPI to differentiate the cytoplasm. The cells were centrifuged and supernatant was removed. After the samples were fixed with 4% paraformaldehyde for 10 minutes, the paraformaldehyde was removed and the samples were mounted in 1x PBS. Samples were imaged using a Leica SP8 LSCM (Leica, Buffalo Grove, IL, USA) with a x64/1.4 numerical aperture oil objective. A 405 nm GaN diode laser line was used to image DAPI and a 488 nm argon laser line was used to observe GFP and YFP fluorescence. Single optical sections were acquired from cells that had adhered to the coverslip with a pixel resolution of 30 nm. Instrument settings were constant for all imaging to allow for direct comparison. Images were processed with ImageJ so that the fluorescence intensity for each signal was visible. Quantitative analysis of each image was done, and ANOVA was used to establish statistical significance.

Results and Discussion

BPEI localizes on the cell wall of Gram-positive bacteria

Based off the efficacy data in Chapter 3, we anticipate that BPEI re-sensitizes MRSA to β-lactam antibiotics by interacting with teichoic acids. If true, BPEI's interaction with MRSA should be confined to the cell wall. By conjugating BPEI to a fluorescent marker, Alexa Fluor 488, we were able to visualize BPEI localization in bacterial cultures using LSCM. Individual transverse optical sections clearly show BPEI

interaction with the MRSA 700787 cell wall region (Figure 21A). Using DAPI, a DNA-binding fluorescent dye, as a marker for the cytoplasm within the cells (Figure 21B), the merged image (Figure 21C) confirms that BPEI was not detected within the cytoplasm, verifying that BPEI does not traverse the lipid bilayer membrane. BPEI: Alexa-Fluor 488 similarly bound to the perimeter of *B. subtilis* 6051 cells (Figure 21D-E). Control images of *B. subtilis* cells (Figure 22) show that the signal was not caused by unconjugated Alexa Fluor 488 or auto-fluorescence. *B. subtilis* and MRSA are both Gram-positive bacteria with similar cell wall structures.

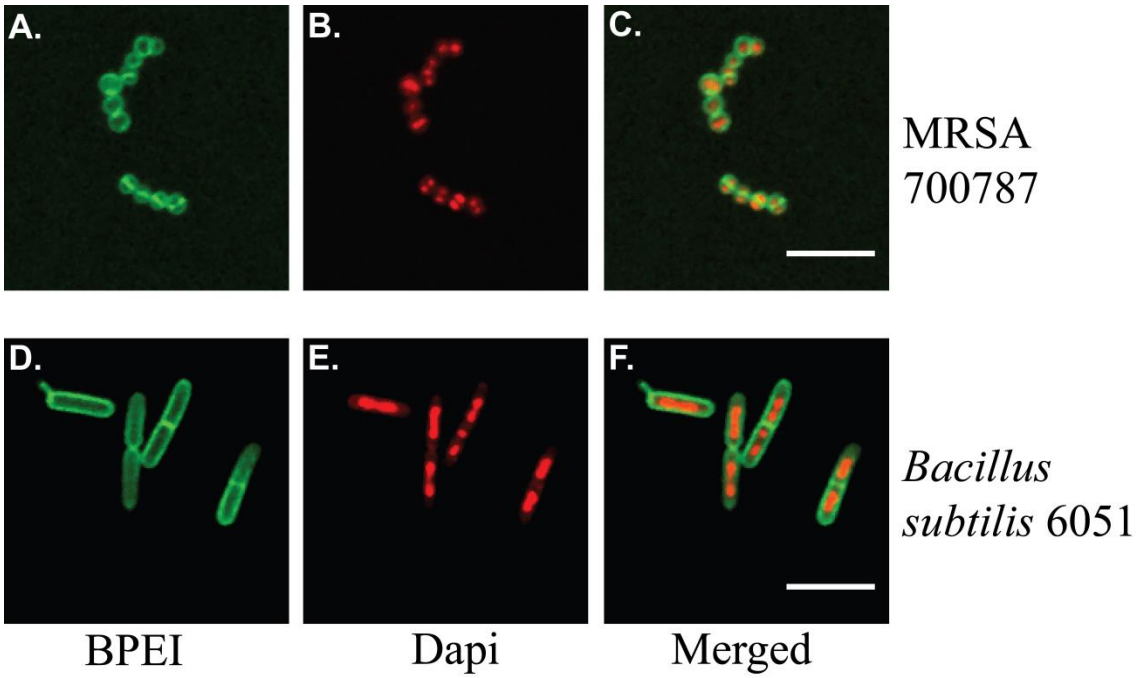


Figure 21. Optical sections of BPEI binding to MRSA and *B. subtilis*. MRSA, stained with BPEI: Alexa Fluor 488 (A) and DAPI (B), is imaged by LSCM. The merged image (C) shows BPEI binding to the cell surface but not within the cytoplasm. Similarly, *B. subtilis* stained with BPEI: Alexa Fluor 488 (D) and DAPI (E), and the merged image (F), shows a high affinity between BPEI and *B. subtilis*. Scale bars equal 5 µm.

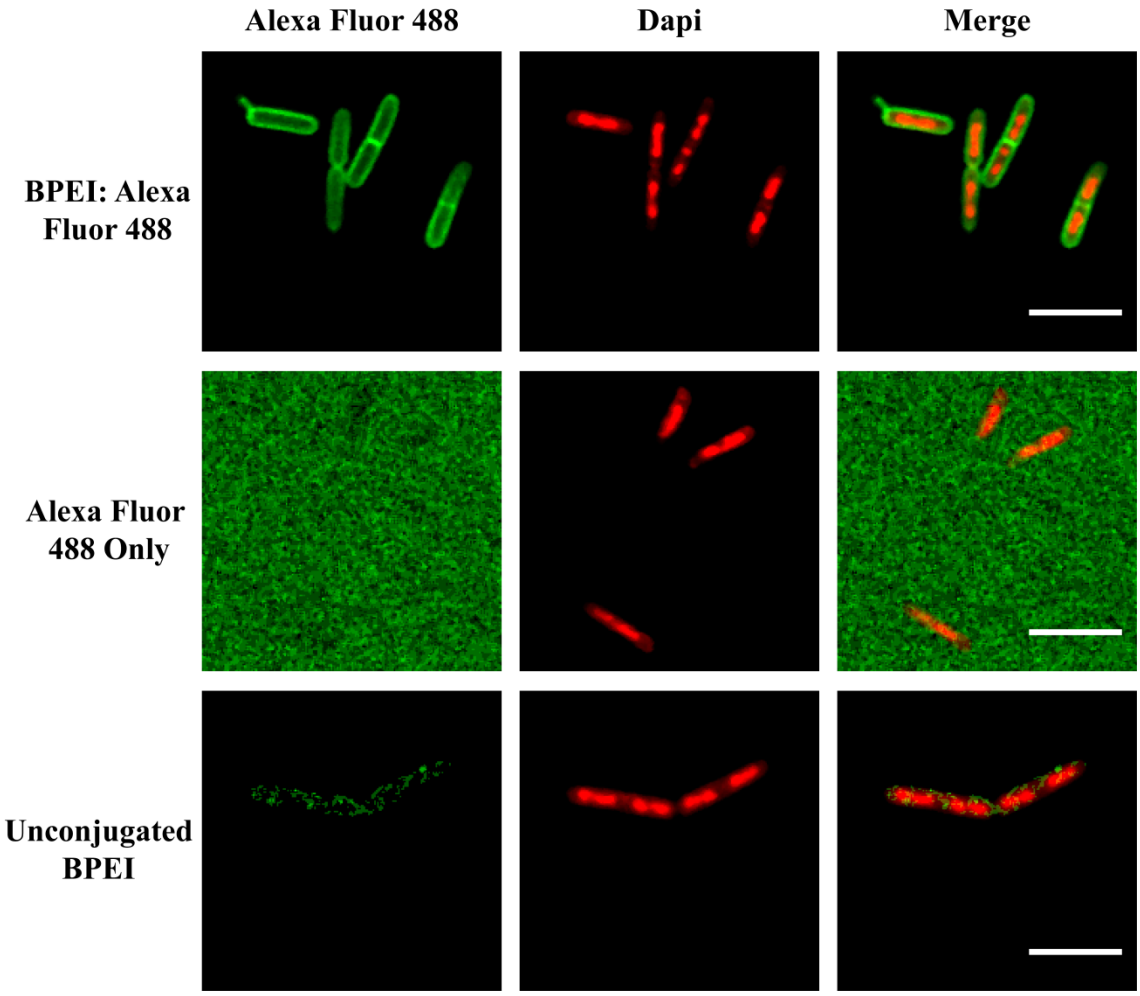


Figure 22. Alexa Fluor 488 signal was caused by conjugated BPEI. Images shown are *B. subtilis* cells treated with BPEI:Alexa Fluor 488 (top row), unconjugated Alexa Fluor 488 (middle row), or unconjugated BPEI (bottom row). The left column shows the detected Alexa Fluor 488 signal. The middle column shows the detected DAPI signal. The right column shows the merged images with both signals. Each image shows raw intensity. Scale bars equal 5 μm.

Optical sections of *E. coli* cells treated with BPEI: Alexa-Fluor 488 revealed minimal fluorescence intensity within the cell envelope, indicating a weaker interaction between the *E. coli* cell envelope and BPEI (Figures 23). This may explain the absence of antibiotic potentiation against *E. coli* in our study (Figure 16D). The absolute intensity shows non-specific interaction (Figure 23A-C). When the fluorescence signal intensity is normalized to the MRSA signal, no Alexa Fluor 488 signal is detected

(Figure 23D-E). *E. coli*, a Gram-negative bacteria, has an outer cell membrane that may prevent BPEI from getting to the cell wall to localize. Also, Gram-negative bacteria do not have teichoic acids.

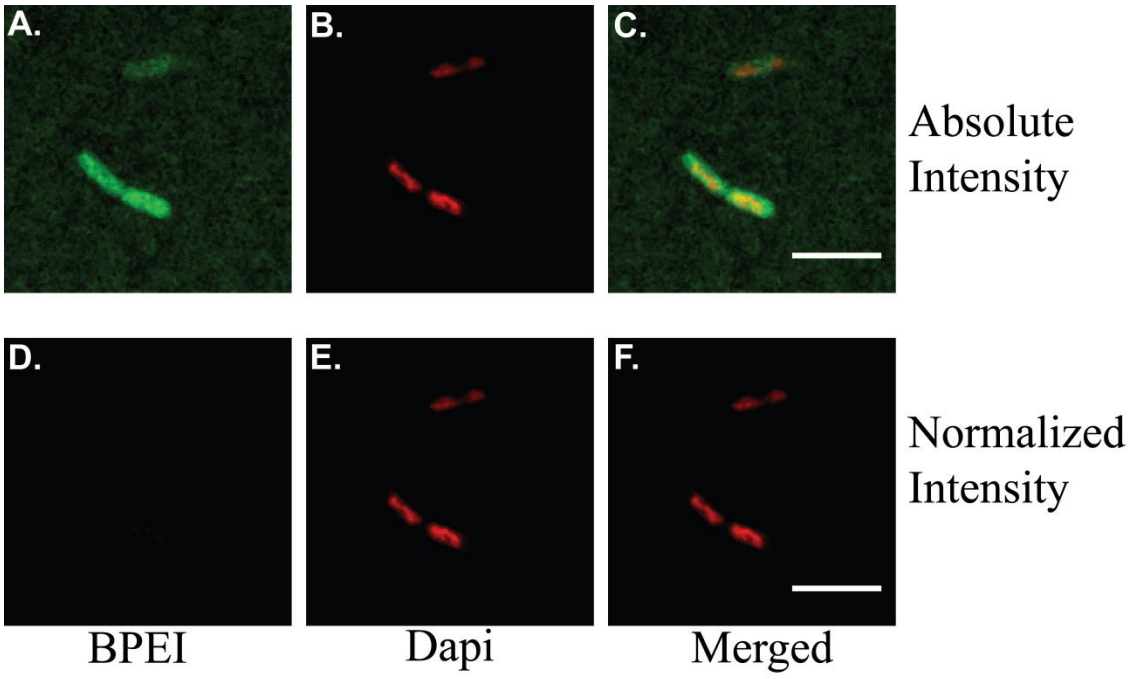


Figure 23. Optical sections of BPEI binding to *E. coli* 11775. *E. coli* stained with BPEI-Alexa Fluor 488 (A) and DAPI (B), is imaged by LSCM and the absolute fluorescence intensity is shown. The merged image (C) shows non-specific localization of BPEI. BPEI is not seen when normalized to the fluorescence intensity of BPEI on *B. subtilis* (D-F). Scale bars equal 5 µm.

The microscopy data, showing BPEI located in the cell wall region and not the cytoplasm, suggests that the observed antibiotic potentiation against MRSA is caused by an interaction of BPEI with some component of the bacterial cell wall. One major component of the Gram-positive cell wall is teichoic acid, a phosphodiester polymer whose anionic phosphate groups have been shown to interact strongly with metal cations.(*134-136*) BPEI, with its polycationic properties, has the potential for very strong electrostatic interactions with the polyanionic WTA molecules. This interaction

would involve the primary amines of BPEI and the phosphate groups of WTA (Figure 24). This interaction can be observed using nuclear magnetic resonance (NMR) studies of mixed BPEI-teichoic acid solutions and compared to NMR spectra of pure teichoic acid.

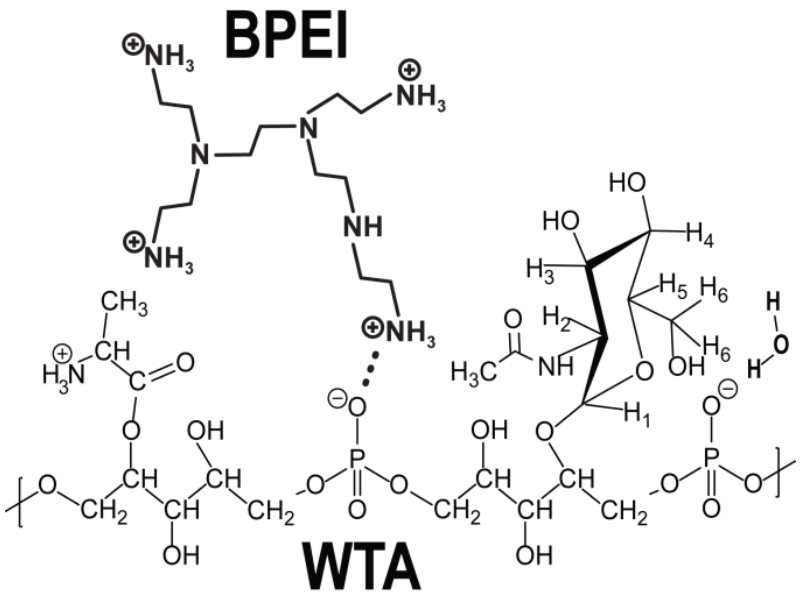


Figure 24. The cationic amine groups of BPEI electrostatically bind to the anionic phosphate groups of WTA.

BPEI electrostatically binds to WTA

The 1-D ^{31}P spectra (Figures 25A, B) show significant changes after mixing WTA with low-M_W BPEI. WTA is a phosphodiester polymer with a heterogeneous arrangement of N-acetylglucosamine (NAG), D-alanine, and hydroxyl groups. This creates variations in conformation of the poly(ribitol) backbone and differences in the phosphate conformations that generate distinct ^{31}P NMR peaks. In the presence of low-M_W BPEI, the ^{31}P NMR peak at 1.3 ppm is very intense, demonstrating that a large fraction of the phosphates have similar conformations. However, signals near 4 ppm are produced by phosphates in a de-shielded environment. The downfield shift arises from a

loss of electron density around the phosphorous nucleus, an effect that could be caused by a hydrogen bond between the phosphate oxygen and a BPEI amine group. The addition of BPEI also increases the intensity of cross peaks in the $^{1}H^{31}P$ HMBC (heteronuclear multiple bond coupling) NMR data (Figure 26A, B). This experiment relies on strong through-bond coupling between the ^{1}H and ^{31}P nuclei. For flexible molecules, internal motion and dynamics causes relaxation of NMR signals;(*148, 149*) and thus, the $^{1}H^{31}P$ HMBC signals are difficult to observe. When molecular motion is restricted, the signals are stronger. Phosphate:amine binding from the WTA:BPEI interactions likely occurs through electrostatic attraction between the numerous cationic primary amines of BPEI and anionic phosphate groups of WTA (Figure 24). Low molecular weight quaternary ammonium compounds have recently been shown to overcome resistance if the number of cationic sites is increased.(*150*) Therefore, the optimal cationic amine polymer should have a high number of primary amines while minimizing cytotoxicity with a low molecular weight.

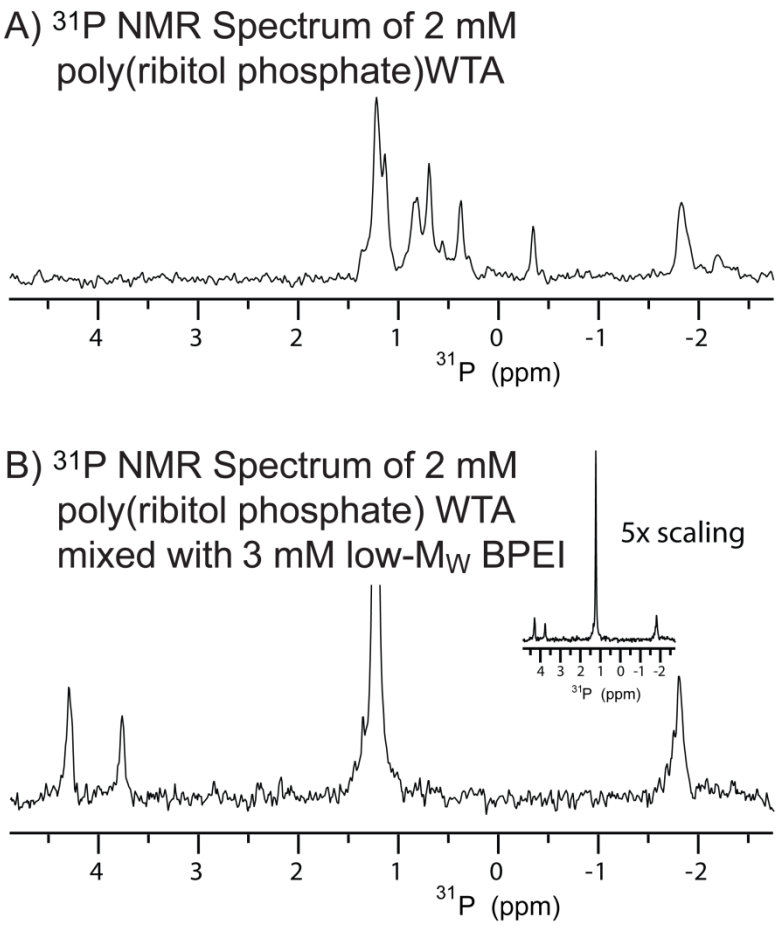


Figure 25. ^{31}P NMR spectra of WTA before (A) and after the addition of low-M_W BPEI (B) show significant changes in phosphate chemical shift caused by changes in the chemical environment.

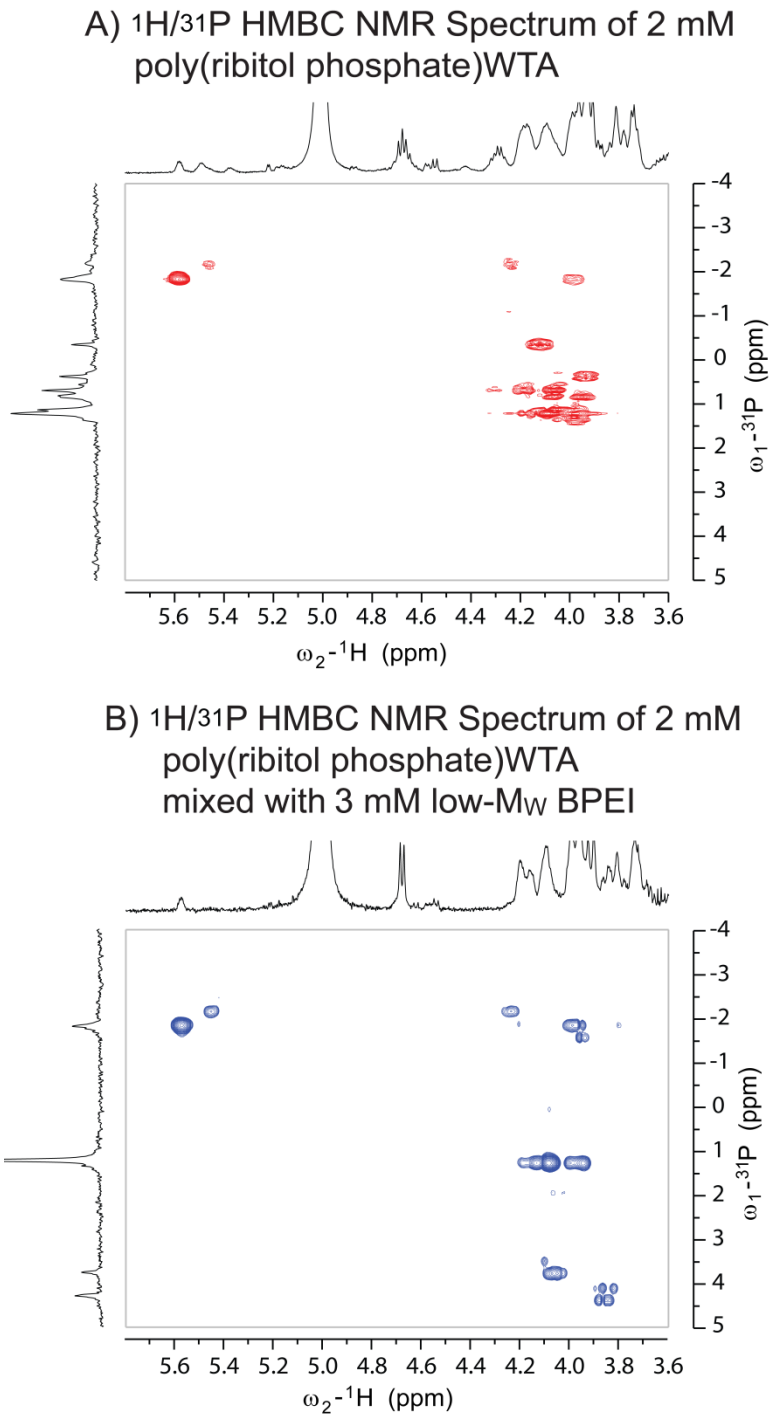


Figure 26. Spectral changes are also manifested in the heteronuclear multiple-bond correlation (HMBC) spectra when comparing pure WTA (A) and WTA with BPEI (B). The P-31 signals near 4 ppm are correlated with the proton signals of NAG sugar groups. However, clear identification of specific interactions is prevented by the heterogeneous nature of WTA functional groups, BPEI branching, and WTA:BPEI binding interactions.

Because low-M_W BPEI binds to WTA, the cationic polymer has the ability to change WTA properties by altering molecular structure and/or creating steric bulk from the branched polymer. This would change or prevent the interaction of WTA with PBP2a and thus disable the enzyme. The same effect can be created through WTA-deficient strains of MRSA, which are re-sensitized to amoxicillin, ampicillin, methicillin, nafcillin, and ceftizoxime.(*41*) An inhibitor of WTA synthesis, tunicamycin, re-sensitizes MRSA to β-lactams such as methicillin, oxacillin, cefotaxime, and several others.(*145*) Inhibition of another regulatory gene, *tarG*, also re-sensitizes MRSA strains to traditional β-lactams(*132, 140, 151*) like imipenem.(*119*) Thus WTA, while not essential to viability,(*132, 140, 151*) is involved in β-lactam resistance.(*152*) WTA helps to optimally localize PBP2a, and WTA-deficient mutants show a decreased functionality of the protein.(*41*) It additionally localizes PBP4, which is essential for the highly cross-linked peptidoglycan exhibited by MRSA and for the expression of β-lactam resistance in CA-MRSA strains.(*137*) Thus, restoration of β-lactam activity in therapeutic clinical usage could be achieved with antibiotics or other compounds that target WTA synthesis or interrupt the ability of WTA to localize PBP2a in the proper configuration required for peptidoglycan crosslinking. If this perspective is true, there should be little or no benefit when BPEI and β-lactam antibiotics are used to treat non-resistant *S. aureus* (MSSA) strains that do not express PBP2a. BPEI and β-lactam antibiotics did not have synergy against non-MRSA strains such as MSSA, *B. subtilis* 6051, and *E. coli* 11775. Also, BPEI did not provide a benefit for potentiating non-β-lactam antibiotics.

WTA is important for BPEI potentiation of β-lactam antibiotics

We hypothesized that BPEI potentiation of β-lactam antibiotics requires WTA. Studies have shown that WTA is important for β-lactam resistance in MRSA and aids with the localization of PBP4 to the division septum.(*41*, *145*, *153, 154*) WTA is dispensable for cell growth; however, WTA-deficient mutants of MRSA have an increased susceptibility to β-lactam antibiotics.(*145*) Also, inhibiting WTA synthesis by chemical inhibition of TarO, the protein responsible for the first step of WTA synthesis, results in a decreased resistance.(*145*) Recent work focused on development of new WTA inhibitors to fight MRSA with reduced protein binding effects.(*154-156*) Removal of WTA through genetic or chemical means reduced CFUs in mice treated with imipenem.(*153*) Disabling mature WTA in the cell wall should have a similar effect.

The cationic amines of BPEI electrostatically interact with the phosphate groups of WTA, sterically hindering the WTA and cell wall. Thus, we wanted to evaluate the requirement of WTA for synergy seen between oxacillin and BPEI against MRSA. MRSA MW2 Δ*tarO*, a WTA-deficient mutant, was used for this purpose.(*145*) For wild-type MRSA MW2, oxacillin and BPEI had synergy (FICI= 0.250; Figure 27A). The MIC of oxacillin was 64-fold lower against MRSA MW2 Δ*tarO* (0.5 μg/mL) in comparison to the wild-type MRSA MW2 (32 μg/mL), which supports the premise that WTA is important for β-lactam resistance in MRSA. For MRSA MW2 Δ*tarO*, the MIC of oxacillin only dropped 2-fold so that the FICI of the BPEI:oxacillin combination was 0.531, indicating additivity instead of synergy (Figure 27B) Also, a checkerboard assay was performed using sub-lethal tunicamycin, a drug found to inhibit WTA

synthesis.(*145*) Although tunicamycin is a good potentiator of β-lactams against MRSA, it cannot be used clinically because of severe neurological toxicity.(*157, 158*) Tunicamycin decreased the MIC of oxacillin to 0.250 μg/mL (128-fold) against wild-type MRSA MW2 (Figure 27D). Adding tunicamycin to the checkerboard assay of oxacillin and BPEI removed synergy against MRSA MW2 (Figure 27C). Both of the assays for MRSA MW2 Δ*tarO* and MRSA MW2 with tunicamycin showed no synergy between oxacillin and BPEI, which tells us that WTA is essential for the synergistic mechanism of BPEI and oxacillin. The combination of BPEI and ampicillin was also tested against MRSA MW2 and MRSA MW2 Δ*tarO*. BPEI and ampicillin have synergy against MRSA MW2 (FICI= 0.188; Figure 28A). However, BPEI did not exhibit synergy with ampicillin against MRSA MW2 Δ*tarO* (FICI= 0.500; Figure 28B). These data suggest that the synergistic effects seen between BPEI and β-lactam antibiotics require WTA and that WTA is likely the target of BPEI.

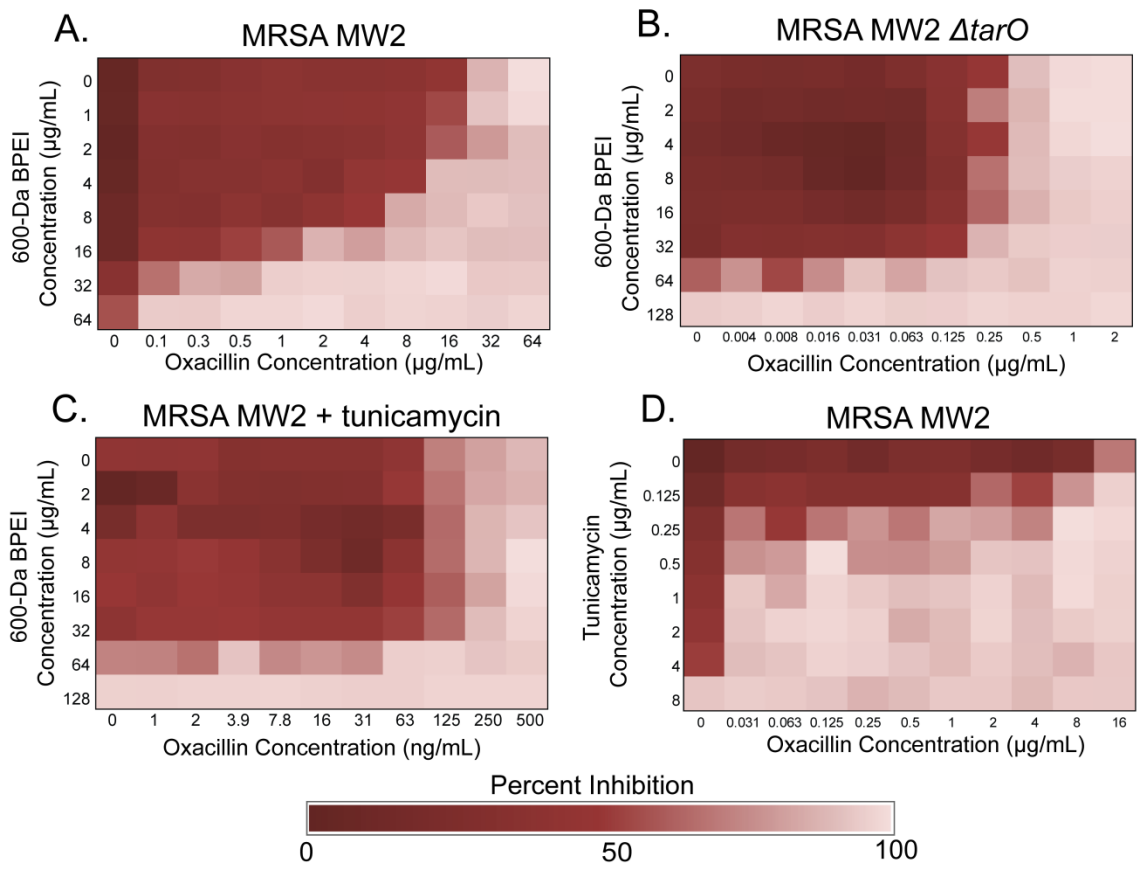


Figure 27. Mechanism by which BPEI makes MRSA susceptible to oxacillin is through WTA. BPEI and oxacillin have synergy against MRSA MW2 (A). Synergy is lost against MRSA MW2 Δ*tarO* (B) and MRSA MW2 with sub-lethal tunicamycin (0.250 µg/mL; C). Tunicamycin potentiates oxacillin against MRSA MW2 (D). Each assay was performed as three separate trials, and the presented data is shown as the average change in OD_{600}.

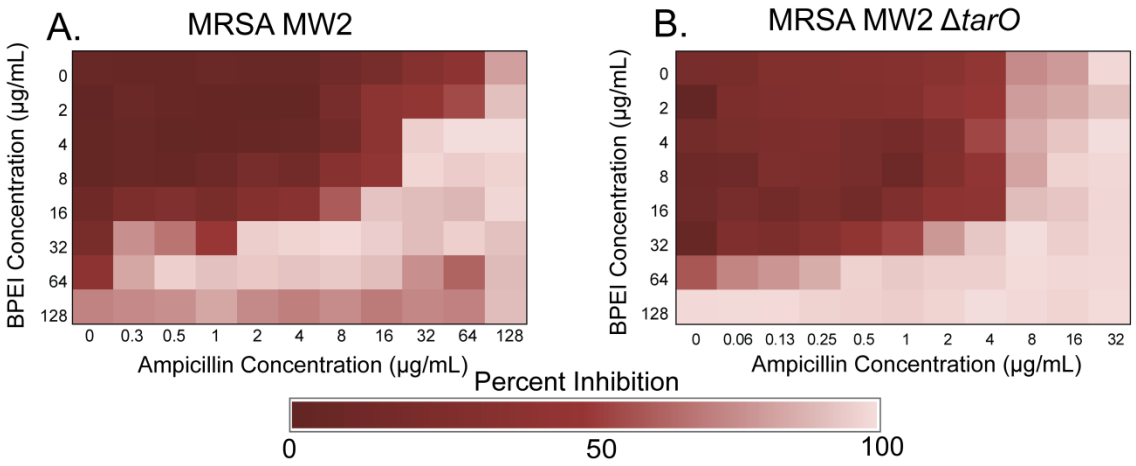


Figure 28. WTA is required for synergy between ampicillin and 600-Da BPEI. BPEI and ampicillin are synergistic (FIC=0.188) on the wild-type MRSA MW2 (A). MRSA cells lacking WTA through deletion of *tarO* (B) do not have synergy (FIC=0.5). Each assay was performed as three separate trials, and the presented data is shown as the average change in OD_{600}.

BPEI prevents proper localization of cell wall machinery

BPEI localizes in the cell wall of Gram-positive bacteria (including MRSA) where it electrostatically binds to WTA. We hypothesize that *in situ* binding of BPEI to WTA would delocalize PBP4 and PBP2a to prevent proper function of MRSA's resistance factors. Although all *S. aureus* strains have three PBPs that crosslink the cell wall (PBP1, PBP2, and PBP3), some MRSA strains also have PBP4 which aids in resistance for CA-MRSA.(*47*) WTA not only localizes PBP4 but also appears to be important for PBP2a, as indicated by the fact that genetic modification and chemical inhibition of WTA synthesis causes MRSA to become re-sensitized to β-lactams.(*137, 145, 159*) This led to the hypothesis that BPEI sterically hinders WTA, thereby preventing proper localization of PBP2a and PBP4. This *in situ* binding of WTA with BPEI has not been investigated previously, though chemical inhibition of WTA synthesis has been shown to work in combination with β-lactam antibiotics to kill

MRSA.(*145, 153-156, 159*) MRSA COL strains with GFP-labelled PBP2 or YFP-labelled PBP4 were obtained from Professor Mariana Gomes de Pinho. PBP4:YFP normally localizes at the division septum of dividing cells. However, PBP4:YFP delocalizes throughout the entire cell wall when WTA synthesis is prevented.(*137*) PBP2:GFP delocalizes when FtsZ (membrane-associated filaments that form the Z-ring of cell division) is altered. PBP delocalization of MRSA COL PBP2:GFP (strain referenced in Tan et al.)(*160*) and MRSA COL PBP4:YFP (strain reference in Atilano et al.)(*137*) by BPEI was tested. Because BPEI electrostatically binds to WTA, we expected BPEI to prevent proper localization of PBP4:YFP but to not necessarily alter localization patterns of PBP2:GFP.

A WTA-deficient mutant had a decreased level of peptidoglycan cross-linking, which Atilano et al. proposed was due to delocalization of PBP4.(*137*) Further analysis showed that TagO (the protein responsible for WTA synthesis) localizes at the division septum prior to PBP4, which suggests a direct protein-protein interaction.(*137*) Atilano et al. found that WTA knockout mutants with a defective TagO protein led to PBP4 delocalization throughout the cell wall during division.(*137*) This result was confirmed using a different probe by Gautam et al.(*141*) Atilano et al. found a direct interaction between the amount of WTA present (not just the TarO protein) and the amount of PBP4 recruited to the division septum.(*137*) Using the same MRSA COL PBP4:YFP as was used by Atilano et al., we found that BPEI similarly prevents proper localization of PBP4 to the division septum (Figure 29). We found that calculating the fluorescence content of the septa versus the non-septa area of the cell wall showed that the proportion of fluorescence intensity in the septa is higher for untreated cells (62 ± 18 %) versus

treated cells (47 ± 18 %). Imaging showed no qualitative difference of septal fluorescence proportion between untreated and treated cells for the PBP2:GFP (Figure 30). Other PBPs, such as PBP1 and PBP2, did not have abnormal localization in the Δ*tarO* mutant.(*137*) PBP2a fluorescently labelled proteins have yet to be reported, but we hypothesize that a similar localization pattern would be seen for PBP2a. MRSA loses resistance to β-lactam antibiotics when treated with WTA synthesis inhibitors such as targosil, ticlopidine, and tunicamycin.(*41, 139, 153*) PBP2a interactions with WTA were determined using SDS-PAGE experiments.(*138*) Thus, it has been suggested that WTA is important for recruitment of PBP2a to the division septum.

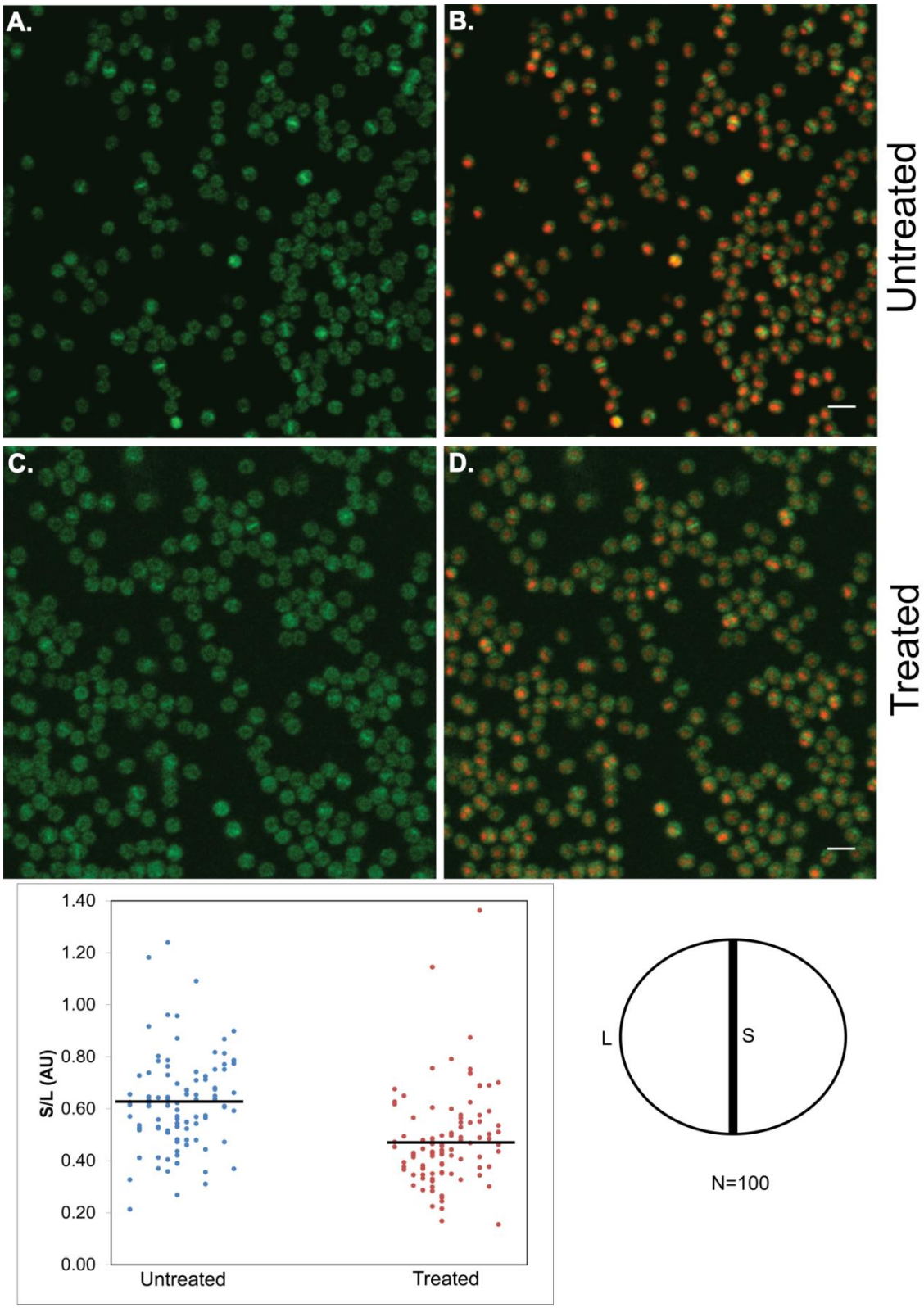


Figure 29. LSCM of MRSA Col PBP4:YFP shows that PBP4 primarily localizes at the division septum of dividing cells (A, B). BPEI delocalizes the PBP4 from the division

septum (C, D). Quantitative analysis of the fluorescence intensity at the division septum (S) versus fluorescence intensity at non-septum regions (L) was performed for untreated and BPEI-treated samples. Analysis was done for 100 cells of each sample that shows a visible closed septum. The PBP4 for untreated cells (S/L= 0.62 ± 0.18) localized heavier at the division than the BPEI-treated samples (S/L= 0.47 ± 0.18). p-values < 0.0001. Scale bars equal 2 μm.

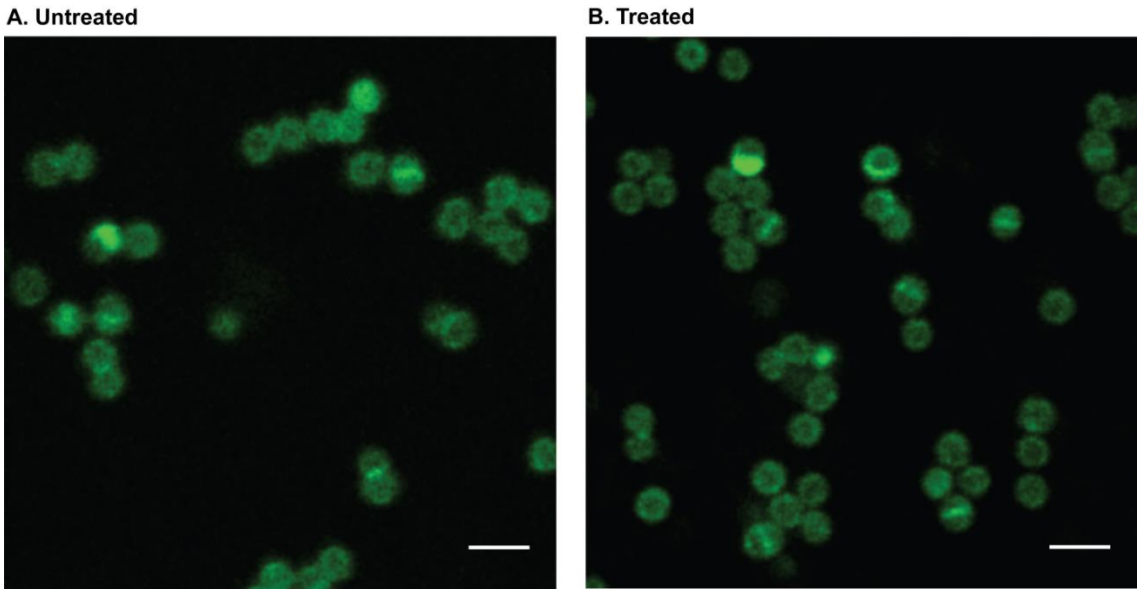


Figure 30. LSCM of MRSA PBP2:GFP shows that PBP2 primarily localizes at the division septum of dividing cells. BPEI does not appear to delocalize PBP2. Scale bars equal 2 μm.

Conclusions

We have shown here that BPEI localizes on the cell wall of Gram-positive bacteria but not Gram-negative bacteria. Specifically, BPEI electrostatically binds the WTA of MRSA and *B. subtilis*. For MRSA, WTA is necessary for localizing cell wall machinery. Thus, by inhibiting WTA function *in situ*, MRSA loses resistance to β-lactams through delocalization of PBP4 and PBP2a.

Since the golden age of antibiotic development, very few new classes of antibiotics have been discovered. Here, we have found a novel mechanism to target MRSA. By blocking the PBP2a and PBP4 resistance pathways with BPEI, β-lactam

antibiotics were able to kill MRSA. Previous research focused on inhibition of WTA synthesis to prevent PBP2a/4 function.(*41, 139, 161*) Here, we have described a different approach that, in our opinion, departs from the status quo by deactivating mature WTA within the cell wall through electrostatic interactions with BPEI. Non-toxic 600-Da BPEI was able to potentiate β-lactam efficacy against MRSA. The mechanism of action involves BPEI electrostatically binding to WTA and thereby preventing WTA from properly localizing PBP2a/PBP4 (Figure 31). The importance of this discovery is finding a new target for MRSA drug development. Although we envision improving human health with β-lactam plus polymer combinations, this represents a new pathway to develop other antibiotic treatments. Disabling PBP2a with cationic polymers enables advancement of antibiotic drug discovery by providing ways for other researchers to reinvigorate antibiotic development efforts that have stalled in the face of PBP2a.

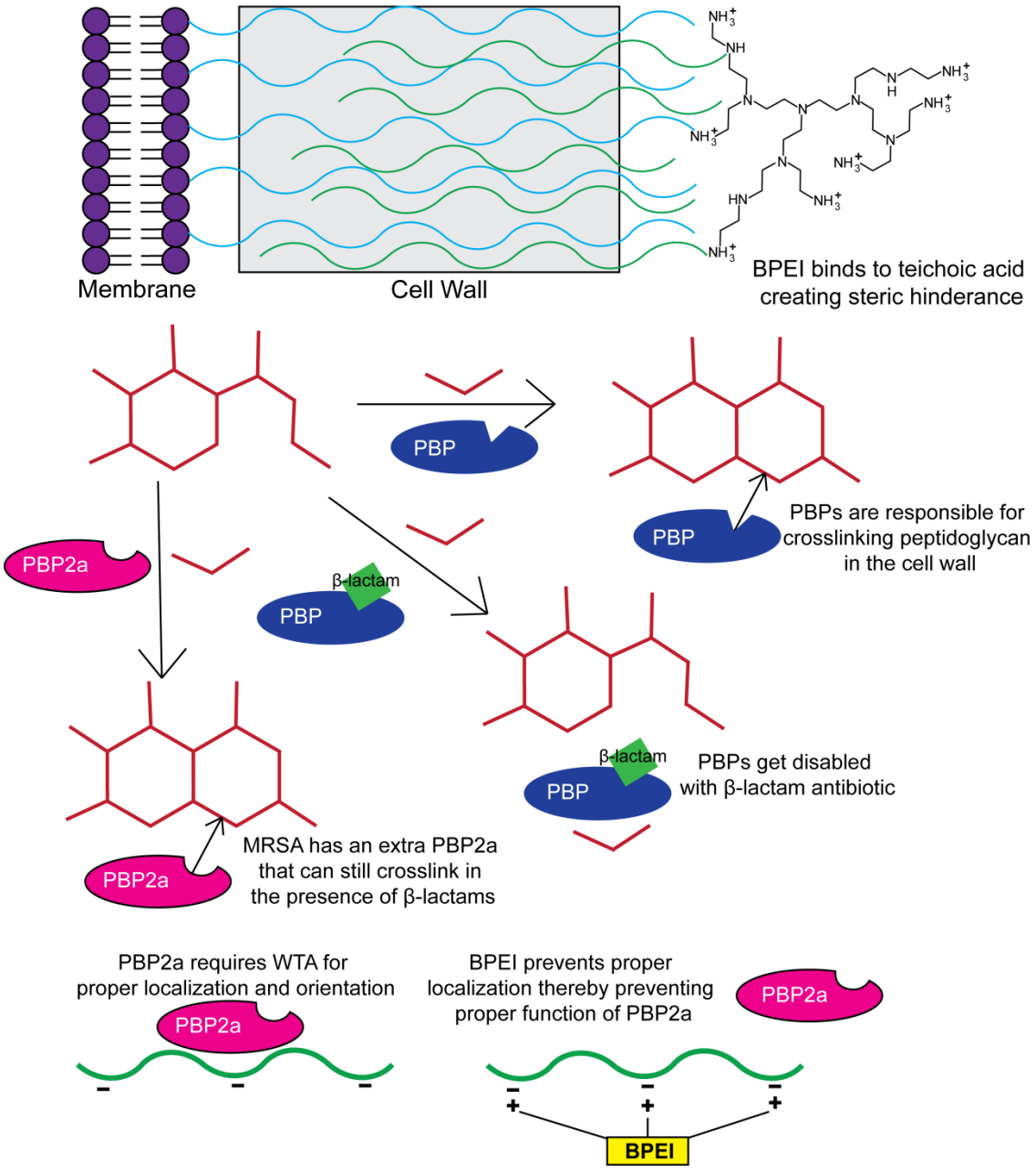


Figure 31. Our proposed mechanism of action is that BPEI electrostatically binds to WTA, which creates steric hindrance and prevents proper localization of PBP2a. Therefore, BPEI disables PBP2a through delocalization, and β-lactam antibiotics disable the other PBPs, which results in cells that are unable to crosslink the cell wall.

Chapter 5: Morphological Examination of the Effect of BPEI on MRSA

Background

BPEI electrostatically binds to WTA in the MRSA cell wall which creates steric hindrance and prevents proper function of WTA. WTA is required for proper localization of cell wall machinery. Of importance for MRSA's resistance to β-lactam antibiotics, WTA is required for proper localization of PBP4 (*137, 141*) and has been suggested to be important for localization of PBP2a.(*41, 137*) WTA-deficient cells were unable to localize PBP4 to the division septum of actively dividing cells and lost resistance to β-lactam antibiotics.(*41, 137*) We were able to replicate these results using BPEI to inhibit mature WTA through *in situ* binding. Additionally, WTA is important for localization and function of Atl, the main autolysin in MRSA,(*142*) and FmtA, another resistance factor in MRSA.(*138*) Atl localizes at the division septum of dividing cells, similar to PBP4 and PBP2.(*142*) However, Schlag et al. found that Atl distributes evenly over the cell wall of WTA-deficient mutants.(*142*) FmtA is upregulated in the presence of β-lactam antibiotics.(*162*) Qamar and Golemi-Kotra found that FmtA binds to WTA and has a conformational change when bound.(*138*) FmtA localizes at the division septum of actively dividing cells. However, WTA-deficient mutants of *S. aureus* showed FmtA localization to be scattered all over the cell wall.(*138*) FmtA is suggested to be a penicillin-binding protein with cross-linking abilities similar to PBP2 and PBP4.(*138, 162*) Thus, the importance of WTA for localization and function of numerous cell wall proteins indicates that removal or inhibition of WTA would cause drastic morphological changes.

Multiple studies have confirmed that WTA is important for morphology of Gram-positive bacteria. Since WTA and LTA are structurally similar, we also anticipate that BPEI interacts with the phosphate groups of LTA, which is also important for morphology. SEM images of *S. aureus* showed an increased cell diameter and rougher cell surface when WTA synthesis is prevented.(*142*) Genetic removal of WTA results in severe aberrations in cell septa, cell wall flaking, and altered morphologies.(*139, 142*) Similar effects are seen with chemical inhibition of WTA.(*139, 163*) Removal of LTA through genetic mutation caused morphological defects in *S. aureus* such as multiple septa formation, thickened wall envelope, and unrounded shapes.(*164, 165*) Richter et al. found a small molecule that inhibits LTA synthesis and causes an increase in cell size, cell surface deformities, and thicker cell wall envelope.(*166*) WTA is also important for morphology of *B. subtilis* cells. WTA-deficient *B. subtilis* cells have an enlarged rounded shape instead of the typical short rod-shape.(*132, 167*) LTA-deficient *B. subtilis* cells have smaller diameters, abnormal septa formation, and cell bending.(*133*) Thus, teichoic acids are important for bacterial cell morphology.

Principle of Electron Microscopy

The first electron microscope was invented in 1931 by Hans Busch. Since then, numerous modifications have made electron microscopy one of the most commonly utilized scientific instruments today. Electron microscopy utilizes the principle of Abbe's equation which states that the maximum resolution that can be obtained is diffraction limited by the size of a particle's wavelength. For light microscopy, the best possible resolution is proportional to the wavelength of the light and inversely

proportional to the numerical aperture. Thus, the absolute best resolution that can be obtained is approximately 200 nm. However, electrons have much smaller wavelengths than photons which results in resolution limits around 50 pm at best. For an electron microscope, Abbe's equation states that the maximum resolution is inversely proportional to the accelerating voltage of the electron beam. Same as light microscopy, resolution for electron microscopes is typically limited by aberrations.

Electron microscopy utilizes many similar principles to light microscopy. However, the use of electrons instead of photons requires special modifications. An electron gun, often made of tungsten, generates a beam of electron. In order to maintain a coherent beam, the microscope system is kept under high vacuum (less than 10^{-6} mbar). Instead of glass lens, electromagnetic lens are used to focus and disperse the electron beam through the column of the microscope. In order to view images generated by an electron microscope, special detectors, cameras, or viewing screens are used.

Scanning electron microscopy (SEM) scans electrons on the surface of a specimen. The produced signal then reconstructs the topography of the specimen (Figure 32). SEM uses a relatively low accelerating voltage (5-30 kV) to prevent full penetration of the electron beam through the sample. The electron gun, vacuum system, and lenses are similar for all electron microscopes. The lenses in SEM work to focus the final ray into a fine point. For SEM, a scanning coil scans the electron beam along the imaging plane. Each signal from the detector represents a pixel in the final image. Commonly used SEM detectors detect either secondary electrons or backscattered electrons. Secondary electrons are low energy electrons that are ejected from the specimen by inelastic scattering with the electron beam. An Everhart-Thornley detector

detects the secondary electrons by attracting them to the biased grid with a low voltage. The brightness of the signal is dependent on the number of electrons that reach the detector. Everhart-Thornley detectors are placed at an angle to the sample which gives the resulting image a 3-dimensional appearance. Backscattered electrons are high energy electrons that elastically scatter when the electron beam interacts with the specimen. A backscattered detector is placed directly above the sample. At best, SEM is able to reach resolution limits around 1-10 nm.

Transmission electron microscopy (TEM) transmits a beam of electrons through a sample, and an image forms based off the interaction with the sample (Figure 32). TEM uses a higher accelerating voltage (greater than 100 kV) in order to fully penetrate through the sample. Samples for TEM must be thin enough to allow for full electron transmission. The lenses for TEM create a coherent electron beam. The electron waves that penetrate through the specimen directly form the image. Since some of the electrons interact with the sample, contrast is seen between differences in electron densities. Phosphor screens or TEM cameras record and display the final image. At best, TEM is able to reach resolution limits around 50 pm.

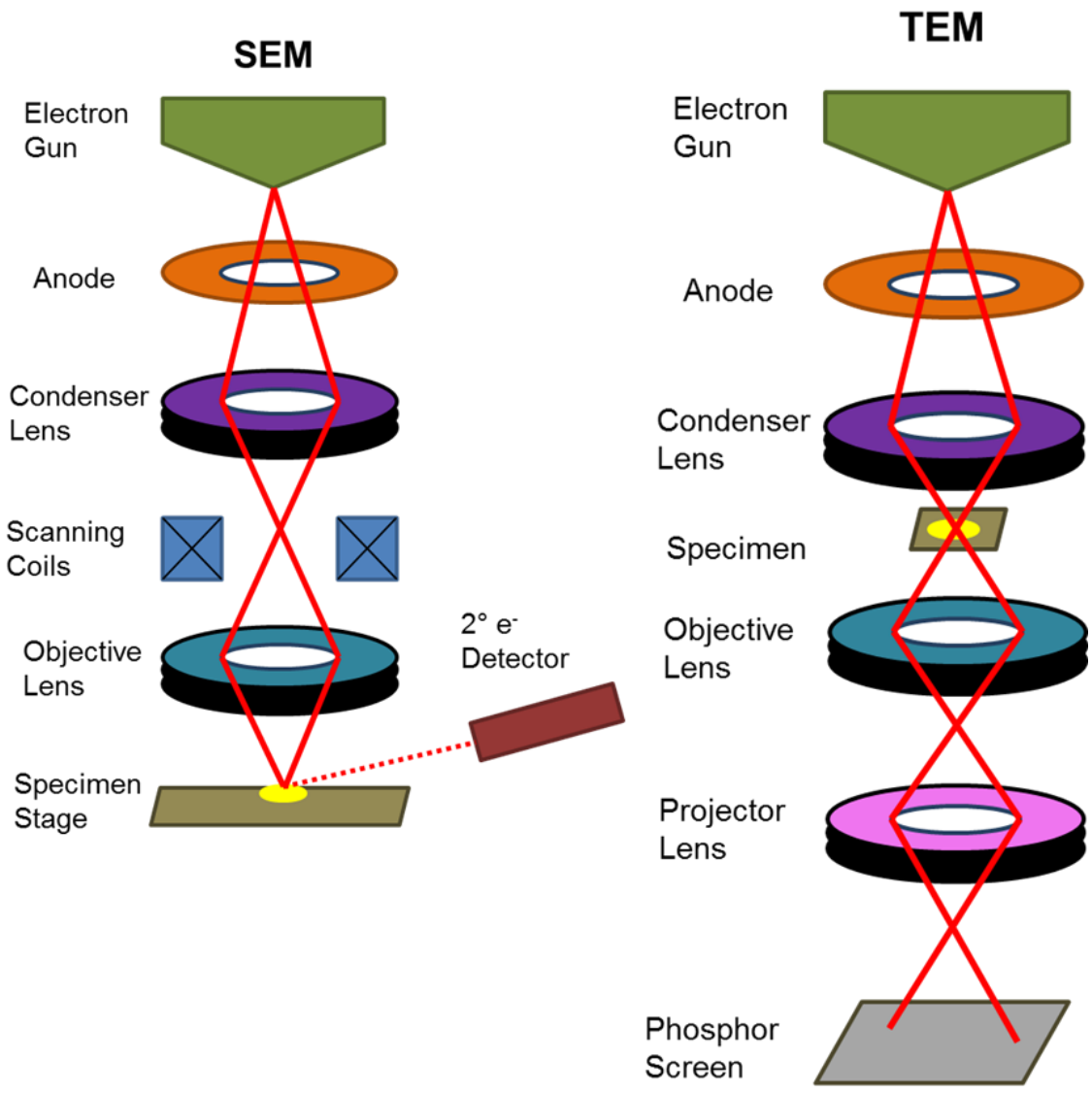


Figure 32. Simplified diagrams of an SEM (left) and TEM (right).

Contrast is found in electron microscopy based off how much the electron beam interacts with the sample. Organic materials do not provide sufficient interaction to be imaged on an electron microscope. Thus, imaging of biological samples typically requires heavy metal staining to increase contrast of the sample. Higher molecular weight metals have better stain efficiency. Thus, the most commonly used TEM stains contain lead or uranium because of their high molecular weights and small grain sizes.

For SEM, sputter coating minimizes charging and increases contrast for imaging. Sputter coating deposits a thin layer of conductive material, most commonly gold palladium or iridium, on the sample. Uncoated biological material will cause charging from the electrical current on the sample and severely hinder the image quality.

Besides staining of samples, other techniques are required to prepare a sample for electron microscopy. First, the samples must be fixed to stop all biological processes and preserve the sample. Commonly used fixatives for bacteria are formaldehyde, glutaraldehyde, and osmium tetroxide (also used as a stain). Water cannot be placed in a conventional electron microscope. Thus, ethanol or acetone are used to dehydrate the bacteria. The cells must also be dried prior to imaging. For SEM, use of a critical point dryer or a drying agent such as hexamethyldisilazane (HMDS) prior to sputter coating prevents the bacteria from being crushed. For TEM, instead of drying the cells, the cells are placed in an embedding medium which replaces any liquid in and around the bacteria with a plastic resin. Then, an ultramicrotome cuts the resin-embedded bacteria to a thickness less than 100 nm. The thin sections are placed on copper grids to be imaged in a TEM.

Purpose of Experiment

We examined morphological abnormalities to MRSA and *B. subtilis* cells caused by BPEI. Specifically, we found that BPEI caused *B. subtilis* cells to become elongated and twisting as opposed to their normal short, rod-shaped morphology. Similarly, MRSA cells had difficulty dividing, increased in size, and displayed cell wall degradation when treated with BPEI. Also, an autolysis assay showed that BPEI

prevents autolysis in MRSA. Thus, inhibiting the function of mature WTA using BPEI negatively impacts cell division and alters morphology. Ultimately, the purpose of the experiment was to determine whether electrostatic binding of WTA would cause morphology alterations similar to those seen when WTA synthesis is inhibited genetically or chemically.

Experimental Procedures

Phase Contrast Imaging

Bacillus subtilis 6051 cells were inoculated in LB growth media 1% from an overnight inoculation. Cells were grown at 37 °C with shaking in either the presence or absence of 130 μg/ml BPEI. At OD_{600} readings of approximately (± 10%) 0.2, 0.5, and 1.0, the cell morphology was observed using an Olympus BX50 phase contrast microscope with a 100X / 1.30 NA oil immersion objective. The procedure was replicated to confirm results.

Scanning Electron Microscopy

Bacteria cells were inoculated 0.5% from an overnight culture and grown at 37 °C with shaking (with or without BPEI). The optical density was monitored, and growth was stopped when the bacteria reached late-lag phase. Aliquots were fixed with a mixture of 2% glutaraldehyde and 2% formaldehyde in 0.1 M cacodylate buffer for 30 minutes at room temperature. The cells were washed and fixed with 1% OsO_4 for 30 minutes at room temperature in the dark. Afterwards, the cells were washed three times with water. One drop of each sample was placed on poly-L-lysine coated coverslips.

The samples immediately underwent a dehydration series by immersion in ethanol solutions (20%, 35%, 50%, 70%, 95%, and 100%) for 15 minutes each. The samples were dried with HMDS and then sputter-coated with AuPd. The samples were imaged on a Zeiss NEON SEM. Size analysis was performed on ImageJ, and ANOVA was used to establish statistical significance.

Autolysis Assay

The autolysis protocol used was modified from Mani et al.(*168*) MRSA 700787 cells were inoculated 0.5% from an overnight culture in TSB (some with the addition of BPEI) and grown to an OD_{600} of approximately 0.450. The cells were pelleted and washed once with cold water. The cells were then resuspended in 0.05 M Tris-HCl (pH of 7.5) with 0.05% Triton X-100, and incubated at 30 °C without shaking. The OD_{600} was monitored every 20 minutes with a single flip of the cuvette. The percentage drop in OD_{600} was calculated for each measurement. The study was done in triplicate, and values are reported as the average with standard deviation.

Transmission Electron Microscopy

Preparation for TEM was modified from Campbell et al.(*139*) Cells were grown in TSB media (some with BPEI) at 37 °C with shaking from a 0.5% overnight inoculation for 2 hours (late-lag phase). The samples were spun down and fixed with 2.5% glutaraldehyde, 2% formaldehyde in 0.1 M cacodylate buffer for 2 hours at room temperature and then washed three times with cacodylate buffer. The cells were stained with 1% OsO_4 in 1.5% PFA for 2 hours at room temperature in the dark and washed

three times with water. The samples were stained with 1% uranyl acetate for 30 minutes at room temperature in the dark and washed three times with water. A dehydration series with ethanol (50%, 70%, 95%, 95%, and 100%) was done for 20 minutes each. The samples were placed in propylene oxide (PO) for 1 hour with one change of solvent at the 30 minute mark. The cells were infiltrated with freshly made Epon in increasing increments of Epon:PO (1:2, 1:1, 2:1) for 1 to 2 hours each. The samples were then placed in 100% Epon and left overnight at room temperature. The cells were transferred to fresh Epon and allowed to sink to the bottom of an embedding mold. The samples were embedded for 24 hours at 60 °C. An ultramicrotome with a glass knife was used to thin-section the blocks to 90 nm thickness. Sections were placed on 200-mesh copper grids. The grids were stained for 30 minutes with 1% uranyl acetate. Imaging was done on a JEOL 2000-FX TEM at 200 kV accelerating voltage.

Results and Discussion

BPEI alters the cell morphology of Bacillus subtilis cells

Deleting WTA/LTA synthesis genes leads to abnormal cell shape and length because the absence of teichoic acids disrupts the proper function of cell wall enzymes. These morphology changes can be duplicated *in situ* by exposing *B. subtilis* cells to BPEI. Abnormal morphology was observed for *B. subtilis* 6051 cells grown in sub-lethal BPEI. *B. subtilis* cells grown in sub-lethal BPEI had an elongated, curling morphology (Figure 33D-E) that was most prominent during late lag phase (~0.2 OD_{600}). At mid-log phase (~0.5 OD_{600}), the morphological difference is less prominent. After stationary phase (~1.0 OD_{600}) was reached, the difference between treated and

untreated cells was unnoticeable. Cells grown under normal conditions remained rod-shaped during the three stages of growth (Figure 33A-C). Without BPEI, the bacteria typically produce individual rods 1 μm in diameter and 2-3 μm in length. In the presence of BPEI, the bacteria produce cells which appear to grow without dividing. Rather than producing straight filaments, the cells have sharp twists and bends accompanied with an increase in diameter (Figure 34). We are uncertain of why this morphological change happens in the presence of BPEI but believe that WTA and LTA are involved.

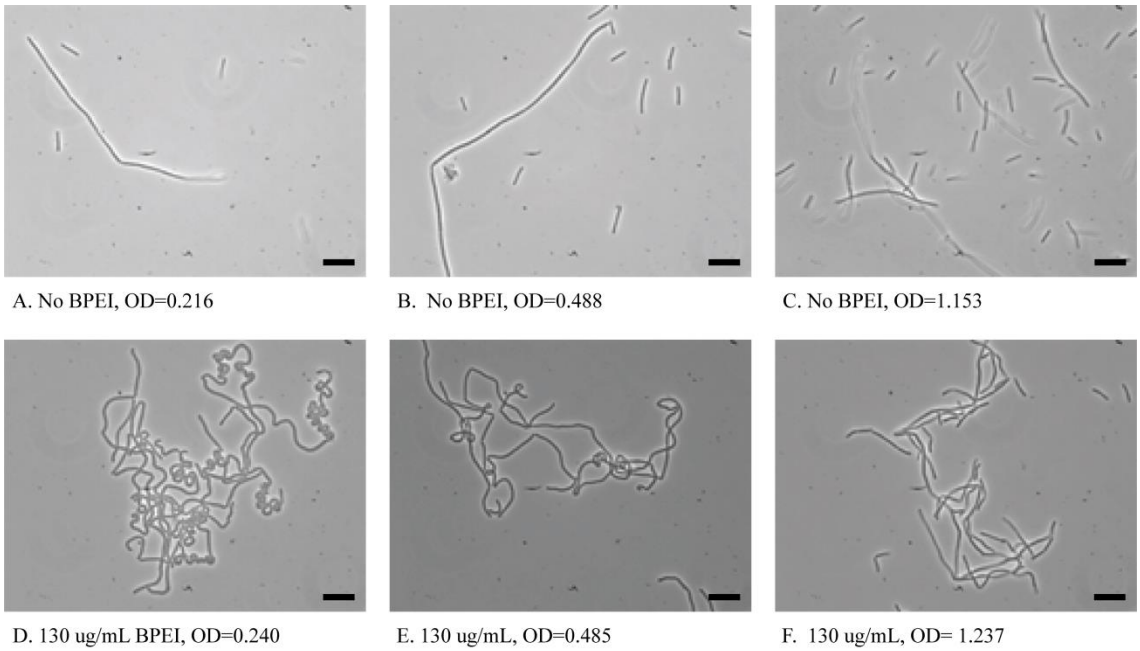


Figure 33. Changes in morphology of *B. subtilis* due to exposure to BPEI during growth, observed using phase contrast microscopy. Cells not grown in BPEI (A-C) have a short, rod-shaped morphology. Cells grown in 128 μg/mL BPEI (D-F) have an elongated, curling morphology. Images on the left (A, D) were grown to an OD_{600} of ~0.2. Middle images (B, E) were grown to an OD_{600} of ~0.5. Images on the right (C, F) were grown to an OD_{600} of ~1.0. Scale bars equal 3 μm.

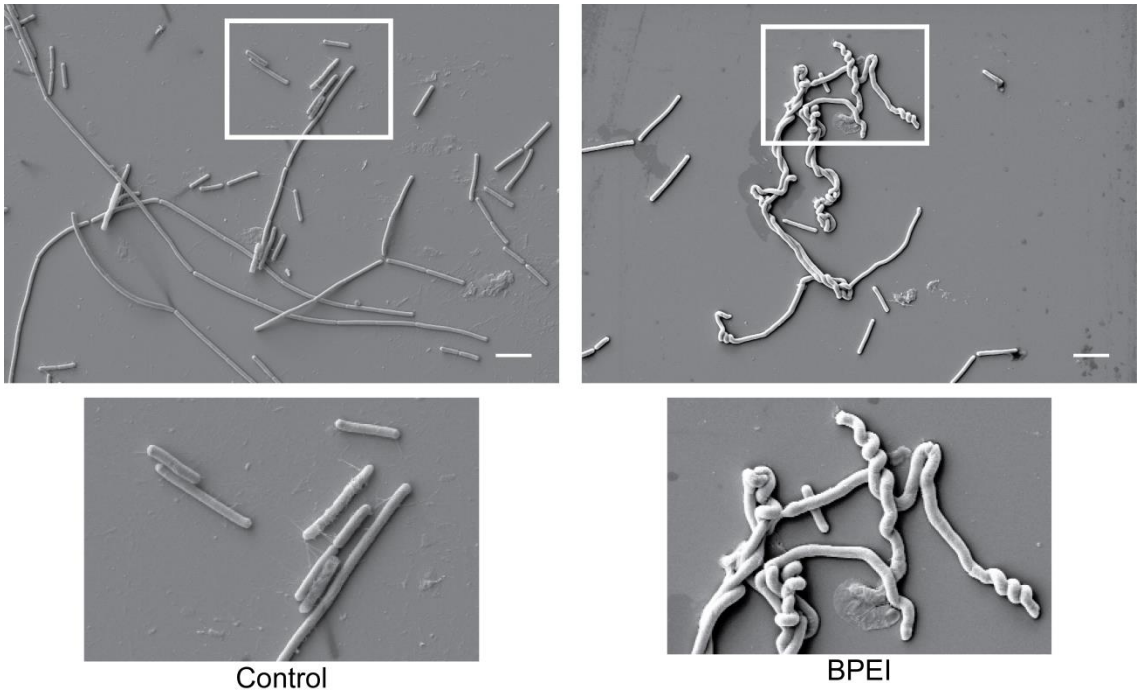


Figure 34. SEM images show the curling morphology of *B. subtilis* 6051 cells grown in BPEI. Cells were grown in the absence of BPEI (left) and in the presence of 150 μg/mL BPEI (right). The images were taken in early exponential phase of cell growth. Growth in the presence of BPEI shows a curling and twisting morphology that lacks septa formation. Scale bars equal 5 μm.

WTA is nonessential for survival in *B. subtilis* cells. Deletion of the *tagO* gene, codes for the enzyme responsible for the first step of WTA synthesis, causes *B. subtilis* cells to have a decreased growth rate and a rounded, thickened morphology in comparison to the wild-type strain.(*132*) Removal of LTA in *B. subtilis* elongates the bacteria which suggests that LTA is important for localization of cell division proteins.(*133*) *B. subtilis* bacteria grown in BPEI displayed characteristics similar to WTA and LTA-deficient cells such as elongation and thickening of the cells and clumping. This effect could be due to BPEI's interaction with WTA. Binding of BPEI to LTA may explain the elongated morphology of the *B. subtilis* cells grown in BPEI. These data suggest that BPEI is interrupting fundamental biochemical processes in the

bacterial cell wall. WTA is important in localization of cell wall machinery. D'elia et al. presented TEM images that showed that WTA knockout *B. subtilis* mutants could not form proper septa and also had asymmetrical thickening of the cell wall.(*132*) Schirner et al. found that *B. subtilis* cells grown in targosil, a drug that prevents a late step of WTA synthesis, have a reduced amount of MreB filaments.(*133*) MreB and Mbl are actin-like filaments that create the rod-shaped morphology in *B. subtilis* and knockout mutants of these filaments have morphological defects similar to cells grown in BPEI.(*169*) It has been suggested that WTA may be important for localization of MreB but the mechanism is not understood.(*170*) Our hypothesis is that BPEI binding to WTA or LTA prevents proper function of MreB or Mbl which causes dramatic morphological distortions of *B. subtilis* cells.

BPEI prevented autolysis of MRSA cells

Bacterial cells use autolysins to lyse peptidoglycan strands during cell division, allowing separation of daughter cells. The importance of WTA and LTA in the regulation of autolysin activity is well known. Schlag et al. found that autolysis increased in WTA knockout mutants and proposed that mature WTA prevents binding of Atl, an autolytic protein in *S. aureus*, to the mature cell wall.(*142*) WTA knockout mutants were unable to correctly localize Atl to the division septum.(*142*) Campbell et al. suggest that when WTA is absent, inefficient septal formation occurs due to the degradation of the autolysins track that allows for cell separation.(*139*) Triton X-100 induced autolytic rate measurements were performed to determine if BPEI affects autolysis in MRSA 700787. The autolytic rate of MRSA cells grown in 16 μg/mL of

BPEI was slowed in comparison to control samples (Figure 35). Autolysis was completely stopped for MRSA cells grown in 64 µg/mL of BPEI. Due to a larger initial cell density (~1 x 10^8 CFUs/mL), the concentration of BPEI used was higher than the MIC found in the checkerboard assays (~5 x 10^5 CFUs/mL). Triton X-100 induced autolysis is believed to occur via the release of LTA from the cell wall.(*171*) The origin of BPEI-induced slowing of autolysis is unknown, but a possible explanation is the prevention of LTA release by the electrostatic binding of BPEI to LTA, which causes steric restraint and prevents Atl localization. Further work is necessary to test this hypothesis.

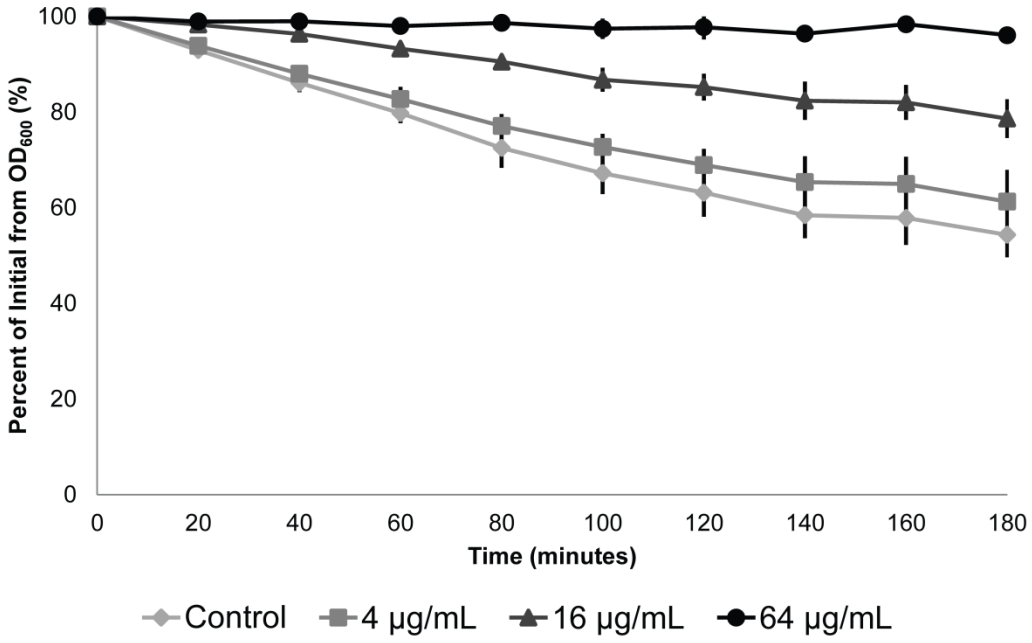


Figure 35. BPEI prevents Triton X-100 induced autolysis in MRSA 700787 in a concentration dependent manner. As the concentration of BPEI increased, the rate of autolysis decreased. Data points are presented as the average of three trials and error bars denote the standard deviation.

WTA-deficient knockout mutants have altered cell wall structure and cell division

Bacteria morphology, cell wall, and division septum are altered when WTA is inhibited or absent because WTA is important for localization of cell wall proteins. WTA-deficient mutants of MRSA have thicker cell walls. Additionally, the division septa of WTA-deficient mutants tend to have multiple formations, be asymmetrical, and lack full expansion or separation.(*139, 142*) These observations are confirmed here. Normally, MRSA MW2 is cocci-shaped with one division septum spanning through the center of the cell (Figure 36A). MRSA MW2 Δ*tarO*, a mutant that lacks WTA, had many septa formations on one cell (Figure 36B). The multiple septa are also at asymmetric and abnormal angles. Additionally, the widths of the septa appear thicker in comparison to the wild-type cells. The wild-type cells (Figure 36) display unaltered cell walls and division septa. The images seen here correspond to the literature data that show MRSA MW2 Δ*tarO* with altered cell morphology and division septa in comparison to the wild-type strain. The data here shows the impact that affecting WTA has on the morphology of MRSA. Thus, we were motivated to determine if electrostatically binding to WTA would have a similar effect on cell division.

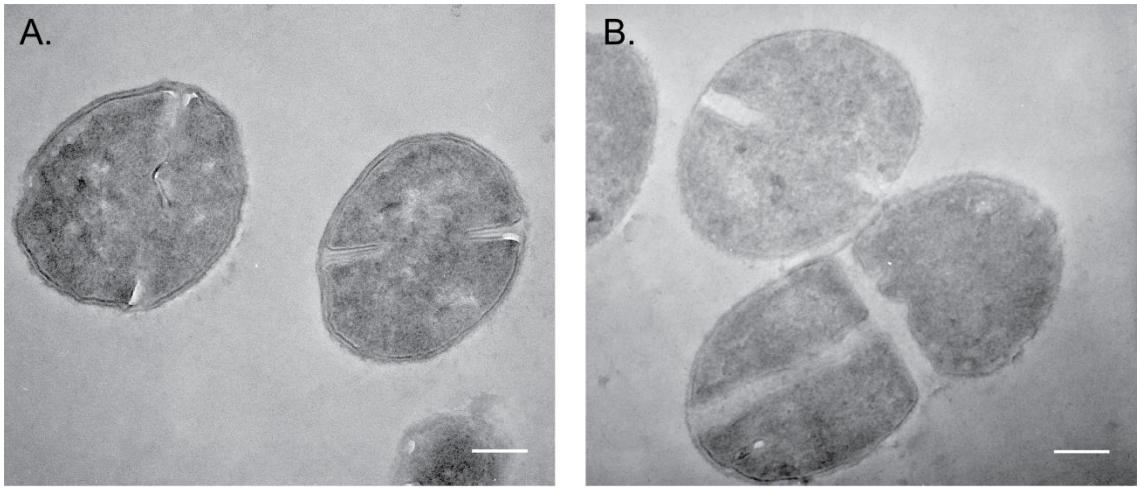


Figure 36. A WTA-deficient mutant, MRSA MW2 Δ*tarO* has altered cell division compared to the wild-type cell. Normal, wild-type MRSA MW2 is cocci shaped with a single division septum across the center (A). MRSA MW2 Δ*tarO* has multiple division septa found on one cell, and the septa are thicker (B). Scale bars equal 200 nm.

BPEI increased cell size of MRSA

WTA-deficient mutants have altered morphologies. SEM images at mid-exponential phase showed that a WTA-deficient mutant was significantly larger and had a rougher surface than the wild-type cells.(*142*) We were motivated to determine if BPEI caused any morphological changes in MRSA. MRSA 700787 cells were grown in sub-lethal concentrations of BPEI, isolated at late-lag phase, and imaged. SEM images show that BPEI does not dramatically alter the shape of MRSA 700787. However, the size of the cells was significantly increased (p-value < 0.001) from 0.86 ± 0.11 μm to 0.98 ± 0.14 μm when grown in BPEI, and the numerous MRSA aggregates suggest the inability to properly form septa and complete the cell division process (Figure 37). The cell morphologies do not appear to be significantly altered; however, the cleavage furrow does not form properly for the cells treated with BPEI. The phenotypic similarity between cells grown in BPEI and knockout mutant cells suggests that the altered

morphologies may arise from an interaction between BPEI and WTA. This data combined with the autolysis data confirm that BPEI prevents cell wall machinery from functioning properly.

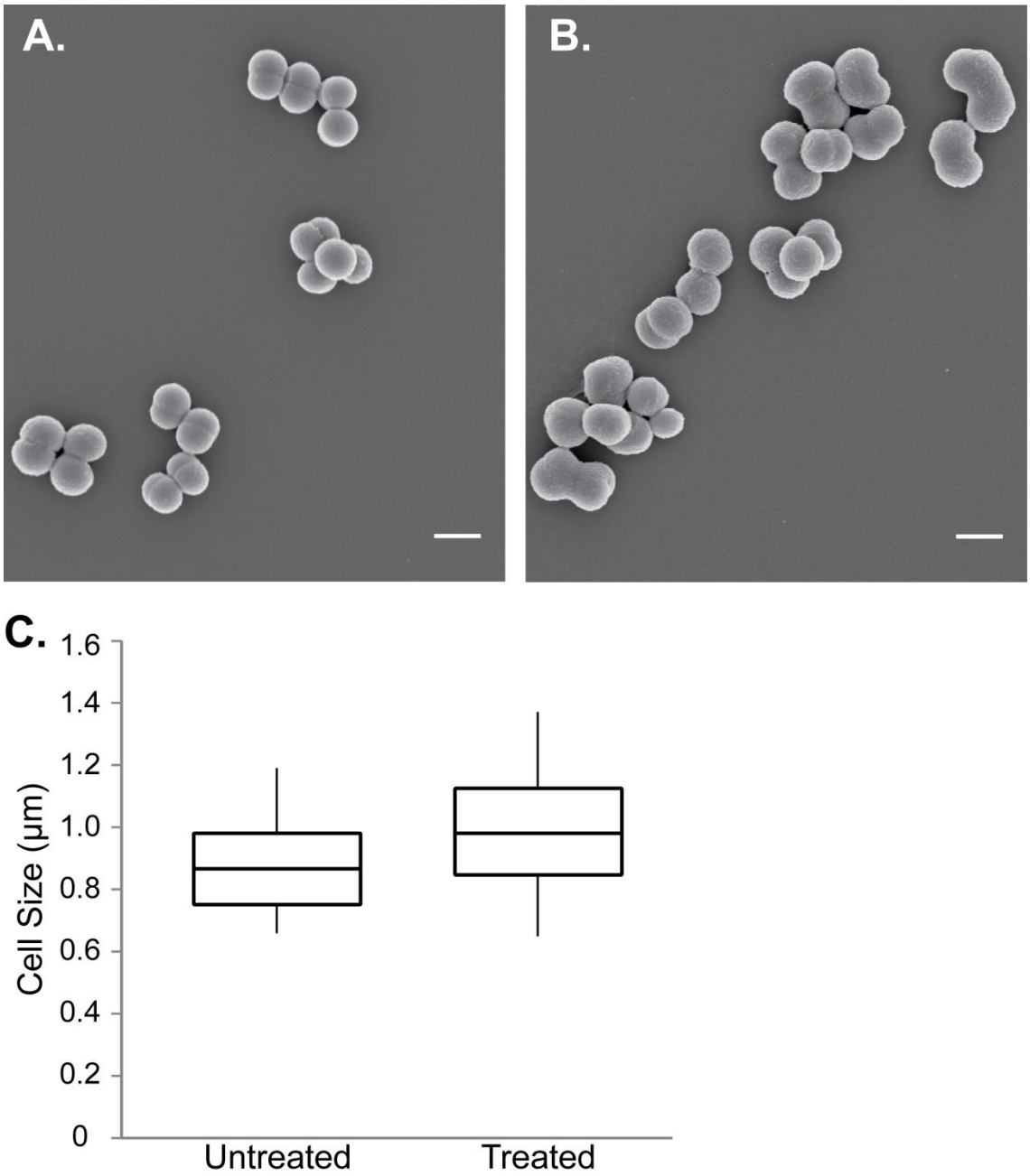


Figure 37. BPEI caused a significant increase in MRSA 700787 cell size. The average cell size (largest diameter) for untreated cells is 0.86 ± 0.11 μm (A) but increases to 0.98 ± 0.14 μm when grown in 64 μg/mL BPEI (B). Normal cleavage furrows are shown with black arrows. Enlarged cells that do not have cleavage furrows present are

shown with white arrows. Cells were fixed and imaged at late-lag phase. Scale bars equal 1 μm. A size analysis graph (C) shows the average cell size (center line), the standard deviation (outside of box), and minimum and maximum values (error bars) of 100 measured cells. (p-value <0.001)

Cell division was altered when cells were treated with BPEI

TEM was used to look at the intracellular area and cross-section of the bacterial cells to determine if BPEI affected the cytoplasmic area, cell wall, or division septum. Negative effects to the division septum were seen when MRSA 700787, MRSA USA300, and MRSA MW2 were treated with sub-inhibitory concentrations of BPEI. However, each strain is phenotypically distinctive from one another. Approximately 25% of untreated MRSA 700787 cells were found to have two septa in dividing cells (Figure 38A). In each case, the first septum is fully complete and the second septum is at the initial stage of septa formation and perpendicular to the first. This type of septa formation was unique to MRSA 700787 and not found in untreated MRSA USA300 or MRSA MW2. When treated with BPEI, approximately 35% of MRSA 700787 cells had cell septa abnormalities including multiple completed septa on each cell or non-perpendicular septa (Figure 38B). Only 7% of untreated bacteria have division septa that would be classified as abnormal. The bacteria were visually larger (Figure 37), as seen with SEM. The large cell sizes of BPEI-treated MRSA 700787 cells seen on SEM images were supported by the absence of septal indents shown in the TEM images. This gives the appearance of each cell being larger because the septa cannot be clearly seen extracellularly. These data clearly show that BPEI impacts the development of the division septa in MRSA 700787.

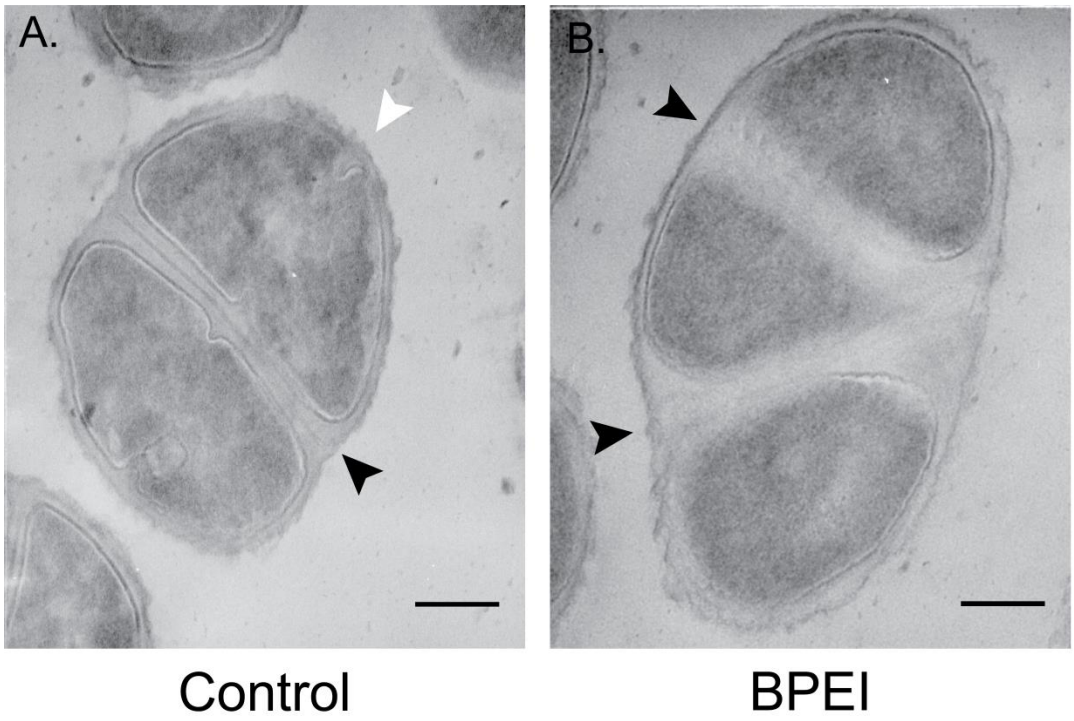


Figure 38. MRSA 700787 cells have abnormal cell division when grown in BPEI. Untreated cells (A) show normal cell division septa versus treated cells (B). Black arrows indicate complete septa formation. White arrows indicate incomplete septa formation. Scale bars equal 200 nm.

MRSA USA300 cells treated with BPEI had difficulty dividing. SEM images of treated versus untreated cells do not show drastic changes in cells morphology, but the BPEI-treated cells contain multiple cell division septa that are not seen in control cells. (Figure 39) When examined using TEM, treated cells were found to have visibly thicker division septa and the electron density of the division septa was lower for the treated cells compared to the control cells (Figure 40). Also, the percentage of cells that were in active cell division was higher for treated samples in comparison to the untreated samples (Table 11). For untreated samples, 75% of cells did not have a visible septum, 12% had a complete septum, and 13% had incomplete septa. For treated samples, only

53% of cells had no septum, 24% had complete septa, and 23% had incomplete septa.

These data suggest that cells are unable to separate efficiently.

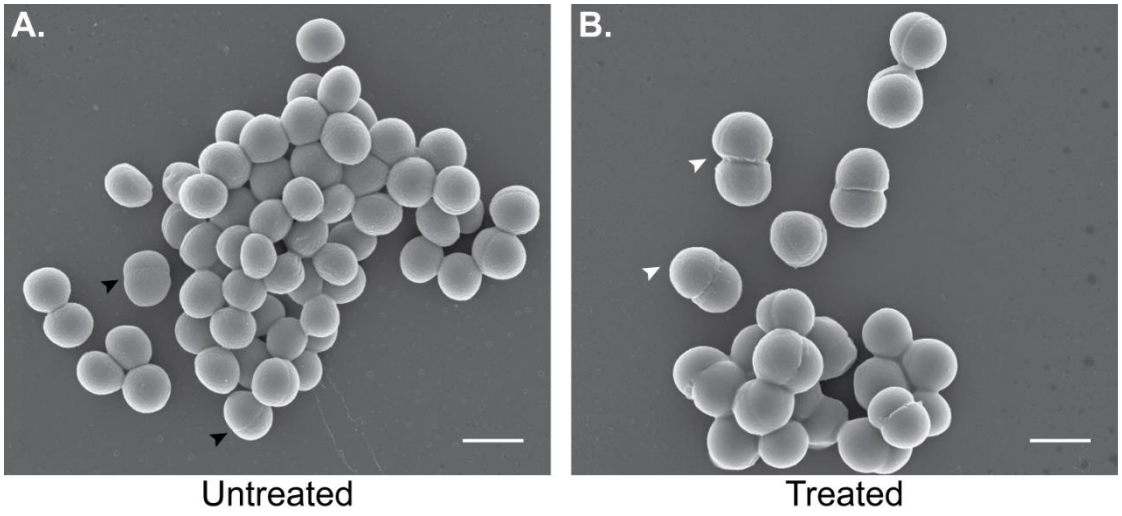


Figure 39. SEM of MRSA USA300 shows multiple septa formations when treated with BPEI. Untreated cells (A) have a single septal formation (black arrows). Some BPEI-treated cells (B) have multiple septa formations (white arrows). Scale bars equal 1 μm.

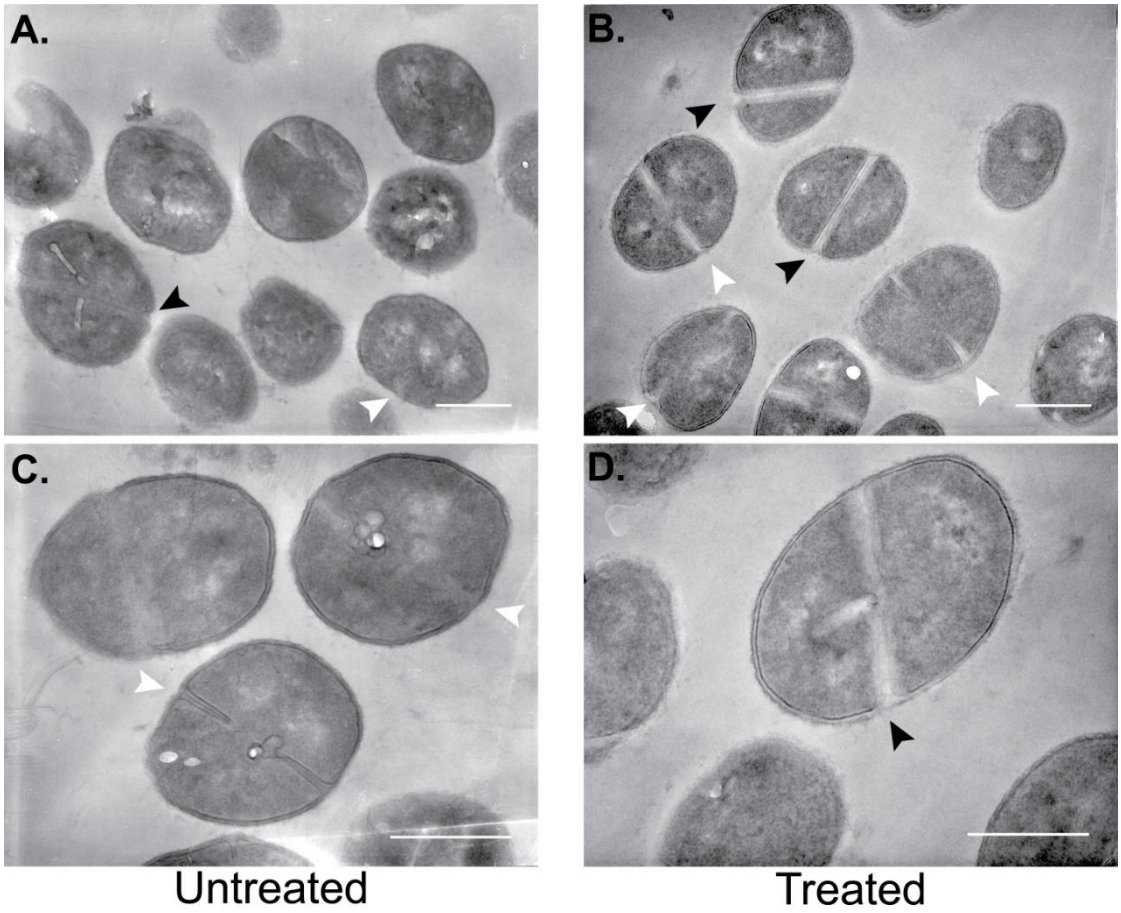


Figure 40. TEM images of MRSA USA300 cells do not show drastic changes in division septa. Cells treated with BPEI (B and D) have thicker division septa in comparison to the untreated cells (A and C). Black arrows indicate complete septa formation. White arrows indicate incomplete septa formation. Scale bars equal 500 nm.

Table 11. BPEI prevents MRSA USA300 cells from separating efficiently.

	Untreated (%)	**Treated (%)**
No Visible Septa	75%	53%
Complete Septa	12%	24%
Incomplete Septum	13%	23%

Notes: 200 cells from each sample were analyzed from TEM images to determine the level of septal formation.

BPEI degraded the cell wall and caused stress response

All strains tested had a different response to treatment with BPEI. MRSA MW2 had an overall stress response to treatment with BPEI. TEM images show that untreated MRSA MW2 cells have a dark, thin cell wall with a clear septum formation (Figure

41A). The septa region is dark in the control cells because the WTA-rich region strongly attracts the metal cations that are used to stain the samples. When treated with BPEI, the bacteria have altered cell division septa and lighter staining septa (Figure 41B). The light septum staining in the treated samples indicates that the amount of WTA found in the septum region is lower than normal. Additionally, the cell wall surface is rougher for treated cells (Figure 41D) in comparison to the untreated cells (Figure 41C). MRSA MW2 cells show signs of universal stress. Stress in bacteria can be caused by a variety of issues including osmotic pressure, nutrient starvation, high or low pH, high cell density, or the presence of toxic chemicals.

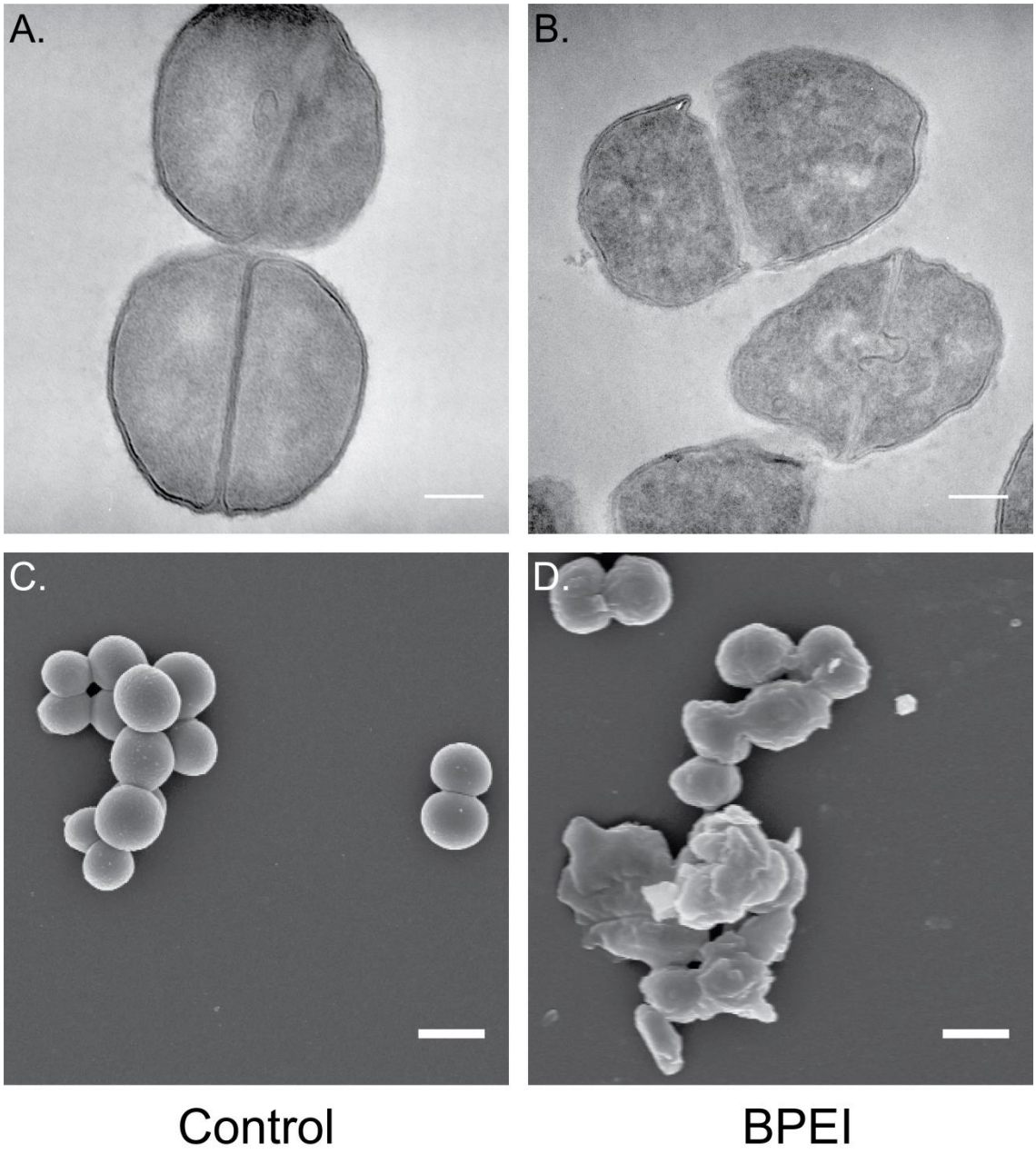


Figure 41. BPEI causes MRSA MW2 to show signs indicative of cell stress. TEM images of untreated (A) and BPEI-treated (B) show the difference in cell wall composition and septum formation. Scale bars equal 200 nm. SEM images of untreated (C) versus treated (D) show drastic alterations to the cell morphology. Scale bars equal 1 μm.

Conclusions

It has been well established that removal of WTA through genetic or chemical means compromises cell morphology and cell division in MRSA and *B. subtilis* bacteria. However, artifacts could arise from gene deletion or by inhibiting the initial steps of WTA synthesis chemically. Therefore, the importance of WTA in cell morphology due to immature WTA, WTA-synthesis machinery, or mature WTA could not be determined. The method for preventing WTA-function changes the morphology outcome. WTA inhibition through genetic modification caused many septa to form.(*139, 142*) Also, septa formations on these cells were at parallel or non-perpendicular angles. Targosil, which inhibits a late step of WTA synthesis by blocking TarG, creates defects that are likely caused by osmotic stress and cell membrane damage. Targosil-treated cells are unable to separate and form increasing cell and cluster size as growth time continues.(*163*) Tunicamycin, which blocks the first-step of WTA synthesis by inhibiting TarO, have global effects to cell division resulting in multiple septa formations, asymmetric septa, and incomplete septa.(*139*) Removal of LTA creates irregularities to the cell such as thickened wall and impaired cell division which are thought to be due to reduced autolysis activity.(*172*) BPEI does not target WTA-synthesis. However, BPEI electrostatically binds to WTA creating steric hindrance and effectively disabling the mature WTA. Here we show that BPEI caused dramatic morphology changes to *B. subtilis*. *B. subtilis* cells that were treated with sub-lethal BPEI formed elongated, twisting, and curling cells. Against MRSA, the effects of BPEI on cell morphology were less pronounced. However, BPEI increased cell size, prevented the cells from dividing properly, and created cell wall destruction. Autolysis

data showed that BPEI prevents autolysis in MRSA cells. Although removal of WTA through genetic manipulation causes more drastic effects to the division septum of dividing MRSA cells, BPEI prevents MRSA from dividing properly. These data reveal that mature WTA plays a role in cell division and morphology.

References

1. Dantes, R., Mu, Y., Belflower, R., Aragon, D., Dumyati, G., Harrison, L. H., Lessa, F. C., Lynfield, R., Nadle, J., Petit, S., Ray, S. M., Schaffner, W., Townes, J., Fridkin, S., and Emerging Infections Program-Active Bacterial Core Surveillance, M. S. I. (2013) National burden of invasive methicillin-resistant Staphylococcus aureus infections, United States, 2011, *JAMA internal medicine 173*, 1970-1978.
2. Centres for Disease, C., and Prevention (2013) *Antibiotic resistance threats in the United States, 2013*, Centres for Disease Control and Prevention, US Department of Health and Human Services.
3. Foxley, M. A., Friedline, A. W., Jensen, J. M., Nimmo, S. L., Scull, E. M., King, J. B., Strange, S., Xiao, M. T., Smith, B. E., Thomas Iii, K. J., Glatzhofer, D. T., Cichewicz, R. H., and Rice, C. V. (2016) Efficacy of ampicillin against methicillin-resistant Staphylococcus aureus restored through synergy with branched poly(ethylenimine), *The Journal of antibiotics 69*, 871.
4. Foxley, M. A., Wright, S. N., Lam, A. K., Friedline, A. W., Strange, S. J., Xiao, M. T., Moen, E. L., and Rice, C. V. (2017) Targeting Wall Teichoic Acid in Situ with Branched Polyethylenimine Potentiates β-Lactam Efficacy against MRSA, *ACS Medicinal Chemistry Letters 8*, 1083-1088.
5. O'Neil, J. (2014) Review on Antimicrobial Resistance. Antimicrobial Resistance: Tackling a Crisis for the Health and Wealth of Nations 2014.
6. Gandra, S., Barter, D. M., and Laxminarayan, R. (2014) Economic burden of antibiotic resistance: how much do we really know?, *Clinical Microbiology and Infection 20*, 973-979.
7. Okeke, I. N., Lamikanra, A., and Edelman, R. (1999) Socioeconomic and behavioral factors leading to acquired bacterial resistance to antibiotics in developing countries, *Emerging Infectious Diseases 5*, 18-27.
8. Fleming-Dutra, K. E., Hersh, A. L., Shapiro, D. J., and et al. (2016) Prevalence of inappropriate antibiotic prescriptions among us ambulatory care visits, 2010-2011, *Jama 315*, 1864-1873.
9. Butler, M. S., Blaskovich, M. A. T., and Cooper, M. A. (2016) Antibiotics in the clinical pipeline at the end of 2015, *The Journal of antibiotics 70*, 3.
10. Raja, A., LaBonte, J., Lebbos, J., and Kirkpatrick, P. (2003) Daptomycin, *Nature Reviews Drug Discovery 2*, 943.
11. Eliopoulos, G. M., Willey, S., Reiszner, E., Spitzer, P. G., Caputo, G., and Moellering, R. C. (1986) In vitro and in vivo activity of LY 146032, a new cyclic lipopeptide antibiotic, *Antimicrobial Agents and Chemotherapy 30*, 532-535.
12. World Health, O. (2014) *Antimicrobial resistance: global report on surveillance*, World Health Organization.
13. Lewis, K. (2013) Platforms for antibiotic discovery, *Nature Reviews Drug Discovery 12*, 371.
14. Fernandes, P. (2015) The global challenge of new classes of antibacterial agents: an industry perspective, *Current Opinion in Pharmacology 24*, 7-11.

15. Law, G. L., Tisoncik-Go, J., Korth, M. J., and Katze, M. G. (2013) Drug repurposing: a better approach for infectious disease drug discovery?, *Current Opinion in Immunology 25*, 588-592.
16. Andersson, J. A., Fitts, E. C., Kirtley, M. L., Ponnusamy, D., Peniche, A. G., Dann, S. M., Motin, V. L., Chauhan, S., Rosenzweig, J. A., Sha, J., and Chopra, A. K. (2016) New Role for FDA-Approved Drugs in Combating Antibiotic-Resistant Bacteria, *Antimicrobial Agents and Chemotherapy 60*, 3717-3729.
17. Ogston, A. (1882) Micrococcus Poisoning, *Journal of Anatomy and Physiology 16*, 526-567.
18. P R, V., and M, J. (2013) A Comparative Analysis of Community Acquired and Hospital Acquired Methicillin Resistant Staphylococcus Aureus, *Journal of Clinical and Diagnostic Research : JCDR 7*, 1339-1342.
19. Gordon, R. J., and Lowy, F. D. (2008) Pathogenesis of Methicillin-Resistant Staphylococcus aureus Infection, *Clinical Infectious Diseases 46*, S350-S359.
20. von Eiff, C., Becker, K., Machka, K., Stammer, H., and Peters, G. (2001) Nasal Carriage as a Source of Staphylococcus aureus Bacteremia, *New England Journal of Medicine 344*, 11-16.
21. Wertheim, H. F. L., Vos, M. C., Ott, A., van Belkum, A., Voss, A., Kluytmans, J. A. J. W., van Keulen, P. H. J., Vandenbroucke-Grauls, C. M. J. E., Meester, M. H. M., and Verbrugh, H. A. (2004) Risk and outcome of nosocomial Staphylococcus aureus bacteraemia in nasal carriers versus non-carriers, *The Lancet 364*, 703-705.
22. Williams, R. E. O., Jevons, M. P., Shooter, R. A., Hunter, C. J. W., Girling, J. A., Griffiths, J. D., and Taylor, G. W. (1959) Nasal Staphylococci and Sepsis in Hospital Patients, *British Medical Journal 2*, 658-662.
23. Ogawa, S. K., Yurberg, E. R., Hatcher, V. B., Levitt, M. A., and Lowy, F. D. (1985) Bacterial adherence to human endothelial cells in vitro, *Infection and Immunity 50*, 218-224.
24. Almeida, R. A., Matthews, K. R., Cifrian, E., Guidry, A. J., and Oliver, S. P. (1996) Staphylococcus aureus Invasion of Bovine Mammary Epithelial Cells, *Journal of Dairy Science 79*, 1021-1026.
25. Proctor, R. A., von Eiff, C., Kahl, B. C., Becker, K., McNamara, P., Herrmann, M., and Peters, G. (2006) Small colony variants: a pathogenic form of bacteria that facilitates persistent and recurrent infections, *Nature Reviews Microbiology 4*, 295.
26. O'Riordan, K., and Lee, J. C. (2004) Staphylococcus aureus Capsular Polysaccharides, *Clinical Microbiology Reviews 17*, 218-234.
27. Bhakdi, S., and Tranum-Jensen, J. (1991) Alpha-toxin of Staphylococcus aureus, *Microbiological reviews 55*, 733-751.
28. Otto, M. (2014) Staphylococcus aureus toxins, *Current Opinion in Microbiology 17*, 32-37.
29. Freer, J. H., and Arbuthnoti, J. P. (1982) Toxins of staphylococcus aureus, *Pharmacology & Therapeutics 19*, 55-106.
30. Gladstone, G. P., and van Heyningen, W. E. (1957) Staphylococcal Leucocidins, *British journal of experimental pathology 38*, 123-137.

31. Moreillon, P., Entenza, J. M., Francioli, P., McDevitt, D., Foster, T. J., François, P., and Vaudaux, P. (1995) Role of Staphylococcus aureus coagulase and clumping factor in pathogenesis of experimental endocarditis, *Infection and Immunity 63*, 4738-4743.
32. Weckman, B. G., and Catlin, B. W. (1957) DEOXYRIBONUCLEASE ACTIVITY OF MICROCOCCI FROM CLINICAL SOURCES, *Journal of Bacteriology 73*, 747-753.
33. Jin, T., Bokarewa, M., Foster, T., Mitchell, J., Higgins, J., and Tarkowski, A. (2004) Staphylococcus aureus Resists Human Defensins by Production of Staphylokinase, a Novel Bacterial Evasion Mechanism, *The Journal of Immunology 172*, 1169.
34. Vandenesch, F., Naimi, T., Enright, M. C., Lina, G., Nimmo, G. R., Heffernan, H., Liassine, N., Bes, M., Greenland, T., Reverdy, M.-E., and Etienne, J. (2003) Community-Acquired Methicillin-Resistant Staphylococcus aureus Carrying Panton-Valentine Leukocidin Genes: Worldwide Emergence, *Emerging Infectious Diseases 9*, 978-984.
35. Lina, G., Piémont, Y., Godail-Gamot, F., Bes, M., Peter, M.-O., Gauduchon, V., Vandenesch, F., and Etienne, J. (1999) Involvement of Panton-Valentine Leukocidin—Producing Staphylococcus aureus in Primary Skin Infections and Pneumonia, *Clinical Infectious Diseases 29*, 1128-1132.
36. Stock, J. B., Rauch, B., and Roseman, S. (1977) Periplasmic space in Salmonella typhimurium and Escherichia coli, *Journal of Biological Chemistry 252*, 7850-7861.
37. Fleming, A. (1929) On the Antibacterial Action of Cultures of a Penicillium, with Special Reference to their Use in the Isolation of B. influenzæ, *British journal of experimental pathology 10*, 226-236.
38. Skinner, D., and Keefer, C. S. (1941) Significance of bacteremia caused by staphylococcus aureus: A study of one hundred and twenty-two cases and a review of the literature concerned with experimental infection in animals, *Archives of Internal Medicine 68*, 851-875.
39. Hicks, L. A., Bartoces, M. G., Roberts, R. M., Suda, K. J., Hunkler, R. J., Taylor, J. T. H., and Schrag, S. J. (2015) US Outpatient Antibiotic Prescribing Variation According to Geography, Patient Population, and Provider Specialty in 2011, *Clinical Infectious Diseases 60*, 1308-1316.
40. Peacock, S. J., and Paterson, G. K. (2015) Mechanisms of Methicillin Resistance in Staphylococcus aureus, *Annual review of biochemistry 84*, 577-601.
41. Farha, M. A., Leung, A., Sewell, E. W., D'Elia, M. A., Allison, S. E., Ejim, L., Pereira, P. M., Pinho, M. G., Wright, G. D., and Brown, E. D. (2013) Inhibition of WTA Synthesis Blocks the Cooperative Action of PBPs and Sensitizes MRSA to β-Lactams, *ACS Chem. Biol. 8*, 226-233.
42. Łęski, T. A., and Tomasz, A. (2005) Role of Penicillin-Binding Protein 2 (PBP2) in the Antibiotic Susceptibility and Cell Wall Cross-Linking of Staphylococcus aureus: Evidence for the Cooperative Functioning of PBP2, PBP4, and PBP2A, *Journal of Bacteriology 187*, 1815-1824.

43. Chambers, H. F., and Sachdeva, M. (1990) Binding of β-Lactam Antibiotics to Penicillin-Binding Proteins in Methicillin-Resistant Staphylococcus aureus, *The Journal of Infectious Diseases 161*, 1170-1176.
44. Bondi, A., and Dietz, C. C. (1945) Penicillin Resistant Staphylococci, *Proceedings of the Society for Experimental Biology and Medicine 60*, 55-58.
45. Jevons, M. P. (1961) "Celbenin" - resistant Staphylococci, *British Medical Journal 1*, 124-125.
46. Sabath, L. D., Wallace, S. J., and Gerstein, D. A. (1972) Suppression of Intrinsic Resistance to Methicillin and Other Penicillins in Staphylococcus aureus, *Antimicrobial Agents and Chemotherapy 2*, 350-355.
47. Memmi, G., Filipe, S. R., Pinho, M. G., Fu, Z., and Cheung, A. (2008) Staphylococcus aureus PBP4 is essential for beta-lactam resistance in community-acquired methicillin-resistant strains, *Antimicrobial agents and chemotherapy 52*, 3955-3966.
48. Hanssen, A.-M., and Ericson Sollid, J. U. (2006) SCCmec in staphylococci: genes on the move, *FEMS Immunology & Medical Microbiology 46*, 8-20.
49. Reichmann, N. T., and Pinho, M. G. (2017) Role of SCCmec type in resistance to the synergistic activity of oxacillin and cefoxitin in MRSA, *Scientific Reports 7*, 6154.
50. Gosbell, I. B., Mercer, J. L., Neville, S. A., Crone, S. A., Chant, K. G., Jalaludin, B. B., and Munro, R. (2001) Non-multiresistant and multiresistant methicillin-resistant Staphylococcus aureus in community-acquired infections, *The Medical journal of Australia 174*, 627-630.
51. Voyich, J. M., Braughton, K. R., Sturdevant, D. E., Whitney, A. R., Saïd-Salim, B., Porcella, S. F., Long, R. D., Dorward, D. W., Gardner, D. J., Kreiswirth, B. N., Musser, J. M., and DeLeo, F. R. (2005) Insights into Mechanisms Used by Staphylococcus aureus to Avoid Destruction by Human Neutrophils, *The Journal of Immunology 175*, 3907.
52. Boyle-Vavra, S., and Daum, R. S. (2006) Community-acquired methicillin-resistant Staphylococcus aureus: the role of Panton–Valentine leukocidin, *Laboratory Investigation 87*, 3.
53. van Hal, S. J., and Fowler, V. G. (2013) Is It Time to Replace Vancomycin in the Treatment of Methicillin-Resistant Staphylococcus aureus Infections?, *Clinical Infectious Diseases: An Official Publication of the Infectious Diseases Society of America 56*, 1779-1788.
54. Liu, C., Bayer, A., Cosgrove, S. E., Daum, R. S., Fridkin, S. K., Gorwitz, R. J., Kaplan, S. L., Karchmer, A. W., Levine, D. P., Murray, B. E., Rybak, M. J., Talan, D. A., and Chambers, H. F. (2011) Clinical Practice Guidelines by the Infectious Diseases Society of America for the Treatment of Methicillin-Resistant Staphylococcus aureus Infections in Adults and Children, *Clinical Infectious Diseases 52*, e18-e55.
55. Mellor, J. A., Kingdom, J., Cafferkey, M., and Keane, C. T. (1985) Vancomycin toxicity: a prospective study, *Journal of Antimicrobial Chemotherapy 15*, 773-780.
56. Chang, S., Sievert, D. M., Hageman, J. C., Boulton, M. L., Tenover, F. C., Downes, F. P., Shah, S., Rudrik, J. T., Pupp, G. R., Brown, W. J., Cardo, D., and

Fridkin, S. K. (2003) Infection with Vancomycin-Resistant Staphylococcus aureus Containing the vanA Resistance Gene, *New England Journal of Medicine 348*, 1342-1347.
57. Sievert, D. M., Rudrik, J. T., Patel, J. B., McDonald, L. C., Wilkins, M. J., and Hageman, J. C. (2008) Vancomycin-Resistant Staphylococcus aureus in the United States, 2002–2006, *Clinical Infectious Diseases 46*, 668-674.
58. World Health, O. (2011) WHO model list of essential medicines: 17th list, March 2011.
59. Mangili, A., Bica, I., Snydman, D. R., and Hamer, D. H. (2005) Daptomycin-Resistant, Methicillin-Resistant Staphylococcus aureus Bacteremia, *Clinical Infectious Diseases 40*, 1058-1060.
60. Tsiodras, S., Gold, H. S., Sakoulas, G., Eliopoulos, G. M., Wennersten, C., Venkataraman, L., Moellering Jr, R. C., and Ferraro, M. J. (2001) Linezolid resistance in a clinical isolate of Staphylococcus aureus, *The Lancet 358*, 207-208.
61. Ishikawa, T., Matsunaga, N., Tawada, H., Kuroda, N., Nakayama, Y., Ishibashi, Y., Tomimoto, M., Ikeda, Y., Tagawa, Y., Iizawa, Y., Okonogi, K., Hashiguchi, S., and Miyake, A. (2003) TAK-599, a novel N-Phosphono type prodrug of anti-MRSA cephalosporin T-91825: synthesis, physicochemical and pharmacological properties, *Bioorganic & Medicinal Chemistry 11*, 2427-2437.
62. Higgins, D. L., Chang, R., Debabov, D. V., Leung, J., Wu, T., Krause, K. M., Sandvik, E., Hubbard, J. M., Kaniga, K., Schmidt, D. E., Gao, Q., Cass, R. T., Karr, D. E., Benton, B. M., and Humphrey, P. P. (2005) Telavancin, a Multifunctional Lipoglycopeptide, Disrupts both Cell Wall Synthesis and Cell Membrane Integrity in Methicillin-Resistant Staphylococcus aureus, *Antimicrobial Agents and Chemotherapy 49*, 1127-1134.
63. Grosse, E. J. E., Babinchak, T., Dartois, N., Rose, G., and Loh, E. (2005) The Efficacy and Safety of Tigecycline in the Treatment of Skin and Skin-Structure Infections: Results of 2 Double-Blind Phase 3 Comparison Studies with Vancomycin-Aztreonam, *Clinical Infectious Diseases 41*, S341-S353.
64. Rybak, M. J., Hershberger, E., Moldovan, T., and Grucz, R. G. (2000) In Vitro Activities of Daptomycin, Vancomycin, Linezolid, and Quinupristin-Dalfopristin against Staphylococci and Enterococci, Including Vancomycin-Intermediate and -Resistant Strains, *Antimicrobial Agents and Chemotherapy 44*, 1062-1066.
65. Hitchings, G. H. (1973) Mechanism of Action of Trimethoprim-Sulfamethoxazole—I, *The Journal of Infectious Diseases 128*, S433-S436.
66. Markowitz, N., Quinn, E. L., and Saravolatz, L. D. (1992) Trimethoprim-sulfamethoxazole compared with vancomycin for the treatment of Staphylococcus aureus infection, *Annals of internal medicine 117*, 390-398.
67. Groisman, E. A., Hollands, K., Kriner, M. A., Lee, E.-J., Park, S.-Y., and Pontes, M. H. (2013) Bacterial Mg(2+) Homeostasis, Transport, and Virulence, *Annual review of genetics 47*, 625-646.
68. Domínguez, D. C., Guragain, M., and Patrauchan, M. (2015) Calcium binding proteins and calcium signaling in prokaryotes, *Cell Calcium 57*, 151-165.

69. Smith, R. J. (1995) Calcium and Bacteria, In *Advances in Microbial Physiology* (Poole, R. K., Ed.), pp 83-133, Academic Press.
70. Thomas, K. (2014) Kieth Thomas Ph.D. Dissertation, University of Oklahoma.
71. Fischer, D., Bieber, T., Li, Y., Elsasser, H.-P., and Kissel, T. (1999) A novel non-viral vector for DNA delivery based on low molecular weight, branched polyethylenimine: effect of molecular weight on transfection efficiency and cytotoxicity, *Pharm. Res. 16*, 1273-1279.
72. Gibney, K., Sovadinova, I., Lopez, A. I., Urban, M., Ridgway, Z., Caputo, G. A., and Kuroda, K. (2012) Poly(ethylene imine)s as antimicrobial agents with selective activity, *Macromolecular bioscience 12*, 1279-1289.
73. Keim, G. I. (1960) Wet-strength paper and method of making same, Google Patents.
74. Glaser, H. T., and Edzwald, J. K. (1979) Coagulation and direct filtration of humic substances with polyethylenimine, *Environmental Science & Technology 13*, 299-305.
75. Cordes, R. M., Sims, W. B., and Glatz, C. E. (1990) Precipitation of nucleic acids with poly (ethyleneimine), *Biotechnology progress 6*, 283-285.
76. Kirk, N., and Cowan, D. (1995) Optimising the recovery of recombinant thermostable proteins expressed in mesophilic hosts, *Journal of Biotechnology 42*, 177-184.
77. Milburn, P., Bonnerjea, J., Hoare, M., and Dunnill, P. (1990) Selective flocculation of nucleic acids, lipids, and colloidal particles from a yeast cell homogenate by polyethyleneimine, and its scale-up, *Enzyme and Microbial Technology 12*, 527-532.
78. Vancha, A. R., Govindaraju, S., Parsa, K. V. L., Jasti, M., González-García, M., and Ballestero, R. P. (2004) Use of polyethyleneimine polymer in cell culture as attachment factor and lipofection enhancer, *BMC Biotechnology 4*, 23-23.
79. Mady, M. M., Mohammed, W. A., El-Guendy, N. M., and Elsayed, A. A. (2011) Interaction of DNA and polyethylenimine: Fourier-transform infrared (FTIR) and differential scanning calorimetry (DSC) studies, *International Journal of Physical Sciences 6*, 7328-7334.
80. Boussif, O., Lezoualc'h, F., Zanta, M. A., Mergny, M. D., Scherman, D., Demeneix, B., and Behr, J. P. (1995) A versatile vector for gene and oligonucleotide transfer into cells in culture and in vivo: polyethylenimine, *Proceedings of the National Academy of Sciences 92*, 7297-7301.
81. Hall, A., Parhamifar, L., Lange, M. K., Meyle, K. D., Sanderhoff, M., Andersen, H., Roursgaard, M., Larsen, A. K., Jensen, P. B., Christensen, C., Bartek, J., and Moghimi, S. M. (2015) Polyethylenimine architecture-dependent metabolic imprints and perturbation of cellular redox homeostasis, *Biochimica et Biophysica Acta (BBA) - Bioenergetics 1847*, 328-342.
82. Ferrari, S., Moro, E., Pettenazzo, A., Behr, J. P., Zacchello, F., and Scarpa, M. (1997) ExGen 500 is an efficient vector for gene delivery to lung epithelial cells in vitro and in vivo, *Gene Therapy 4*, 1100.
83. Wiseman, J. W., Goddard, C. A., McLelland, D., and Colledge, W. H. (2003) A comparison of linear and branched polyethylenimine (PEI) with DCChol//DOPE

liposomes for gene delivery to epithelial cells in vitro and in vivo, *Gene Ther 10*, 1654-1662.
84. Godbey, W. T., Wu, K. K., and Mikos, A. G. (1999) Size matters: molecular weight affects the efficiency of poly (ethyleneimine) as a gene delivery vehicle, *Journal of biomedical materials research 45*, 268-275.
85. Muñoz-Bonilla, A., and Fernández-García, M. (2012) Polymeric materials with antimicrobial activity, *Progress in Polymer Science 37*, 281-339.
86. Gao, B., Zhang, X., and Zhu, Y. (2007) Studies on the preparation and antibacterial properties of quaternized polyethyleneimine, *Journal of Biomaterials Science, Polymer Edition 18*, 531-544.
87. Pasquier, N., Keul, H., Heine, E., Moeller, M., Angelov, B., Linser, S., and Willumeit, R. (2008) Amphiphilic branched polymers as antimicrobial agents, *Macromolecular bioscience 8*, 903-915.
88. Lipinski, C. A., Lombardo, F., Dominy, B. W., and Feeney, P. J. (2001) Experimental and computational approaches to estimate solubility and permeability in drug discovery and development settings1PII of original article: S0169-409X(96)00423-1. The article was originally published in Advanced Drug Delivery Reviews 23 (1997) 3–25.1, *Advanced Drug Delivery Reviews 46*, 3-26.
89. Lipinski, C. A. (2004) Lead- and drug-like compounds: the rule-of-five revolution, *Drug Discovery Today: Technologies 1*, 337-341.
90. Wenlock, M. C., Austin, R. P., Barton, P., Davis, A. M., and Leeson, P. D. (2003) A Comparison of Physiochemical Property Profiles of Development and Marketed Oral Drugs, *Journal of Medicinal Chemistry 46*, 1250-1256.
91. O'Shea, R., and Moser, H. E. (2008) Physicochemical Properties of Antibacterial Compounds: Implications for Drug Discovery, *Journal of Medicinal Chemistry 51*, 2871-2878.
92. Comer, J., and Tam, K. (2001) *Lipophilicity profiles: theory and measurement*, Wiley-VCH: Zürich, Switzerland.
93. David, T. M. (2007) The pKa Distribution of Drugs: Application to Drug Discovery, *Perspectives in Medicinal Chemistry 1*, 1177391X0700100003.
94. Brown, E. D., and Wright, G. D. (2016) Antibacterial drug discovery in the resistance era, *Nature 529*, 336.
95. Burgett, A. W. G., Poulsen, T. B., Wangkanont, K., Anderson, D. R., Kikuchi, C., Shimada, K., Okubo, S., Fortner, K. C., Mimaki, Y., Kuroda, M., Murphy, J. P., Schwalb, D. J., Petrella, E. C., Cornella-Taracido, I., Schirle, M., Tallarico, J. A., and Shair, M. D. (2011) Natural products reveal cancer cell dependence on oxysterol-binding proteins, *Nature Chemical Biology 7*, 639-647.
96. Haynes, W. M. (2014) *CRC handbook of chemistry and physics*, CRC press.
97. Gallardo-Godoy, A., Muldoon, C., Becker, B., Elliott, A. G., Lash, L. H., Huang, J. X., Butler, M. S., Pelingon, R., Kavanagh, A. M., Ramu, S., Phetsang, W., Blaskovich, M. A. T., and Cooper, M. A. (2016) Activity and Predicted Nephrotoxicity of Synthetic Antibiotics Based on Polymyxin B, *Journal of Medicinal Chemistry 59*, 1068-1077.
98. Huang, J. X., Kaeslin, G., Ranall, M. V., Blaskovich, M. A., Becker, B., Butler, M. S., Little, M. H., Lash, L. H., and Cooper, M. A. (2015) Evaluation of

biomarkers for in vitro prediction of drug-induced nephrotoxicity: comparison of HK-2, immortalized human proximal tubule epithelial, and primary cultures of human proximal tubular cells, *Pharmacology Research & Perspectives 3*, e00148-n/a.

99. Tang, G. P., Guo, H. Y., Alexis, F., Wang, X., Zeng, S., Lim, T. M., Ding, J., Yang, Y. Y., and Wang, S. (2006) Low molecular weight polyethylenimines linked by β-cyclodextrin for gene transfer into the nervous system, *The Journal of Gene Medicine 8*, 736-744.
100. Wiegand, C., Bauer, M., Hipler, U.-C., and Fischer, D. (2013) Poly(ethyleneimines) in dermal applications: Biocompatibility and antimicrobial effects, *International Journal of Pharmaceutics 456*, 165-174.
101. Fischer, D., Li, Y., Ahlemeyer, B., Krieglstein, J., and Kissel, T. (2003) In vitro cytotoxicity testing of polycations: influence of polymer structure on cell viability and hemolysis, *Biomaterials 24*, 1121-1131.
102. Veni, E. J. K., Baliga, S., Shenoy, M., and Gopalkrishna, B. K. (2014) Community-acquired methicillin resistant Staphylococcus aureus, *Int. J. Curr. Res. Rev. 6*, 1-10, 10 pp.
103. Pastagia, M., Kleinman, L. C., Lacerda de la Cruz, E. G., and Jenkins, S. G. (2012) Predicting Risk for Death from MRSA Bacteremia, *Emerging Infectious Diseases 18*, 1072-1080.
104. Cosgrove, S. E., Qi, Y., Kaye, K. S., Harbarth, S., Karchmer, A. W., and Carmeli, Y. (2005) The Impact of Methicillin Resistance in Staphylococcus aureus Bacteremia on Patient Outcomes: Mortality, Length of Stay, and Hospital Charges, *Infection Control & Hospital Epidemiology 26*, 166-174.
105. O'Daniel, P. I., Peng, Z., Pi, H., Testero, S. A., Ding, D., Spink, E., Leemans, E., Boudreau, M. A., Yamaguchi, T., Schroeder, V. A., Wolter, W. R., Llarrull, L. I., Song, W., Lastochkin, E., Kumarasiri, M., Antunes, N. T., Espahbodi, M., Lichtenwalter, K., Suckow, M. A., Vakulenko, S., Mobashery, S., and Chang, M. (2014) Discovery of a New Class of Non-β-lactam Inhibitors of Penicillin-Binding Proteins with Gram-Positive Antibacterial Activity, *J. Am. Chem. Soc. 136*, 3664-3672.
106. Zhanel, G. G., Love, R., Adam, H., Golden, A., Zelenitsky, S., Schweizer, F., Gorityala, B., Lagace-Wiens, P. R. S., Rubinstein, E., Walkty, A., Gin, A. S., Gilmour, M., Hoban, D. J., Lynch, J. P., III, and Karlowsky, J. A. (2015) Tedizolid: A Novel Oxazolidinone with Potent Activity Against Multidrug-Resistant Gram-Positive Pathogens, *Drugs 75*, 253-270.
107. Ling, L. L., Schneider, T., Peoples, A. J., Spoering, A. L., Engels, I., Conlon, B. P., Mueller, A., Schaberle, T. F., Hughes, D. E., Epstein, S., Jones, M., Lazarides, L., Steadman, V. A., Cohen, D. R., Felix, C. R., Fetterman, K. A., Millett, W. P., Nitti, A. G., Zullo, A. M., Chen, C., and Lewis, K. (2015) A new antibiotic kills pathogens without detectable resistance, *Nature (London, U. K.) 517*, 455-459.
108. Appelbaum, P. C. (2006) The emergence of vancomycin-intermediate and vancomycin-resistant Staphylococcus aureus, *Clin. Microbiol. Infect. 12*, 16-23.
109. Gardete, S., and Tomasz, A. (2014) Mechanisms of vancomycin resistance in Staphylococcus aureus, *J. Clin. Invest. 124*, 2836-2840.

110. Jiang, W., Li, B., Zheng, X., Liu, X., Pan, X., Qing, R., Cen, Y., Zheng, J., and Zhou, H. (2013) Artesunate has its enhancement on antibacterial activity of β-lactams via increasing the antibiotic accumulation within methicillin-resistant Staphylococcus aureus (MRSA), *J. Antibiot. 66*, 339-345.
111. Suzuki, M., Yamada, K., Nagao, M., Aoki, E., Matsumoto, M., Hirayama, T., Yamamoto, H., Hiramatsu, R., Ichiyama, S., and Iinuma, Y. (2011) Antimicrobial Ointments and Methicillin-Resistant Staphylococcus aureus USA300, *Emerging Infectious Diseases 17*, 1917-1920.
112. Orhan, G., Bayram, A., Zer, Y., and Balci, I. (2005) Synergy Tests by E Test and Checkerboard Methods of Antimicrobial Combinations against Brucella melitensis, *Journal of Clinical Microbiology 43*, 140-143.
113. Carrel, M., Perencevich, E. N., and David, M. Z. (2015) USA300 Methicillin-Resistant Staphylococcus aureus, United States, 2000–2013, *Emerging Infectious Diseases 21*, 1973-1980.
114. Baba, T., Takeuchi, F., Kuroda, M., Yuzawa, H., Aoki, K.-i., Oguchi, A., Nagai, Y., Iwama, N., Asano, K., Naimi, T., Kuroda, H., Cui, L., Yamamoto, K., and Hiramatsu, K. (2002) Genome and virulence determinants of high virulence community-acquired MRSA, *The Lancet 359*, 1819-1827.
115. Holden, M. T. G., Feil, E. J., Lindsay, J. A., Peacock, S. J., Day, N. P. J., Enright, M. C., Foster, T. J., Moore, C. E., Hurst, L., Atkin, R., Barron, A., Bason, N., Bentley, S. D., Chillingworth, C., Chillingworth, T., Churcher, C., Clark, L., Corton, C., Cronin, A., Doggett, J., Dowd, L., Feltwell, T., Hance, Z., Harris, B., Hauser, H., Holroyd, S., Jagels, K., James, K. D., Lennard, N., Line, A., Mayes, R., Moule, S., Mungall, K., Ormond, D., Quail, M. A., Rabbinowitsch, E., Rutherford, K., Sanders, M., Sharp, S., Simmonds, M., Stevens, K., Whitehead, S., Barrell, B. G., Spratt, B. G., and Parkhill, J. (2004) Complete genomes of two clinical Staphylococcus aureus strains: Evidence for the rapid evolution of virulence and drug resistance, *Proceedings of the National Academy of Sciences of the United States of America 101*, 9786.
116. Levison, M. E., and Levison, J. H. (2009) Pharmacokinetics and Pharmacodynamics of Antibacterial Agents, *Infectious disease clinics of North America 23*, 791-vii.
117. Hartman, B. J., and Tomasz, A. (1984) Low-affinity penicillin-binding protein associated with β-lactam resistance in Staphylococcus aureus, *J. Bacteriol. 158*, 513-516.
118. Fuda, C., Suvorov, M., Vakulenko, S. B., and Mobashery, S. (2004) The Basis for Resistance to β-Lactam Antibiotics by Penicillin-binding Protein 2a of Methicillin-resistant Staphylococcus aureus, *Journal of Biological Chemistry 279*, 40802-40806.
119. Wang, H., Gill, C. J., Lee, S. H., Mann, P., Zuck, P., Meredith, T. C., Murgolo, N., She, X., Kales, S., Liang, L., Liu, J., Wu, J., Santa Maria, J., Su, J., Pan, J., Hailey, J., McGuinness, D., Tan, C. M., Flattery, A., Walker, S., Black, T., and Roemer, T. (2013) Discovery of Wall Teichoic Acid Inhibitors as Potential Anti-MRSA β-Lactam Combination Agents, *Chem. Biol. (Oxford, U. K.) 20*, 272-284.

120. Belcheva, A., and Golemi-Kotra, D. (2008) A close-up view of the VraSR two-component system - A mediator of staphylococcus aureus response to cell wall damage, *Journal of Biological Chemistry 283*, 12354-12364.
121. Roemer, T., Schneider, T., and Pinho, M. G. (2013) Auxiliary factors: a chink in the armor of MRSA resistance to beta-lactam antibiotics, *Current Opinion in Microbiology 16*, 538-548.
122. Xia, G., Kohler, T., and Peschel, A. (2010) The wall teichoic acid and lipoteichoic acid polymers of Staphylococcus aureus, *International Journal of Medical Microbiology 300*, 148-154.
123. Brown, S., Maria, J. P. S., Jr., and Walker, S. (2013) Wall teichoic acids of Gram-positive bacteria, *Annu. Rev. Microbiol. 67*, 313-336.
124. Beveridge, T. J. (1978) The response of cell walls of Bacillus subtilis to metals and to electron-microscopic stains, *Canadian Journal of Microbiology 24*, 89-104.
125. Bera, A., Biswas, R., Herbert, S., Kulauzovic, E., Weidenmaier, C., Peschel, A., and Götz, F. (2007) Influence of Wall Teichoic Acid on Lysozyme Resistance in Staphylococcus aureus, *Journal of Bacteriology 189*, 280-283.
126. Sewell, E. W. C., and Brown, E. D. (2014) Taking aim at wall teichoic acid synthesis: new biology and new leads for antibiotics, *J. Antibiot. 67*, 43-51.
127. Weidenmaier, C., Peschel, A., Xiong, Y.-Q., Kristian, S. A., Dietz, K., Yeaman, M. R., and Bayer, A. S. (2005) Lack of Wall Teichoic Acids in Staphylococcus aureus Leads to Reduced Interactions with Endothelial Cells and to Attenuated Virulence in a Rabbit Model of Endocarditis, *Journal of Infectious Diseases 191*, 1771-1777.
128. Vergara-Irigaray, M., Maira-Litrán, T., Merino, N., Pier, G. B., Penadés, J. R., and Lasa, I. (2008) Wall teichoic acids are dispensable for anchoring the PNAG exopolysaccharide to the Staphylococcus aureus cell surface, *Microbiology 154*, 865-877.
129. Holland, L. M., Conlon, B., and O'Gara, J. P. (2011) Mutation of tagO reveals an essential role for wall teichoic acids in Staphylococcus epidermidis biofilm development, *Microbiology 157*, 408-418.
130. Weidenmaier, C., Kokai-Kun, J. F., Kristian, S. A., Chanturiya, T., Kalbacher, H., Gross, M., Nicholson, G., Neumeister, B., Mond, J. J., and Peschel, A. (2004) Role of teichoic acids in Staphylococcus aureus nasal colonization, a major risk factor in nosocomial infections, *Nature medicine 10*, 243-245.
131. Weidenmaier, C., and Peschel, A. (2008) Teichoic acids and related cell-wall glycopolymers in Gram-positive physiology and host interactions, *Nature reviews. Microbiology 6*, 276-287.
132. D'Elia, M. A., Millar, K. E., Beveridge, T. J., and Brown, E. D. (2006) Wall teichoic acid polymers are dispensable for cell viability in Bacillus subtilis, *Journal of bacteriology 188*, 8313-8316.
133. Schirner, K., Marles-Wright, J., Lewis, R. J., and Errington, J. (2009) Distinct and essential morphogenic functions for wall-and lipo-teichoic acids in Bacillus subtilis, *The EMBO Journal 28*, 830-842.
134. Thomas, K. J., 3rd, and Rice, C. V. (2014) Revised model of calcium and magnesium binding to the bacterial cell wall, *Biometals : an international*

journal on the role of metal ions in biology, biochemistry, and medicine 27, 1361-1370.
135. Halye, J. L., and Rice, C. V. (2010) Cadmium Chelation by Bacterial Teichoic Acid from Solid-State Nuclear Magnetic Resonance Spectroscopy, *Biomacromolecules 11*, 333-340.
136. Wickham, J. R., Halye, J. L., Kashtanov, S., Khandogin, J., and Rice, C. V. (2009) Revisiting Magnesium Chelation by Teichoic Acid with Phosphorus Solid-State NMR and Theoretical Calculations, *The Journal of Physical Chemistry B 113*, 2177-2183.
137. Atilano, M. L., Pereira, P. M., Yates, J., Reed, P., Veiga, H., Pinho, M. G., and Filipe, S. R. (2010) Teichoic acids are temporal and spatial regulators of peptidoglycan cross-linking in Staphylococcus aureus, *Proceedings of the National Academy of Sciences of the United States of America 107*, 18991-18996.
138. Qamar, A., and Golemi-Kotra, D. (2012) Dual roles of FmtA in Staphylococcus aureus cell wall biosynthesis and autolysis, *Antimicrobial agents and chemotherapy 56*, 3797-3805.
139. Campbell, J., Singh, A. K., Maria, J. P. S., Kim, Y., Brown, S., Swoboda, J. G., Mylonakis, E., Wilkinson, B. J., and Walker, S. (2011) Synthetic Lethal Compound Combinations Reveal a Fundamental Connection between Wall Teichoic Acid and Peptidoglycan Biosyntheses in Staphylococcus aureus, *Acs Chem Biol 6*, 106-116.
140. Bhavsar, A. P., Erdman, L. K., Schertzer, J. W., and Brown, E. D. (2004) Teichoic acid is an essential polymer in Bacillus subtilis that is functionally distinct from teichuronic acid, *Journal of bacteriology 186*, 7865-7873.
141. Gautam, S., Kim, T., and Spiegel, D. A. (2015) Chemical probes reveal an extraseptal mode of cross-linking in Staphylococcus aureus, *Journal of the American Chemical Society 137*, 7441-7447.
142. Schlag, M., Biswas, R., Krismer, B., Kohler, T., Zoll, S., Yu, W., Schwarz, H., Peschel, A., and Gotz, F. (2010) Role of staphylococcal wall teichoic acid in targeting the major autolysin Atl, *Mol Microbiol 75*, 864-873.
143. Shimomura, O., Johnson, F. H., and Saiga, Y. (1962) Extraction, purification and properties of aequorin, a bioluminescent protein from the luminous hydromedusan, Aequorea, *Journal of Cellular Physiology 59*, 223-239.
144. Moreillon, P. (2008) New and emerging treatment of Staphylococcus aureus infections in the hospital setting, *Clin. Microbiol. Infect. 14*, 32-41.
145. Campbell, J., Singh, A. K., Santa Maria, J. P., Jr., Kim, Y., Brown, S., Swoboda, J. G., Mylonakis, E., Wilkinson, B. J., and Walker, S. (2011) Synthetic lethal compound combinations reveal a fundamental connection between wall teichoic acid and peptidoglycan biosyntheses in Staphylococcus aureus, *ACS chemical biology 6*, 106-116.
146. Swoboda, J. G., Campbell, J., Meredith, T. C., and Walker, S. (2010) Wall Teichoic Acid Function, Biosynthesis, and Inhibition, *Chembiochem 11*, 35-45.
147. Brown, S., Meredith, T., Swoboda, J., and Walker, S. (2010) Staphylococcus aureus and Bacillus subtilis W23 Make Polyribitol Wall Teichoic Acids Using Different Enzymatic Pathways, *Chemistry & Biology 17*, 1101-1110.

148. Webba da Silva, M. (2007) NMR methods for studying quadruplex nucleic acids, *Methods 43*, 264-277.
149. Gotfredsen, C. H., Meissner, A., Duus, J. Ø., and Sørensen, O. W. (2000) New methods for measuring 1H–31P coupling constants in nucleic acids, *Magnetic Resonance in Chemistry 38*, 692-695.
150. Jennings, M. C., Minbiole, K. P. C., and Wuest, W. M. (2015) Quaternary Ammonium Compounds: An Antimicrobial Mainstay and Platform for Innovation to Address Bacterial Resistance, *ACS Infectious Diseases 1*, 288-303.
151. Swoboda, J. G., Meredith, T. C., Campbell, J., Brown, S., Suzuki, T., Bollenbach, T., Malhowski, A. J., Kishony, R., Gilmore, M. S., and Walker, S. (2009) Discovery of a Small Molecule that Blocks Wall Teichoic Acid Biosynthesis in Staphylococcus aureus, *ACS chemical biology 4*, 875-883.
152. Pasquina, L. W., Santa Maria, J. P., and Walker, S. (2013) Teichoic acid biosynthesis as an antibiotic target, *Curr. Opin. Microbiol. 16*, 531-537.
153. Lee, S. H., Wang, H., Labroli, M., Koseoglu, S., Zuck, P., Mayhood, T., Gill, C., Mann, P., Sher, X., Ha, S., Yang, S.-W., Mandal, M., Yang, C., Liang, L., Tan, Z., Tawa, P., Hou, Y., Kuvelkar, R., DeVito, K., Wen, X., Xiao, J., Batchlett, M., Balibar, C. J., Liu, J., Xiao, J., Murgolo, N., Garlisi, C. G., Sheth, P. R., Flattery, A., Su, J., Tan, C., and Roemer, T. (2016) TarO-specific inhibitors of wall teichoic acid biosynthesis restore β-lactam efficacy against methicillin-resistant staphylococci, *Science Translational Medicine 8*, 329ra332.
154. Mandal, M., Tan, Z., Madsen-Duggan, C., Buevich, A. V., Caldwell, J. P., Dejesus, R., Flattery, A., Garlisi, C. G., Gill, C., Ha, S. N., Ho, G., Koseoglu, S., Labroli, M., Basu, K., Lee, S. H., Liang, L., Liu, J., Mayhood, T., McGuinness, D., McLaren, D. G., Wen, X., Parmee, E., Rindgen, D., Roemer, T., Sheth, P., Tawa, P., Tata, J., Yang, C., Yang, S.-W., Xiao, L., Wang, H., Tan, C., Tang, H., Walsh, P., Walsh, E., Wu, J., and Su, J. (2017) Can We Make Small Molecules Lean? Optimization of a Highly Lipophilic TarO Inhibitor, *Journal of Medicinal Chemistry*.
155. Farha, M. A., Koteva, K., Gale, R. T., Sewell, E. W., Wright, G. D., and Brown, E. D. (2014) Designing analogs of ticlopidine, a wall teichoic acid inhibitor, to avoid formation of its oxidative metabolites, *Bioorganic & Medicinal Chemistry Letters 24*, 905-910.
156. Yang, S.-W., Pan, J., Yang, C., Labroli, M., Pan, W., Caldwell, J., Ha, S., Koseoglu, S., Xiao, J. C., Mayhood, T., Sheth, P. R., Garlisi, C. G., Wu, J., Lee, S. H., Wang, H., Tan, C. M., Roemer, T., and Su, J. (2016) Benzimidazole analogs as WTA biosynthesis inhibitors targeting methicillin resistant Staphylococcus aureus, *Bioorganic & Medicinal Chemistry Letters 26*, 4743-4747.
157. Chang, J. Y., and Korolev, V. V. (1996) Specific Toxicity of Tunicamycin in Induction of Programmed Cell Death of Sympathetic Neurons, *Experimental Neurology 137*, 201-211.
158. Lin, T. Y., Wang, S. M., Fu, W. M., Chen, Y. H., and Yin, H. S. (1999) Toxicity of tunicamycin to cultured brain neurons: Ultrastructure of the degenerating neurons, *Journal of Cellular Biochemistry 74*, 638-647.

159. Farha, M. A., Leung, A., Sewell, E. W., D'Elia, M. A., Allison, S. E., Ejim, L., Pereira, P. M., Pinho, M. G., Wright, G. D., and Brown, E. D. (2013) Inhibition of WTA synthesis blocks the cooperative action of PBPs and sensitizes MRSA to beta-lactams, *Acs Chem Biol 8*, 226-233.
160. Tan, C. M., Therien, A. G., Lu, J., Lee, S. H., Caron, A., Gill, C. J., Lebeau-Jacob, C., Benton-Perdomo, L., Monteiro, J. M., Pereira, P. M., Elsen, N. L., Wu, J., Deschamps, K., Petcu, M., Wong, S., Daigneault, E., Kramer, S., Liang, L., Maxwell, E., Claveau, D., Vaillancourt, J., Skorey, K., Tam, J., Wang, H., Meredith, T. C., Sillaots, S., Wang-Jarantow, L., Ramtohul, Y., Langlois, E., Landry, F., Reid, J. C., Parthasarathy, G., Sharma, S., Baryshnikova, A., Lumb, K. J., Pinho, M. G., Soisson, S. M., and Roemer, T. (2012) Restoring Methicillin-Resistant Staphylococcus aureus Susceptibility to β-Lactam Antibiotics, *Science Translational Medicine 4*, 126ra135.
161. Lee, K., Campbell, J., Swoboda, J. G., Cuny, G. D., and Walker, S. (2010) Development of improved inhibitors of wall teichoic acid biosynthesis with potent activity against Staphylococcus aureus, *Bioorganic & Medicinal Chemistry Letters 20*, 1767-1770.
162. Komatsuzawa, H., Ohta, K., Labischinski, H., Sugai, M., and Suginaka, H. (1999) Characterization of fmtA, a Gene That Modulates the Expression of Methicillin Resistance in Staphylococcus aureus, *Antimicrobial Agents and Chemotherapy 43*, 2121-2125.
163. Campbell, J., Singh, A. K., Swoboda, J. G., Gilmore, M. S., Wilkinson, B. J., and Walker, S. (2012) An Antibiotic That Inhibits a Late Step in Wall Teichoic Acid Biosynthesis Induces the Cell Wall Stress Stimulon in Staphylococcus aureus, *Antimicrobial Agents and Chemotherapy 56*, 1810-1820.
164. Gründling, A., and Schneewind, O. (2007) Synthesis of glycerol phosphate lipoteichoic acid in <em>Staphylococcus aureus</em&gt, *Proceedings of the National Academy of Sciences 104*, 8478.
165. Oku, Y., Kurokawa, K., Matsuo, M., Yamada, S., Lee, B.-L., and Sekimizu, K. (2009) Pleiotropic Roles of Polyglycerolphosphate Synthase of Lipoteichoic Acid in Growth of Staphylococcus aureus Cells, *Journal of Bacteriology 191*, 141-151.
166. Richter, S. G., Elli, D., Kim, H. K., Hendrickx, A. P. A., Sorg, J. A., Schneewind, O., and Missiakas, D. (2013) Small molecule inhibitor of lipoteichoic acid synthesis is an antibiotic for Gram-positive bacteria, *Proc. Natl. Acad. Sci. U. S. A. 110*, 3531-3536, S3531/3531-S3531/3536.
167. Schirner, K., Eun, Y. J., Dion, M., Luo, Y., Helmann, J. D., Garner, E. C., and Walker, S. (2015) Lipid-linked cell wall precursors regulate membrane association of bacterial actin MreB, *Nature chemical biology 11*, 38-45.
168. Mani, N., Tobin, P., and Jayaswal, R. K. (1993) Isolation and characterization of autolysis-defective mutants of Staphylococcus aureus created by Tn917-lacZ mutagenesis, *Journal of Bacteriology 175*, 1493-1499.
169. Carballido-López, R., and Errington, J. (2003) The Bacterial Cytoskeleton: In Vivo Dynamics of the Actin-like Protein Mbl of Bacillus subtilis, *Developmental cell 4*, 19-28.

170. Formstone, A., Carballido-López, R., Noirot, P., Errington, J., and Scheffers, D.-J. (2008) Localization and interactions of teichoic acid synthetic enzymes in Bacillus subtilis, *Journal of Bacteriology 190*, 1812-1821.
171. Suzuki, J., Komatsuzawa, H., Sugai, M., Ohta, K., Kozai, K., Nagasaka, N., and Suginaka, H. (1997) Effects of various types of Triton X on the susceptibilities of methicillin-resistant staphylococci to oxacillin, *FEMS Microbiology Letters 153*, 327-331.
172. Bæk, K. T., Bowman, L., Millership, C., Dupont Søgaard, M., Kaever, V., Siljamäki, P., Savijoki, K., Varmanen, P., Nyman, T. A., Gründling, A., and Frees, D. (2016) The Cell Wall Polymer Lipoteichoic Acid Becomes Nonessential in Staphylococcus aureus Cells Lacking the ClpX Chaperone, *mBio 7*.

[Appendix A: Table of Abbreviations]

Abbreviation	Explanation
ANOVA	Analysis of variance
BSL	Biosafety level
BPEI	Branched polyethylenimine
CA-MRSA	Community-acquired methicillin-resistant *Staphylococcus aureus*
CFU	Colony-forming unit
COSY	Correlation spectroscopy
Da	Dalton
DNA	Deoxyribonucleic acid
EPS	Extrapolymeric substance
FDA	Food and Drug Administration
FIC	Fractional inhibitory concentration
FICI	Fractional inhibitory concentration index
GFP	Green fluorescent protein
HA-MRSA	Hospital-acquired methicillin-resistant *Staphylococcus aureus*
HMBC	Heteronuclear multiple-bond correlation spectroscopy
HMDS	Hexamethyldisilazane
hRPTECs	Primary human renal proximal tubule epithelial cells
HSQC	Heteronuclear single-quantum correlation spectroscopy
IC50	Half maximal inhibitory concentration
LB	Lysogeny broth
LDH	Lactase dehydrogenase
LPEI	Linear polyethylenimine
LPS	Lipopolysaccharide
LSCM	Laser scanning confocal microscope
LTA	Lipo teichoic acid
MBC	Minimum bactericidal concentration
MIC	Minimum inhibitory concentration
MRSA	Methicillin-resistant *Staphylococcus aureus*
MSSA	Methicillin-susceptible *Staphylococcus aureus*
MW	Molecular weight
NA	Numerical aperture
NAG	N-acetylglucosamine
NAM	N-acetylmuramic acid
NMR	Nuclear magnetic resonance
OD_{600}	Optical density at 600 nm
PBP	Penicillin binding protein
PBS	Phosphate buffered saline

PEI	Polyethylenimine
PO	Propylene oxide
PVL	Panton–Valentine leukocidin
RO5	Rule of 5
SCCmec	Staphylococcal cassette chromosome *mec*
SEM	Scanning electron microscope
TCA	Trichloroacidic acid
TEM	Transmission electron microscope
TOCSY	Two-dimensional nuclear magnetic resonance spectroscopy
TSB	Tryptic soy broth
VISA	Vancomycin-intermediate-resistant *Staphylococcus aureus*
VRSA	Vancomycin-resistant *Staphylococcus aureus*
WTA	Wall teichoic acid
YFP	Yellow fluorescent protein